Monitoring forest fragmentation and carbon storage in the Cerrado Biome of Mato Grosso using optical and SAR satellite images.

Dissertation

for the award of the degree

"Doctor rerum naturalium" (Dr.rer.nat.) in Mathematics and Natural Sciences

of the Georg-August-Universität Göttingen

within the doctoral program of Geoscience and Geography

of the Georg-August University School of Science (GAUSS)

submitted by

Flávia de Souza Mendes

from Cachoeira Paulista, Brazil

Göttingen, 2019

Thesis Commitee

Prof. iR. Dr. Gerhard Gerold (thesis supervisior)

Department of Landscape Ecology, Georg-August Universität Göttingen

Dr. Stefan Erasmi

Department of Physical Geography, Georg-August Universität Göttingen

Members of Examination Board

1st Referee: Prof. iR. Dr. Gerhard Gerold

Department of Landscape Ecology, Georg-August Universität Göttingen

2nd Referee: Prof. Dr. Daniela Sauer

Department of Physical Geography, Georg-August Universität Göttingen

Further members of Examination Board

Prof. Dr. Heiko Faust

Department of Human Geography, Georg-August Universität Göttingen

Dr. Stefan Erasmi

Institute of Farm Economics, Thünen Institute

Prof. Dr. Veraldo Liesenberg

College of Agriculture and Veterinary, Santa Catarina State Universtiy (UDESC)

Prof. Dr. Martin Kappas

Department of Cartography, GIS and Remote Sensing, Georg-August Universität Göttingen

Data of oral examination: 27th January, 2020

"Faith and reason are like two wings on which the human spirit rises to the contemplation of truth..." (Pope St. John Paul II)

Acknowledgments

Table of Contents

List of Figures

List of Tables

Summary

Several studies suggested that forest fragmentation, which is an effect of deforestation, and edge effect have an impact on the biomas and carbon stock in tropical forest. For Amazon and Atlantic Forest biomes, most studies have shown using in situ measurements and remote sensing data that biomass and carbon stock reduce within the first 300 meter of a forest edge to its center. For the Cerrado biome, there is currently no consensus whether or not there is an edge effect on biomass and carbon stock. Therefore, this study aims to better analyze the forest fragmentation and edge effect on the vegetation, such as biomass-carbon stock and canopy greenness, in the Cerrado biome. The most common method used to assess the edge effects on vegetation in tropical forest is direct measurement, which is difficult to replicate, cost intensive and time consuming. Therefore, the use of satellite images may be an alternative to monitor vegetation cover within the context of edge effects. In order to monitor forest fragmentation and carbon storage in the Cerrado biome, different approaches were investigated with fragmented areas in the city of Nova Mutum- Mato Grosso: (1) mapping the different type of vegetation using optical and synthetic aperture radar (SAR) remote sensing images, (2) estimating the biomass and carbon stock from in situ measurements within the context of edge effect and (3) monitoring the edge effect over the long-term using time-series Landsat satellite images.

First, the use of optical and SAR images to map the different types of vegetation in the transitional area between the Cerrado and Amazon biomes was investigated. Using this approach, the diverse vegetation types of the transition areas were studied. The findings indicated that by applying a supervised random forest classification, the highest overall accuracy and kappa coefficient were obtained by using only Sentinel 2A images for the classification process. However, out of the three classifications, two (Sentinel 2A with TanDEM-X and Sentinel 2A with Sentinel 1A) that used radar and optical images recorded the highest overall accuracy and kappa values. Bands 5, 11, and 12 from Sentinel 2A satellite image, texture images from Sentinel 1A cross-polarization, and coherence from TanDEM-X images were the most important variables that separated each vegetation class similar to the variable importance from the random forest algorithm. After obtaining a better understanding of the diverse vegetation types in the study area, we assessed the impact of fragmentation and edge effect on biomass and carbon stock using in situ measurements that were collected in July and August 2017. Using this approach, we investigated the woody components of tree layer and shrub layer by recording key variables such as the diameter at breast height (DBH), total tree-shrub height, wood density, basal area and tree species. Here, the DBH and the total tree-shrub height were the explanatory variables of the allometric model in the Cerradão. For the Cerrado denso on the other hand DBH and the wood density were the explanatory variables of the allometric model. In contrast to our working hypothesis, the results showed no significant differences in the quantity and the distribution of AGB and carbon

stocks between edge and center of the fragments of both vegetation types. Rather, the results showed a significant difference for the AGB and aboveground carbon stocks between the two investigated vegetation types. We thus suggest that the edge effect on biomass patterns found in the Amazon cannot be compared with those of the Cerrado biome. It is important to stress that our analyzes were performed with a single measurement, therefore, to have a better understanding of these impacts, a long-term approach is required. The last analysis of this thesis was to evaluate the edge effect in the long-term based on NDVI values of the transitional area between the Cerrado and Amazon biomes. The method described in this study corroborates studies that assessed edge effect on vegetation within the Cerrado and Amazon biomes. In this study, we applied a different approach to investigate possible edge effects using vegetation index from freely available satellite images. Our results showed a positive significant change (p-value < 0.00005) via the NDVI values in relation to distance from the nearest edge. The closer the vegetation was to the edge, the lower their respective NDVI value. Furthermore, our results showed that long-term edge effect patterns found in the Amazon biome cannot be extrapolated to Cerrado. This observation is mainly due to the stabilization of NDVI trends after two years of deforestation within the area. This suggest that more studies are needed to adequately understand the dynamics of edge effect in Arc of Deforestation, which directly affect biomass and carbon estimations.

In this thesis, different methods were used to assess edge effects on the vegetation, such as biomass-carbon stock and greenness, in the Amazon-Cerrado ecotone. In the small scale, using fieldwork data, we could not find any evidence that fragmentation affects the carbon stock, due to the fact that the natural resources of the Cerrado biome have been widely exploited within the past 50 years, and thus, has a general decreased in biomass and carbon stock in the edge and also the center of the fragment. However, we have significant results from remote sensing long-term data, in which the NDVI is affected by the forest fragmentation and edge effect on the vegetation (canopy greenness), the closer to the edge, the lower the NDVI value. This shows that the use of satellite images has allowed an analysis of a larger period compared to fieldwork. One explanation for these findings is that the natural resources of the Cerrado biome have been widely exploited within the past 50 years, and thus, has decreased an overall biomass and carbon stock in all areas, which was found in the fieldwork data due to the few samples that were measured. However, the use of satellite images has allowed an analysis of the fragmentation effect with a larger amount of samples compared to fieldwork. not only in the edges. These outcomes of this thesis provide a solid research direction for further studies on edge effect in the Amazon-Cerrado ecotone. Long-term analysis using both field data and remote sensing is required to fully understand the fragmentation and edge effects in the Cerrado.

1. General Introduction

1.1 Tropical Savanna

The term savanna is the result of a large number of different concepts based on environmental factors such as climate, soil, hydrology, geomorphology and biotic functions (Bourliere and Hadley 1970). In general, there are two schools of thought for savanna definition, the European and American. The Europeans characterize savanna as 'a tropical grass with herbs and a continuous or discontinuous coverage of trees. The American follows the same definition, but includes areas that are not tropical (Collinson 1988). This thesis focuses on the tropical savanna (Figure 1.1). The tropical savanna biome covers nearly 20% of the Earth's surface (Cole 1963) and concentrates about $1/5^{th}$ of the global population (Goudie and Cuff 2002). This biome is located in the transition between the tropical forests and xeric shrublands (deserts). The vegetation in the savanna is characterized by trees that are widely spaced with an open canopy that allows for the growth of an herbaceous ground layer. The climate in the biome corresponds to Köppen climate classifications "As" and "Aw", with temperatures above 18°C in every month and a clear dry season of varying length (Cole 1963). The largest part of savanna is in the African continent, where it occupies around 50% of the land surface, followed by Asia and South America (Menaut 1983). The savanna offers important ecosystem services, such as carbon storage, pollination, water supply and flow regulation, erosion control, cultural values, and biological control of agricultural pests (Bengtsson et al. 2019). The flat topography, accessibility and the easy management of the soil for agricultural activities makes the savanna the most affected biome in terms of deforestation. Therefore, the major threat to tropical savanna is fire, which is usually used by settlers for the deforestation and preparation of soil before land cultivation. Fire destroys individual organisms, disturbs species, changes the vegetation structure, and alters the biophysical components of the plants (Walker 1987). However, wildfire can also play an important role in the savanna ecosystem. Natural fires are important for the regeneration of the vegetation (Zimmermann et al. 2008).
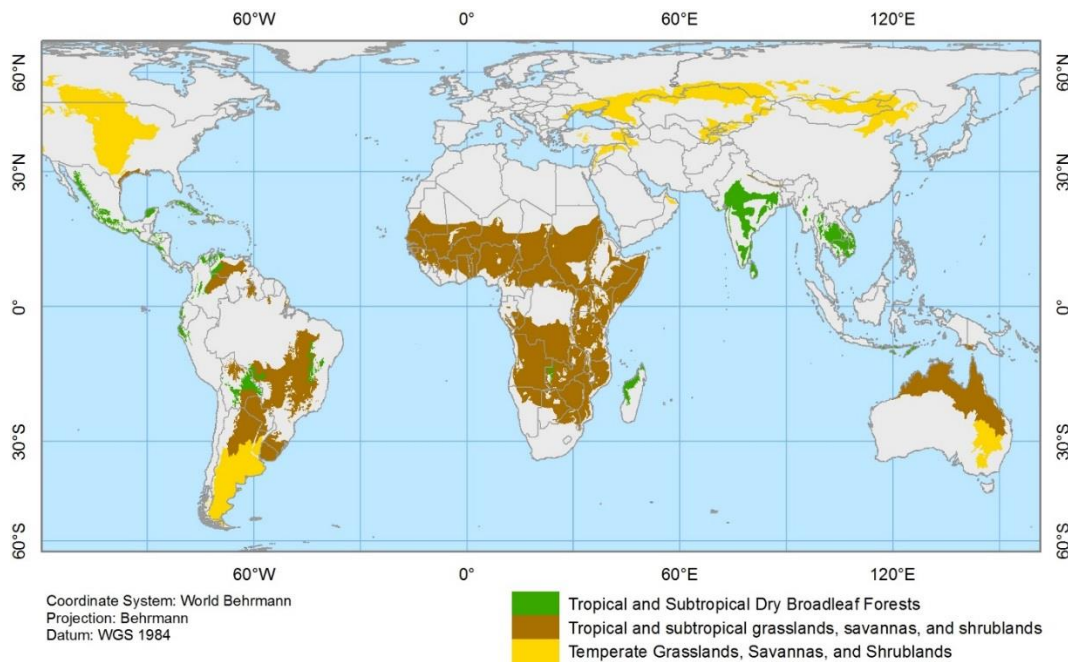
Figure 1.1 The distribution of tropical savanna (including tropical dry forests) in the world (after Olson et al. 2001).

The savannas of Tropical America are mostly located in Brazil, Colombia and Venezuela, some parts of Cuba, Paraguay and Mexico (Figure 1.1). Sarmiento (1983) classified the tropical savannas in America into four types: savanna grassland (dwarf form of trees and shrubs), tree/shrub savanna (continued herby layer), wooded savanna (density of 1000 trees ha) and savanna parkland (grooves of trees and shrubs). Additionally, Venezuela and Colombia have a specific savanna type called Llanos, which is located in wetland environment along the shores of the rivers. Together they represent around 18% of the savanna coverage in South America. However, the majority of savanna coverage is located in Brazil. In Brazil, savanna ecosystems are called Cerrado.

1.2   The Cerrado Biome and the ongoing threat of deforestation and land use

The Cerrado biome is the second largest vegetation complex present in Brazil and occupies about 200 million hectares in 11 Brazilian states and the Federal District, about 24% of Brazilian territory, and altitudes between 300 and 1600 meters. The biome is the most extensive woodland-savanna in South America and presents a great diversity, such as diferent vegetation types. In general, the vegetation of Cerrado in Brazil covers three main different vegetation types: grassland, savannas, and forest formations. The forest formations consist of arboreal species in a continuous canopy and include the Gallery, Dry, and Open Forest. The savanna formation is characterized by a discontinuous herbaceous-shrub and tree canopy. The seven types of savanna formation are Dense Woodland, Woodland, Open Woodland, Park Woodland, Palm, Vereda, and Stone Woodland. The grassland formations include three

vegetation types: Stone Grassland, Shrub Savanna, and Grassland. Each of these types has a high diversity, which is a consequence of the high variability of the soil and microclimates as well as the floristic evolution with plants from different Brazilian biomes (Walter 2006). Due to this diversity, Cerrado was considered a biodiversity hotspot with around 12,000 plant species (1,500 endemic), 251 species of mammals, 856 avifauna species, 800 fish species, 262 reptile species and 204 amphibian species (Myers et al. 2000; Sawyer 2016).

The large size of Cerrado biome is also reflected in the importance of hydrography for the other biomes in Brazil, such as Amazon. In Portuguese, the Cerrado is popularly known as the "cradle of water" or the "water tank of Brazil", as it drains water to eight out of twelve watersheds in the country and contains six basins (the Amazon basin, the Tocantins basin, the North Atlantic/Northeast, from the São Francisco basin, from the Atlantic East and the Paraná/Paraguay River Basin). Especially noteworthy are the hydrological contributions to the flow of the Parana basin (50%), Tocantins basin (62%) and São Francisco basin (94%). Great potential of the Cerrado water resources is given by surface flows (rivers) and groundwater flows. However, these resources are being devastated since the occupants of this region exhaustively exploit water resources for irrigated agriculture (Scariot 2005).

The occupation of Cerrado occurred in multiple different phases. The first phase occurred with the arrival of the Portuguese in Brazil to search for precious stones and metals in the sixteenth century. Between the eighteenth and nineteenth centuries, the mining and livestock were the most important economic activities encouraging the first formations of urban centers. Nevertheless, the intense migration in the region only occurred in the second phase of the occupation with the construction of Brasilia, as a capital city, and the large investments in the economic plans to develop the region. This second phase began in the 1960s when Juscelino Kubitschek's government created the plan for modernizing the country. First, the states, such as Rio Grande do Sul and Santa Catarina, located in the south of the country were occupied and later the lands of the Midwest. From the 1970s, the government invested in infrastructure construction, such as roads and railways, as part of Cerrado's agricultural development incentive projects, such as the Cerrado Development Program (POLOCENTRO), which had the objective to develop and extend the agriculture in Brazil to supply raw materials to national and international markets. This project supported many farmers with rural credit to have technical assistance and budgets to invest in their own farms. These investments supported research in management of the low fertility and high acidity soils, mainly done by the Brazilian Agricultural Research Corporation (EMBRAPA). These initiatives caused the grain acreage to double, in 1970, 5 million hectares were cultivated with grains and today the area covers more than 10 million hectares. During this time, the population density grew even faster, first with the construction of

Brasilia (the capital) and second with investments from the Brazilian government to develop agricultural in the country (Ganem 2008).

The development and investments in Cerrado over these periods increased the agricultural productivity, diversified local economy, improved road infrastructure, increased the income of the cities and improved the public services. However, until now, the focus in economy is on the export of raw material and is based on monoculture, such as soybean. The cost of this has been that Cerrado has had a large environmental degradation, mainly in the last 50 years, due to the expansion and production of agriculture and livestock. This agricultural use begins with the deforestation of the area. Wood with high commercial value is sold, and the rest of the area is usually burned. Then cattle are placed in this area to settle the soil and finally the soil is prepared, grains are planted and chemical and pesticide fertilizers are used. This process modifies the flora and fauna, increase the occurrence of soil erosion, siltation of rivers, and poisoning of ecosystems (Klink and Machado 2005).

The flat topography, accessibility and the easy management of the soil for agricultural activities has led to the Cerrado becoming one of the most affected biomes in terms of deforestation. From 2008 to 2018, the total deforested area per year in Cerrado (9,922 km²) was higher than in the Amazon (6,346 km²), as can be seen in Figure 1.2.
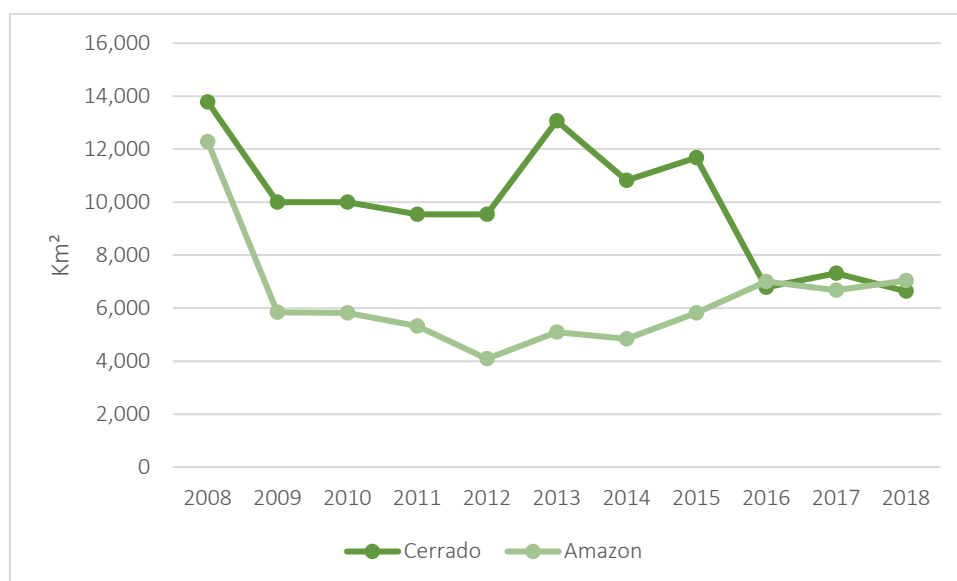
Figure 1.2 Total deforested area per year in Amazon and Cerrado biomes from 2008 to 2018.
Source: (INPE 2011)

Within that period, Brazilian institutes, such as the Instituto Brasileiro do Meio Ambiente e dos Recursos Naturais Renováveis (IBAMA) and National Institute for Space Research (INPE), started to monitor the rate of deforestation in the Cerrado biome. They found that the Cerrado lost around 0.8% of its total vegetation area per year (INPE 2011). The monitoring of the deforestation in the years before

2002 were not as systematic. Nevertheless Machado et al. (2004) analyzed the deforestation rates from 1985 to 1993, and found that the Cerrado lost 1.5% of its total vegetation area annually, approximately 3 million hectares per year. The data presented Machado et al. (2004) do not follow the same methodology of PRODES, which from 2002 was considered the official Brazilian government program to map the deforestation of the Cerrado. However, the results presented by Machado et al. (2004) are still important to have an understanding of the Cerrado deforestation scenario in the years before 2002. Mato Grosso was the state that was most deforested in the last 18 years (Figure 1.3) and remains the largest producer of soybean in Brazil. This region is situated in the transitional zone between Amazon and Cerrado biomes, known as "the arc of deforestation" (AOD).
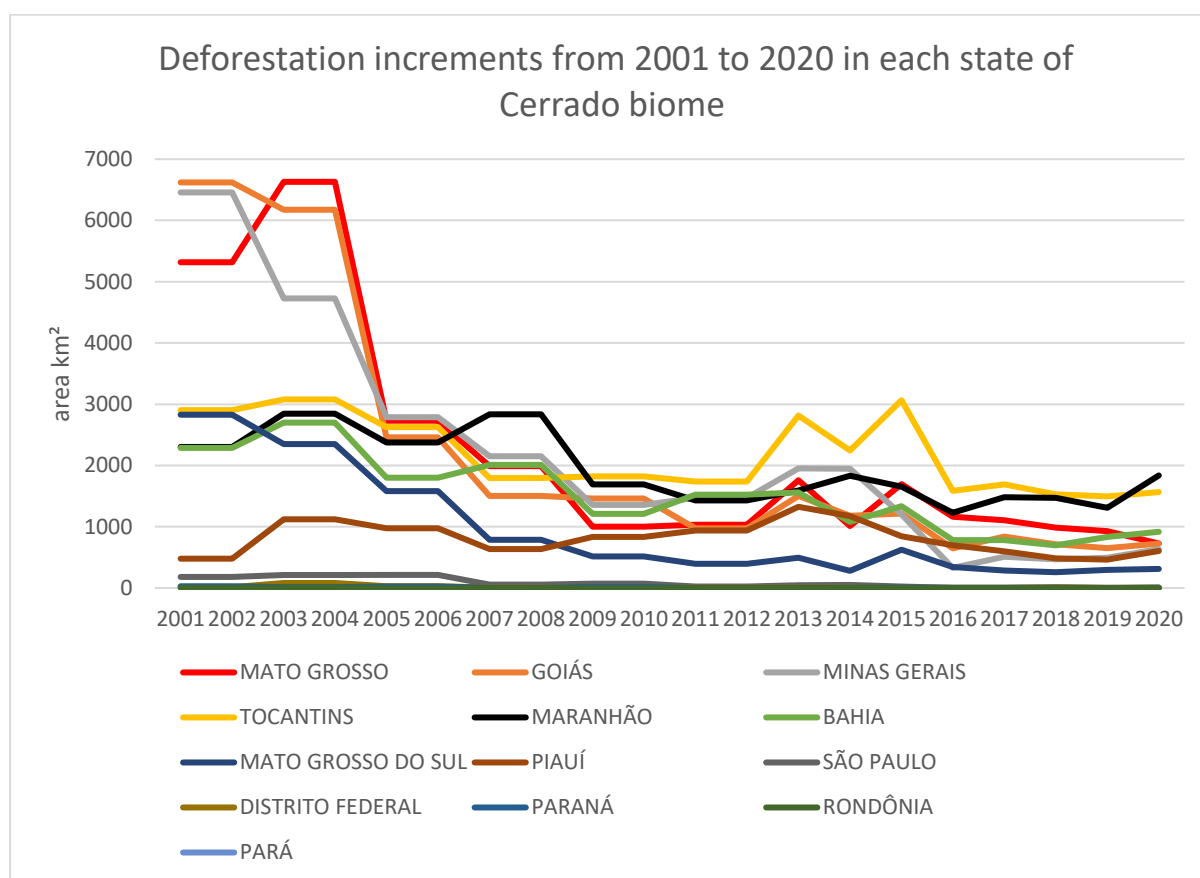
Figure 1.3 Deforestation increments in the states of all Cerrado biome from 2001 to 2020.

Source: (F. G. Assis et al. 2019)

The AOD is located in the frontier states of Mato Grosso, Pará, and Rondônia, and it accounts for 75% of the areas that were deforested between 1996 to 2005 (Macedo et al. 2012; INPE 2011). In these transition areas, the laws that support the protection of forests are weaker and unmanaged. One example is the environmental legislation that defines the amount of natural vegetation that has to be preserved during new deforestation for farmland (80% in the Amazon, 20% in the Cerrado biome) (Soares-Filho et al. 2014). The AOD accounts for 75% of the deforestation in the Legal Brazilian Amazon

and the largest agricultural area in Brazil, mainly soybeans (INPE 2011). Recently, the Brazilian government has established policies to decrease the rates of deforestation in these areas, such as the "Soy Moratorium" (Rudorff et al. 2012), which was an agreement with the major soybean traders not to purchase soybean that was planted in deforested areas after July 2006 in the Brazilian Amazon biome. Policies such as Soy Moratorium decrease the deforestation in Amazon biome, as can be seen in Figure 1.2. Soterroni et al. (2019) estimated if the Soy Moratorium was introduced in the Cerrado, it would prevent the loss of 3.6 million hectares of native vegetation that would otherwise be cleared for soybean production by 2050. The deforestation and expansion of agricultural areas, mainly soybean changed the land use of the Amazon and Cerrado Biome, especially in the last 50 years.

In 2013, MMA (2015) mapped the land use of Cerrado biome and showed that 54% of the Cerrado was covered by native vegetation (111 Mha) and 46% was occupied by anthropogenic uses (93 Mha), such as agriculture (12%) and livestock (30%) (Figure 1.4). The soybean accounts for the largest area of the agricultural use, around 90%. This means that approximately 52% of all soybeans in Brazil is grown in the Cerrado biome. Within the Cerrado, the state of Mato Grosso holds the largest area of soybean (35%). Due to the continual threat of the Cerrado biome, it remains important to monitor the land use change of this area. The field monitoring of Cerrado is a time-consuming challenge, given the large size of the biome. Hence, the use of remote sensing facilitates the monitoring of the status and changes in land cover and land use at large scales.
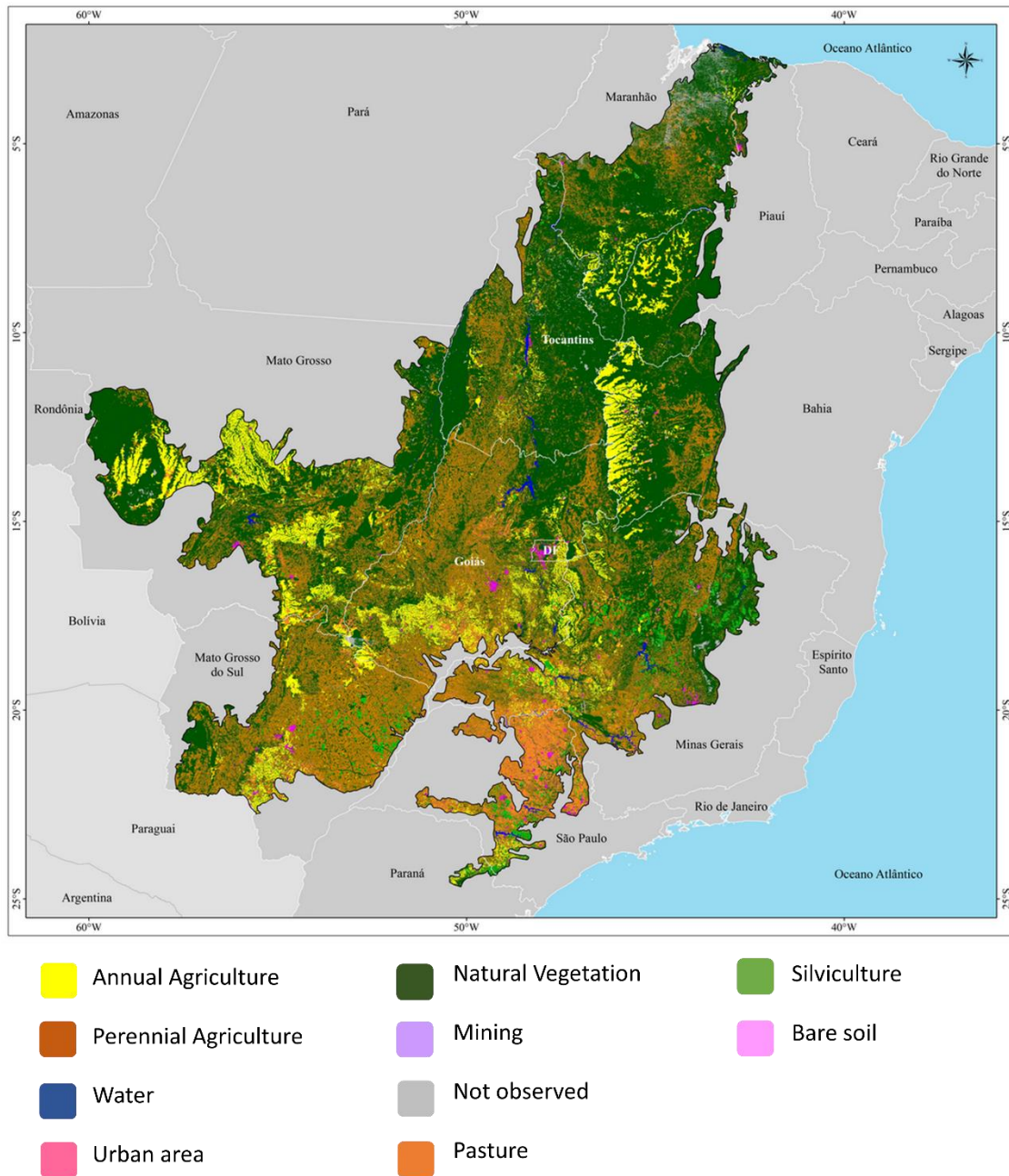
Figure 1.4 Land use map of Cerrado biome in 2013.

Source: (MMA 2015).

1.3   Remote Sensing

Remote sensing is the acquisition of data from a target without direct contact (Colwell 1984). These data can be collected from optical or radar sensors. The optical sensor obtains the data through natural electromagnetic radiation reflected (solar) or emitted from the earth's surface. The radar sensor generates electromagnetic energy, penetrates through cloud cover and registers the backscattering spread back to the sensor (Jensen 2014). Optical sensors have four types of resolution: spatial, spectral,

radiometric and temporal. The spatial resolution is the image quality and its ability to obtain details on the image. The temporal resolution is the time it takes a satellite to image the same area two times. The spectral resolution is related to the number of bands that the sensor and the length of each spectrum. Radiometric resolution is the sensitivity of the sensor to differentiate radiance values or range of numerical values of the digital number associated to the pixels. One of the main advantages of using optical sensors to map and monitor the Savanna biome is the numerous sources of free digital imagery, such as Landsat series (since 1972) and Moderate Resolution Imaging Spectroradiometer (MODIS) (since 1999). Additionally, optical images are more accessible for researchers who have no experience in processing and interpreting these data. However, optical sensors can easily saturate the signal when there is a large biomass, such as in dense forests, especially in the tropical regions. Moreover, optical sensors depend on optimal weather and light conditions to collect the date from the surface. To overcome these disadvantages, radar sensors may be an alternative.

The important advantage that radar sensors have compared to optical sensors is the capability of the radiation to penetrate through cloud cover and a better analysis of the properties of vegetation structure without saturation. These are important when the study area is located in dense forest, such as Tropical Forest or Savanna (Amazon, Cerrado). The depiction of a forest is a sum of factors of different mechanisms of interaction and scattering between sensor, atmosphere and target. The backscattering represents the signal of a microwave scattered from the imaged area and it is a result of the dielectric and geometric propriety of target, the characteristic of the sensor and atmosphere condition. Henderson et al. (1998) mention five main scattering mechanisms in forest environments: i) crown backscattering; ii) direct backscattering trunk; iii) direct backscattering ground; iv) crown-ground backscattering and v) trunk-ground backscattering or double bounce. Le Toan and Kong (1992) described seven scattering mechanisms that further included multiple branch and branch-ground scattering. The influence degree of each scattering mechanism has a strong dependence on wavelength and polarization of the sensor. In the short or intermediate wavelengths such as X and C band, the backscattering represents the radiation interaction of canopy, leaves, branches, secondary branches and part of volumetric scattering (inside crown). Longer wavelengths such as L and P band have the capability of deep penetration and allow for the interaction with the biggest vegetation components such as trunks, crown, ground and branches (Le Toan and Kong 1992). The polarization controls the types of components that interact with the radiation. There are four polarizations system: Vertical transmit and receive (VV), Horizontal transmit and receive (HH), Vertical transmit and Horizontal receive (VH) and Horizontal transmit and Vertical receive (HV). The two first polarization are called co-polarized which interact and reflect with only one orientation. The last two are called cross-polarized, which have a direct relation with volumetric scattering and sensitivity to biomass (Jensen 2014; Sun et

al. 2002). Another component that influences the backscattering is the dielectric constant, which represents the electric conductivity of different materials, such as, vegetation, soil, water and ice. Moreover, the moisture content has an impact on the dielectric constant, therefore, the water content in the leaf plays an important role in the backscattering. The higher the water content, the higher the dielectric constant, and the higher the energy that is reflected (Jensen 2014). Additionally, the radar sensor has important advantages compared with optical sensors in terms of the analysis and extraction of information from the vegetation structure, such as biomass, LAI, volume and basal area. The penetration of the radar sensor into the vegetation with different wavelengths can provide more information about the structure. In overall, the radar system provides many advantages to study tropical forest such as the Cerrado as it can penetrate through cloud cover making the analysis weather independence and it provides low probability of signal saturation in dense forests.

1.4   Remote Sensing for mapping and monitoring Savanna and Cerrado

The mapping and monitoring of the savanna biome are essential to understand the impact of LUCC on global environment, biodiversity, carbon storage, and climate change. Mapping and monitoring vegetation resources at local and global scales using traditional methods (field surveys), is expensive and slow. Remote sensing offers the means for systematic observation and analysis of the surface, which can support important initiatives focus on the impact of the human activity in the context of LUCC on climate change, such as the reduction of emissions from deforestation and forest degradation (REDD+).

In savanna biomes, previous studies mostly focused on land use and forest mapping using optical sensors (Grecchi et al. 2014; Hernandez et al. 1998; Paneque-Galvez et al. 2013; Sabattini 2015; Sano et al. 2008). For example, Anupama et al. (2014) analyzed the land use in the Eastern Gats (India) for the last 200 years using satellite images with medium spatial resolution. They found no significant change in the forest cover in the last 30 years. In Africa, Basommi et al. (2015) and Munyati et al. (2013) mapped the land cover in the East of Ghana and South Africa with Landsat satellite images TM and ETM+. In Australia, Fensham et al. (2011) mapped the forest type and deforestation in the East of the country using high spatial resolution. During the study period from 1952 to 2010, the researchers mapped the three types of forest: mulga, gidgee and miscellaneous and found that they lost 74%, 30% and 82% respectively, of their original area.

The use of SAR has increased over the past decades due to the launching of many SAR sensors such as SIR, ERS, JERS-1, RADARSAT-1, ALOS-PALSAR 2, TerraSAR-X / TanDEM-X and Sentinel 1A. Currently, land use mapping is the most common topic addressed in studies using SAR sensors in savanna biomes.

In Brazil, Evans and Costa (2013) mapped six vegetation habitats using L and C band by the backscattering information from the surface. Additionally, Saatchi et al. (2010) mapped five land cover types in Brazil using the JERS-1 mosaic, using texture measurement. Furthermore, the use of SAR images to assess the biomass and carbon estimation has increased in the last decades. For example, Liu et al. (2015), who used the C band (AMSR-E dual polarization) to estimate the global aboveground biomass (AGB) in a period from 1998 to 2002, finding that 17% of the area belongs to the savanna biome. In the Africa savanna, the studies assessing biomass mostly used L band from ALOS PALSAR quad polarization to estimate the biomass and carbon (Mermoz et al. 2015; Mermoz et al. 2014; Michelakis et al. 2015; Mitchard et al. 2011). While the individual use of optical and SAR sensors to assess the vegetation in savanna remains the most common method, the combination of both sensors for monitoring forest resources has become more used over the last 15 years.

To examine the savanna vegetation, which has one of the largest forest diversity, the combination of different satellite images (optical and SAR) and spatial resolution (low, medium and high) provides substantial improvement in the accuracy (Saatchi et al. 2010). Mapping land use remains the most studied topic using the combination of optical and SAR images. In Brazil, Cremon et al. (2014) used the Landsat TM and ALOS PALSAR images to map the land use and cover. They identified four vegetation classes with an accuracy of 94% using both sensors. In Africa, Haack and Bechdol (2000) evaluated the accuracy of the Landsat TM and SIR-C images in the East of Africa for mapping natural vegetation, scattered agricultural and settlements. Their results showed that both sensors have approximately the same accuracy. Moreover, four geospatial manipulations with the SAR images were tested and the texture applications showed the best classification accuracies. The importance of using different sensors to map the vegetation was shown by Mayaux et al. (2000). They processed data from three satellite systems (AVHRR, ATSR, ERS-1 SAR) to show that each one of them provide better results for different types of targets. AVHRR was most suited to distinguish forest and savanna, ATSR best distinguished secondary forests and ERS-1 was best for gallery-forests, plantations and swamp forests in Central Africa. Moreover, the use of both sensors were applied on biomass estimation, such as Mitchard et al. (2012) who estimated the forest high-biomass and carbon stock (an uncertainly of +/- 25%) using LIDAR, ALOS PALSAR and 96 ground-based plots in Gabon, Africa. One of the main reasons for the uncertainty was the use of a generic allometric equation for an area, which includes a range of different vegetation types.

To date, the mapping and monitoring of Cerrado using optical sensors have been mostly applied on land use change. Sano et al. (2001) used the Landsat series to map the land use change for the Cerrado biome in 1990, 2000 and 2010. In 30 years, Cerrado lost 265,595 km² of its natural vegetation. Moderate-resolution, multi-spectral satellite remote sensing data from 1986 to 2002 were used by

Sano et al. (2005) to assess the land use change in Cerrado. The vegetation areas were converted to agro-pastoral in 31% (3,646 km2) of the study region in western Bahia and 24% (3,011 km2) of the eastern Mato Grosso study region. The use of sar sensors in Cerrado are usually used for mapping land cover and estimate biomass and carbon. For example, Almeida and Shimabukuro (2000) used the L band from JERS-1 to detect cover changes in forest and non-forested in Cerrado biome. Moreover, Santos et al. (1998) used JERS-1 images to show the relation among backscatter and biophysical parameters (biomass values) of forest and savanna formations. The use of both sensors (optical and sar) to assess mapping and monitoring Cerrado can be showed in a limited number of studies. Bitencourt et al. (2007) combined the optical medium spatial resolution images and JERS-1 images to predict vegetation variation in the Cerrado biome. They related the LAI collected in the field campaign with the NDVI from an optical sensor image to obtain the green leaves biomass, which showed a strong relation to each other. For AGB estimation, they used the JERS-1 images, which resulted in a good correlation (R^2=0.8714) and showed better results for Cerradão and cerrado sensu stricto compared to the NDVI of optical images.

1.5   Forest Fragmentation and edge effects

Forest fragmentation is the partitioning of continuous large patches of forest into isolated small patches, which expose the organism in the border of these fragments to a different environmental condition (Laurance et al. 2000, Murcia 1995). In this study we mapped the fragmented forests in the spatial resolution of 20 meters. The process of forest fragmentation exposes a formerly undisturbed forest to an environment with different conditions, which is responsible for the edge effect (Laurance et al. 2000, Murcia 1995).

Edge effect is the result of an abrupt transition between two contrasting habitats, such asforested and non-forested areas. Edge effects can be abiotic (changes in the environmental conditions, such as structure complexity), direct biological (changes in the abundance and distribution of species) and indirect biological (changes in species interaction). Laurance et al. (1997) summarized the edge effects in relation to the distance up to 500 meters and showed the most common edge effects are higher wind intensity, increased edge temperature, low soil moisture, increased tree mortality, reduced biomass, plant germination process, original habitat size reduction, soil erosion, microclimate in the edges and carbon storage capacity (Casenave et al. 1995; Harper et al. 2005; Laurance et al. 1998a; Matlack 1993; Mendonça et al. 2015; Murcia 1995) (Figure 1.5).
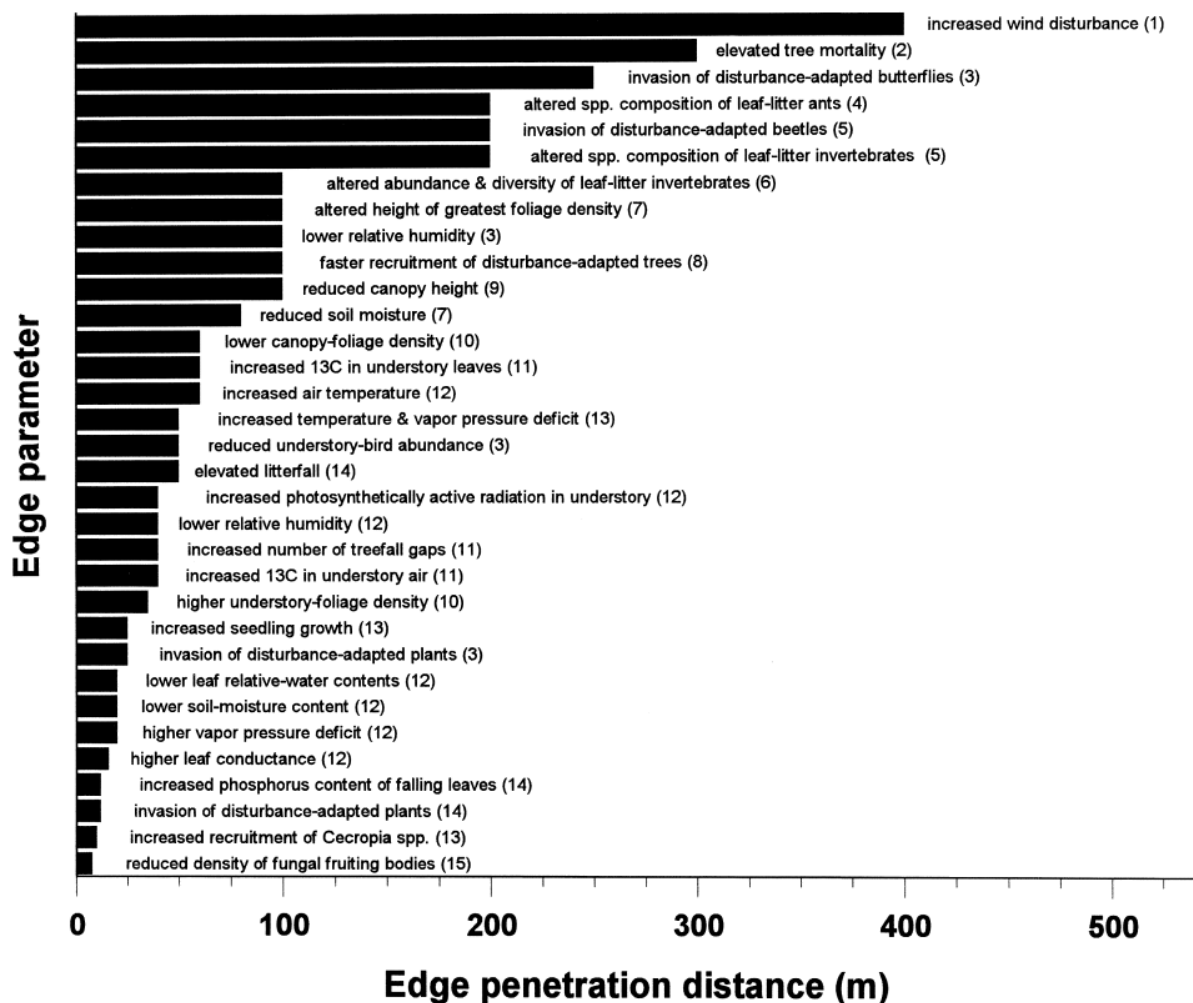
Figure 1.5 Edge effects parameters in relation to the distance up to 500 meters from the border of the fragment (Laurance et al. 1997).

In this study, we mapped the forest fragments in the spatial resolution of 20 meters, therefore an area is considered a forest fragment when there is a distance of 1 pixel (20 meters) between two parallel edges with forest area. We used the edge density (edge to a per unit area), total edge (absolute measure of total edge length) and number of patches (numbers of forest fragments) to support the analysis of this thesis (McGarigal et al. 2002).

To date, there has been no study, which estimated the forest areas that are subject to fragmentation in the entire Cerrado biome. In contrast, the Amazon and Atlantic Forest biomes have been completely analyzed (Pütz et al. 2014). Pütz et al. (2014) found that in the Amazon, the number of fragments are smaller than in the Atlantic forest, 77,038 fragments versus 245,173 fragments, respectively. Additionally, the size of the fragments is greater than in the Atlantic Forest, 8,376 ha versus 64 ha, respectively. The fragmentation patterns caused by deforestation in Amazon can be comparable to the fragmentation of some regions in Cerrado, mainly in our study area, the AOD, where

the border between Cerrado and Amazon biomes lies. The few studies analyzing the fragmentation in parts of Cerrado, found different estimates for the fragment size. For example, Cunha (2007) estimated the size of fragments in Goiás State and found that 82.12% of these fragments were smaller than 1 ha. The authors attribute this to the influence of the forest formation and the high degree of socioeconomic development. In contrast to Cunhan's findings, Jorge and Garcia (1997) found a high frequency of small fragments, around 10 ha, in the region of Sao Paulo.

The studies in the tropical forests in Brazil, which examine edge effects, focus on the impact on biomass and carbon storage. Pütz et al. (2014) analyzed the edge effect in Amazon and Atlantic Forest biomes and found that the Atlantic Forest biome lost about 69 million tons of carbon over a period of 10 years, as a consequence of forest fragmentation. In the Amazon biome, 599 million tons of carbon have been lost during the same period. Chaplin-Kramer et al. (2015) estimated the edge effect in the biomass and carbon in tropical forest across the world and found that a decrease of 25% of carbon within the first 500 meters of the forest edge. Moreover, Brinck et al. (2017) showed that 19% of the tropical forest in the world are within the first 100 meters of a forest fragment. Additionally, the edge effect of these areas caused an additional 19.3 Gt of carbon emissions, representing 31% of the annual carbon releases from the tropical forest. Furthermore, Nascimento and Laurance (2004) assessed the carbon loss in Amazonian forest fragments in a long-term data of 19 years. The results show an increasing of 4 to 5 Mg of carbon emission per hectare within the first 300 meters of forest edges. Laurance et al. (1998c) estimate the carbon emission related to edge effect in parts of Pará and Rondônia States, Brazil. The carbon emission estimations were 0.3 to 42% lower when the edge effect was not considered in the calculation. Moreover, Laurance et al. (1997) analyzed the biomass collapse in central Amazon using permanent plots. The study showed a loss of carbon within de first 100 meters up to 36% in the first 10 to 17 years after fragmentation. The impact on biomass and carbon stock from the edge effect is a consequence of an intensification in land use and cover change (LUCC) in Cerrado during the past decades. Therefore, the biome requires adequate monitoring tools and mechanisms for future sustainable management of these fragile ecosystems.

In Cerrado biome, there is no consensus about the edge effect to date. Regarding the biomass and carbon stock changes by the edge effect, Kulp et al. (2018) did not find any relation between edge effect and biomass in Cerrado located in Mato Grosso State. Additionally, Mendonça et al.; Queiroga (2015; 2001a) did not find differences between the edge distances regarding the species distribution, vegetation structure and microclimate. In contrast, Lima-Ribeiro (2008) showed that microclimate parameters are different in the border and in the interior of the fragments. The soil and air temperature were higher in the border and the humidity was higher in the interior. Additionally, the vegetation structure (V. aurea aggregation index) showed a high edge effect and the height of trees and stem

circumference were higher in the interior. These studies used direct measures within a short temporal analysis, which are limited by the replicability, cost of execution and time consuming. The use of satellite images provides an alternative for analyzing the edge effect in the Cerrado biome. Therefore, more studies are needed to overcome the lack of information on edge effect in Cerrado biome using remote sensing.

1.6   Aim of Thesis

The Cerrado biome plays a critical role in fighting climate change due to the amount of carbon stored. However, in recent decades this biome has been vastly deforested for livestock and agricultural production due to the weak laws of protection compared to Brazilian biomes (Amazon). The vast deforestation has led to fragmentation of the biome and consequently an edge effect, which has been linked to a reduced carbon stock and biodiversity (Laurance et al. 1997, 2006). While edge effects have been extensively studied in the Amazon and Atlantic Forest biomes, mainly effect on biomass, fires susceptibility, biodiversity, only few studies have examined the edge effect in the Cerrado. These studies were performed using only in situ data. However, as the Cerrado covers over 200 million hectares in Brazil, therefore, remote sensing is a useful alternative to map and monitor a large area in the Cerrado biome over a long-time frame.

In this thesis, I examine the edge effect on biomass in a study area within the Cerrado biome using both in situ and remote sensing data. Due to the previously described effect in Amazon and Atlantic Forest biomes, the central hypothesis of this thesis is that we can assess fragmentation which leads to an edge effect on vegetation, such as biomass, using remote sensing data in the endangered Cerrado/Amazon Ecotone of Nova Mutum—Mato Grosso. In order to examine this hypothesis, the aims of this thesis are to:

a) compare and evaluate different combination of optical and SAR satellite systems for the identification of forest fragments and mapping of vegetation types in the study area

b) collect in situ data to assess the vegetation edge effect on biomass and carbon storage

c) use a time-series approach to spatially monitor the fragmentation and edge effects using optical remote sensing data

These aims will allow me to examine the edge effect on vegetation in the study area for a single year (2017) as well as over the time frame (1984-2017) and compare the data to the described effect in the Amazon and Atlantic Forest biomes.

1.7   Outline of the thesis

To achieve the objectives, this thesis is structured in four chapters. In the first chapter, I introduced the concepts of tropical Savanna, Cerrado, remote sensing, fragmentation and edge effect. Moreover, I describe the study area and the general methods. In the second chapter, we identify the forest fragments and classify vegetation types using different types of sensors. This step is important because it helps to understand the edge effect in different types of vegetation, since the edge effect acts differently in each type of vegetation. In the third chapter, we estimate biomass and carbon stock using field data within the context of the edge effect in the different types of vegetation that were identified in the second chapter. In the fourth chapter, we used long-time satellite images series to spatially map and monitor of edge effects and fragmentation. In the fifth chapter, we discuss the general findings of the previous chapter. The thesis concludes with final remarks and recommendations.

1.8   Study Area

The study area is located in the transition area of Cerrado and Amazon biomes in part of Nova Mutum city (Figure 1.6). Nova Mutum is placed in the frontier states of Mato Grosso, Pará, and Rondônia, where the AOD lies.
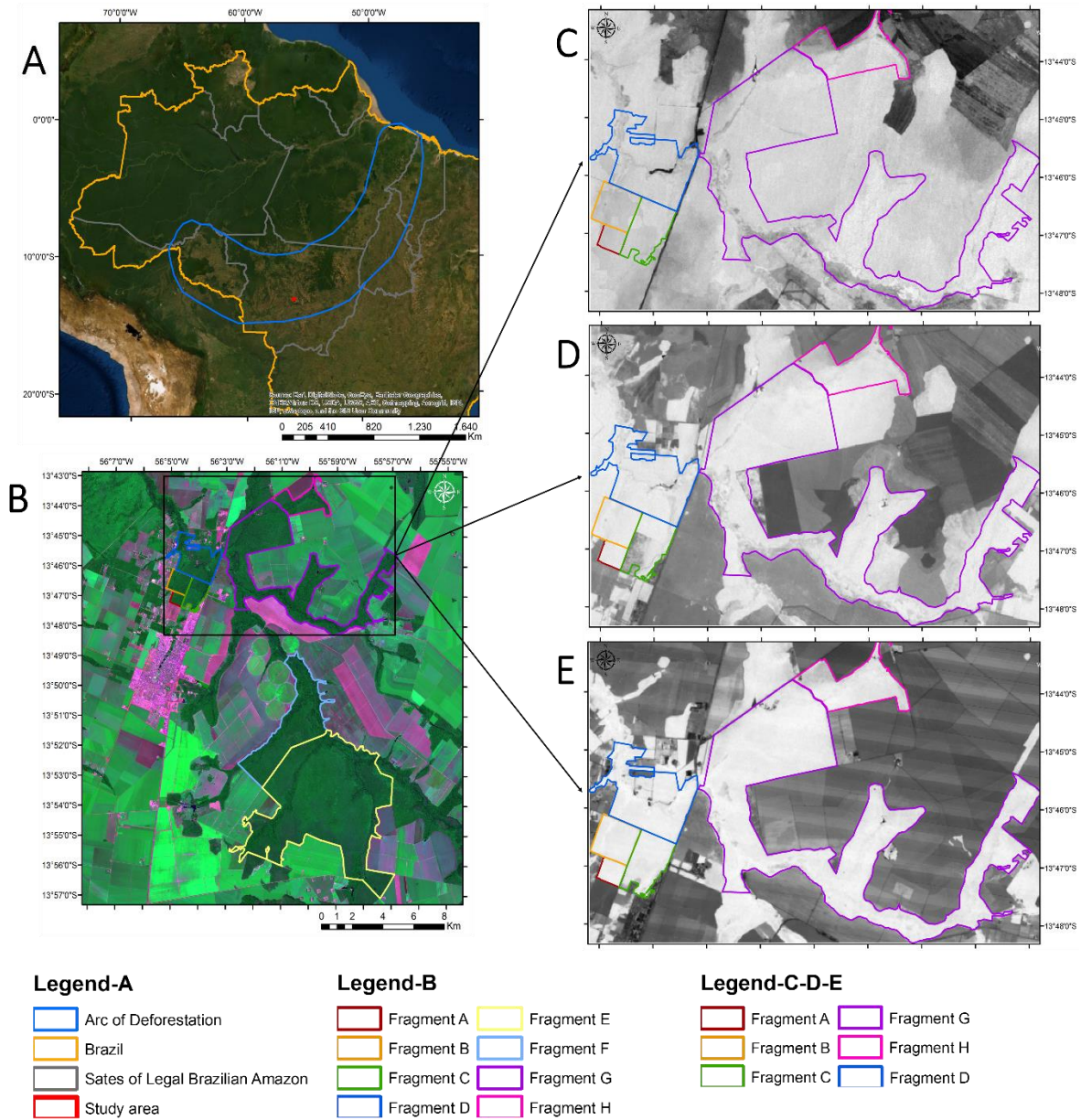
Figure 1.6. Location of the study area in Brazil on top of a Google Earth image (A), in Nova Mutum city and on top of a false color composition of Sentinel 2A Band 3, 4, and 8 in 07 July 2017 (B), in the exact area of analysis from 1985 (C), 1997 (D) and 2017 (E) on top of a NDVI image.

Nova Mutum is an important city in the context of deforestation in the AOD region. Between 2002 and 2010, Nova Mutum was among the 20 cities that most deforested natural vegetation (MMA 2014), which has increased the process of landscape fragmentation (Figure 1.7). Additionally, the city plays an important role in the Brazilian agricultural sector, the city is one of the 20 largest soybean producers in the Brazil. Therefore, Nova Mutum is a key city in relation to the forest fragmentation, which was caused by the strong deforestation process in the last 30 years and the growing importance in the soybean production in Brazil.
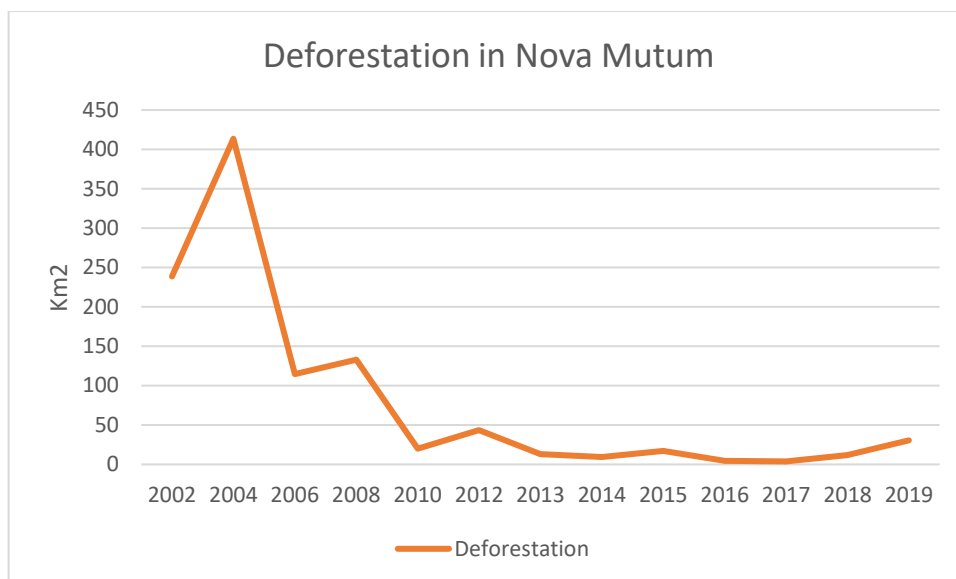
Figure 1.7. Deforestation in Nova Mutum (km2) from 2001 to 2019.

Source: (F. G. Assis et al. 2019)

Nova Mutum, which belongs to the Alto Teles Pires River Basin, has a well defined rainy (October to April) and dry (May to September) season. The climate is classified as Tropical savanna climate (Aw) following the Köppen Climate Classification and the annual temperature and precipitation average are 24 °C and 2200 mm, respectively. This area is dominated by two soils types, Oxisols (80%) and Entisols (20%) and has a flat topography (maximum slope of 3%) (Goedert 1986; IBGE 2001).

In general, the vegetation of the Cerrado consists of three different physiognomic units from dry grasslands to forest formations. The grasslands are characterized by herbaceous plants (principally grasses) with small and thin trees and shrubs. The savanna formations are characterized by a discontinuous herbaceous-shrub and tree canopy. The forest formations consist of arboreal species in a continuous canopy. In our study area, there are four vegetation types, Cerradão (Open Forest), Cerrado denso (Dense Woodland), gallery forest, and secondary forest. Overall, Cerradão has a crown cover between 50 and 90% and the height of the trees varies from 8 to 15 meters. Cerrado denso has a crown cover between 5 to 70% and tree height varies from 5 to 8 meters. The layers of shrubs and herbs are less dense compared to Cerradão. The gallery forest has a crown cover between 70 to 95% and the height of the trees varies from 20 to 30 meters. Secondary forests are formed after clear-cutting and have different structures, depending on the age of the succession (Ferreira 1997). In our study area, the tree height of Cerradão ranges from 4.5 to 21.1 m with an arithmetic mean of 11.1 m and the crown cover ranges between 66.3 to 80.7 %. The wood density and basal area have in average 0.69 g cm^{-3} and 22.1 m^{-2} ha^{-1}, respectively. Cerrado denso has different characteristics compared to the Cerradão, as it is part of savanna formations. The tree height of Cerrado denso ranges from 2.1 to

14.3 m and the crown cover from 61.6 to 72%. The wood density and basal area have in average 0.67 g cm^{-3} and 10.5 m^{-2} ha^{-1}, respectively.

1.9   Materials and Methods

1.9.1   Remote Sensing data

We used a set of images from seven sensors, three SAR and four optical. The SAR sensors were the PALSAR-2 aboard ALOS-2 from the Japan Aerospace Exploration Agency (JAXA); TanDEM-X (TerraSAR-X add-on for Digital Elevation Measurement) from the German Aerospace Center, DLR, and Astrium GmbH and Sentinel 1A from from the European Union's Copernicus programme. The optical were the Sentinel 2A from the European Union's Copernicus programme and Landsat 5, 7 and 8 from NASA and the U.S. Geological Survey (USGS) (Figure 1.8).
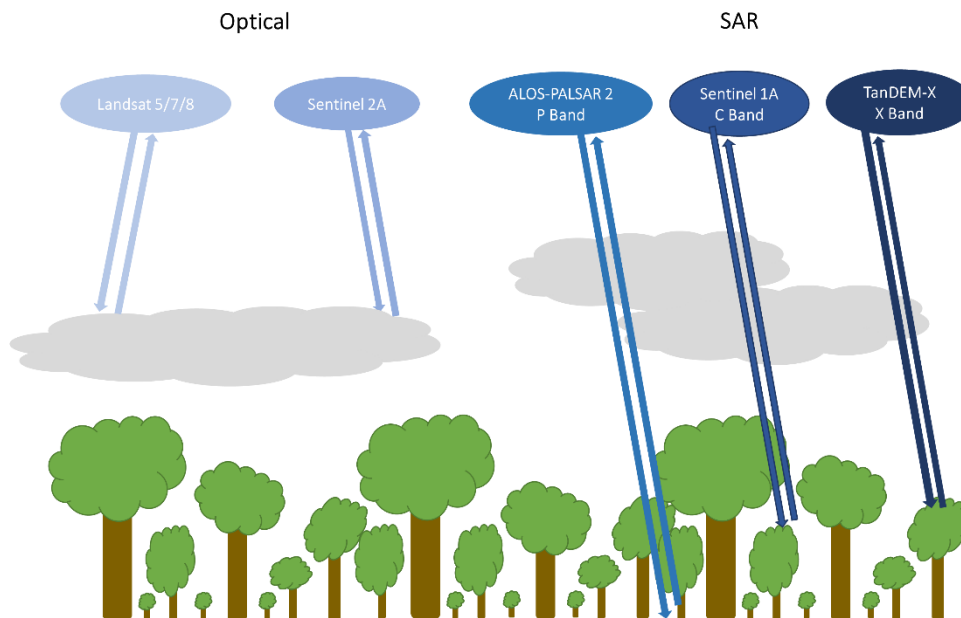
Figure 1.8. Sensors used in this thesis and their respective interaction with the forest.

In the first manuscript, we used seven coverages (using nine Bands altogether, from Band 2 to Band 8A, Band 11, and Band 12) of the Multispectral Instrument (MSI) on-board Sentinel-2A, twenty-three coverages from Sentinel-1A IW Ground Range Detected (GRD) Level-1 product, four coverages of the dual polarization images and one coverage of the full polarization images from ALOS-PALSAR 2 and one coverage from TanDEM-X (Table 1.1). This set of images was used in order to identify the four dominant vegetation types that are prevalent in the Cerrado area (i.e., Cerrado denso, Cerradão, gallery forest, and secondary forest). Therefore, we extracted features from both sources of data such as intensity (Sentinel 1A, TanDEM-X and ALOS-PALSAR 2 dual/full polarimetric), grey level co-occurrence matrix

(Sentinel 1A), coherence (TanDEM-X), and polarimetric decompositions (ALOS-PALSAR 2 full polarimetric) during the dry and rainy season of 2017.

Table 1.1 Characteristics of the selected satellite images.

Sensor	Band	Polarization	Orbit	Features
Sentinel 1A	C	Dual – VH and VV	Descending	Intensity, glcm
TanDEM-X	X	Single – HH	Ascending	Intensity, coherence
ALOS-PALSAR 2 dual	L	Dual – HH and HV	Descending	Intensity
ALOS-PALSAR 2 full	L	Full	Ascending	Intensity, polarimetric decompositions
Sentinel 2A	2 to 8A, 11 and 12			
Landsat 5	3 and 4			
Landsat 7	3 and 4			
Landsat 8	4 and 5			

In the third manuscript, we used 498 images from Landsat 5 Thematic Mapper (TM), 552 images from Landsat 7 Enhanced Thematic Mapper Plus (ETM+) and 144 Landsat 8 Operational Land Imager (OLI) from two different Path/Row (227/069 and 227/070) between March 1984 and September 2018. The images were acquired from TIER 1 collection category, this includes Level-1 Precision, Terrain (L1TP) corrected data and radiometrically calibrated. The Tier 1 is considered the best set of data for time-series analysis (USGS EROS, 2017). The data was available from U.S. Geological Survey (USGS) EROS Science Processing Architecture (ESPA) ordering system. We chose these data to analyze the NDVI time-series in order to create an annual mean value composites from May to September (dry season). The mean value composites processing was necessary to reduce the seasonal variation in the vegetation. By this approach, we obtained 35 annual composites from 1984 to 2018.

1.9.2 Field Data

The sampling was designed in two steps. First, we mapped the vegetation in the study area based on the satellite image of Landsat 8-OLI from (07 July 2017 and separated by types (Cerradão, Cerrado denso, gallery forest and secondary forest). Second, we selected the areas depending on its homogeneity, such as soil type and relief, as well as on a minimum distance of > 100 m of each fragment to rivers. Additionally, the fragments had to be within the first 2 km from a federal or state road due to

the low infrastructure of the region, which often does not allow us to access the forest fragmentation site.

The sampling was executed on four plots along a transect from the edge of each fragment towards its center (Figure 1.9). Therefore, 32 plots were investigated in total. The location of the transect was predominantly defined in the middle of the fragment edge, closest to the next road and – as possible – without further border influences, e.g. by crossroads. The circular plot sampling started at 20 m from the edge of the forest fragment to preserve the characteristic of the vegetation type and still have a significant edge effect at this distance. Additionally, the other three plots were constructed after a horizontal distance of 80 m from center to center of each plot until reach the distance of 260 m towards the center of the fragment. The circular plot had a radius of 12.62 m and an area of approximately 500 m² (Figure 1.9). The distances between the transects as well the size and shape of the plots was recommended by several publications that analyzed the edge effect in the Cerrado and other biomes (Sampaio and Scariot, 2011; Penariol and Madi-Ravazzi, 2013; Benítez-Malvido et al., 2018; Mendonca, 2019).
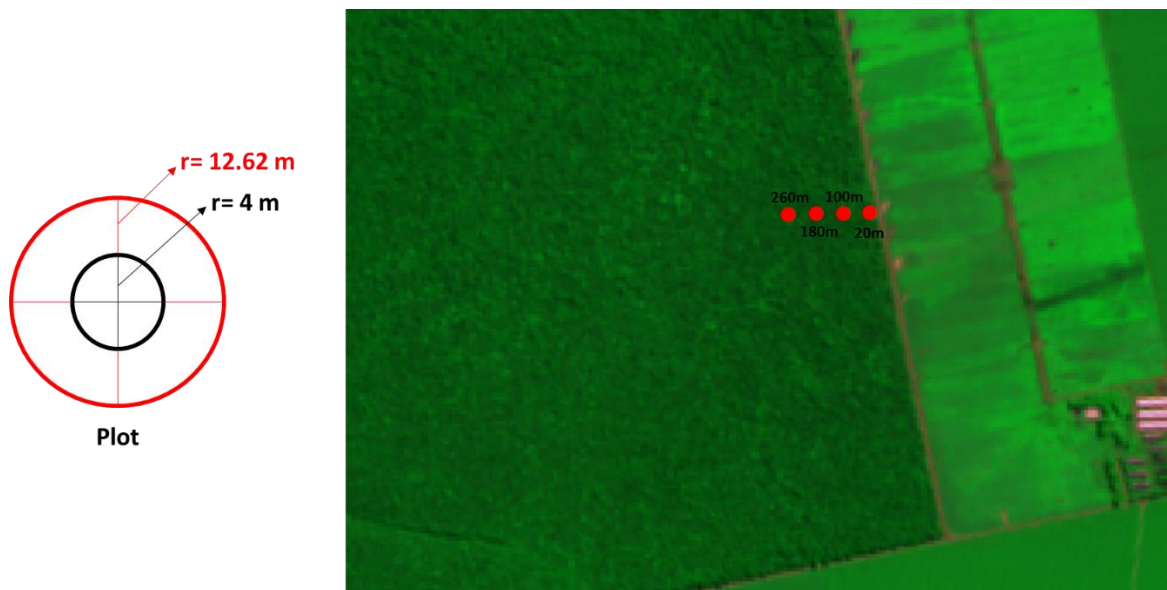
Figure 1.9 Sample design within each fragment (Sentinel 2A 17.07.2017) with the transect (red points) from the edge of the fragment to the center. The red circle represents the shape and size of the circular plot, the black circle represents the shape and size of the circular sub-plot.

The living trees with a DBH1.30 ≥ 10 cm in total height, DBH1.30 and treetop coverage were measured. A Brazilian botanist – specialized in Cerrado/Amazon vegetation – identified each tree species. Each plot was located by recording the coordinates with a GPSMap 60CSx GARMIN hand tool in the plot center and geolocation of the smartphone. Moreover, a 360° photo was taken with a RICOH-THETA S camera. A subplot with a radius of 4 m and a surface area of approximately 50 m² was

established as a part of the center of the plot to include the shrub layer to the field survey, which were measured in DBH0.30 and total height.

1.9.3   Statistical Analysis

In the first manuscript, we used the Random Forests (RF) algorithm implemented in R software for image classification. RF is a supervised classification algorithm that uses multiples decision trees to get an accurate classification and prediction. The N numbers of trees are built by the classifier, contributing each to the assignment of the most frequent class. This algorithm uses the bagging method to produce random samples of training sets for each random decision tree. Every tree uses a random subset from the original set. This original set was created from training samples, where two-thirds were used to train the classifier and one-third of them were used for validation. Two-thirds of the training sample were the out-of-bag (OOB) data and one-third of the training sample were the OOB error estimate (Breiman 2001). Random Forest can be used for classification and regression and is an efficient tool due to measuring the relative importance of each feature. This variable importance measures the decrease of accuracy when a variable is removed from the classification. The higher a variable is ranked, the more it is contributing to the accuracy. Additionally, it has a lower probability to overfit compared to other models if there are enough trees. This method has many improvements: it does not require any input preparation, it is more stable using big data since it works well with variable non-linearity, it provides a pre-feature selection building the trees, and reduces the time required for the process. For remote sensing analysis, RF showed to be a stable and accurate algorithm, especially when it is applied to different types of sensors and large time series. The achievement of this method can be seen in recent studies such as (Baron and Erasmi 2017; Breiman 2001; Bradter et al. 2011), which applied RF for vegetation mapping using different types of data. In this study, the RF models consisted of 1000 trees, and 70% of our samples were used for training the classifier and 30% for validation of the classification results.

In order to analyze the performance of RF we used the confusion matrix. The confusion matrix assesses the accuracy of the classification, showing the relation between classification result and sample site. Column values correspond to the sample site results, rows to the classification results, and diagonal to the correctly classified pixels. The general measurement showed in confusion matrices of q classes is the overall accuracy, which is a result of dividing the total number of pixels and the pixels that were correctly classified. Additionally, the kappa coefficient was largely used to measure the accuracy of the classification. The values of the kappa coefficient range from 0 to 1, where 0 means no relation

between the classification results and the sample site results, and 1 means that both are identical (Congalton 1991).

Finally, for detailed analysis, we calculated both the user's and producer's accuracy. User's accuracy (U_i) is obtained considering the number of the correctly identified pixels of a given class (p_{ii}), divided by the total number of pixels of the class in the classified image ($p_{i.}$).

$$U_i = {p_{ii}}/{p_{i.'}} \qquad (1)$$

On the other hand, producer's accuracy (P_j) is the number of correctly identified pixels (p_{jj}) divided by the total number of pixels in the reference image ($p_{.j}$). A detailed description of the classification assessment can be found in the literature (Congalton 1991; Olofsson et al. 2014).

$$P_j = {p_{jj}}/{p_{.j'}} \qquad (2)$$

In the second manuscript, we statistically evaluate the fieldwork data. Thereby the individual plots of the transect within each fragment were regarded in detail mainly based on boxplots. Besides, the plots were investigated in groups depending on the distance to the fragment border and separated per vegetation type, i.e. all first plots of the Cerradão were analyzed in groups as well as all second plots of the Cerradão were analyzed together. The nonparametric *Kruskal-Wallis* test was used, if there were significant differences within the variable data as well as within the AGB and aboveground carbon stock data from the border of the fragment to the center as well as between the two vegetation types. It was investigated if there were significant differences of the AGB and aboveground carbon stocks between the fragments of one vegetation type to assess whether the fragment size has an impact on the amount of AGB and carbon stocks.

In the third manuscript, in order to analyze the edge effect, we used NDVI mean values and the distance to the nearest edge from each random point created in the six fragments. We used a simple linear regression of the relationship between distance to the nearest edge and NDVI for the thirty-five years, to that we plot the distance to nearest edge in the X-axis and NDVI values in the Y-axis for every year and fragment. Secondly, we calculate a linear regression using the p-value to show how strong and significant theses relations are.

2. Optical and SAR Remote Sensing Synergism for Mapping Vegetation Types in the Endangered Cerrado/Amazon Ecotone of Nova Mutum—Mato Grosso

Abstract

Mapping vegetation types through remote sensing images has proved to be effective, especially in large biomes, such as the Brazilian Cerrado, which plays an important role in the context of management and conservation at the agricultural frontier of the Amazon. We tested several combinations of optical and radar images to identify the four dominant vegetation types that are prevalent in the Cerrado area (i.e., Cerrado denso, Cerradão, gallery forest, and secondary forest). We extracted features from both sources of data such as intensity, grey level co-occurrence matrix, coherence, and polarimetric decompositions using Sentinel 2A, Sentinel 1A, ALOS-PALSAR 2 dual/full polarimetric, and TanDEM-X images during the dry and rainy season of 2017. In order to normalize the analysis of these features, we used principal component analysis and subsequently applied the Random Forest algorithm to evaluate the classification of vegetation types. During the dry season, the overall accuracy ranged from 48 to 83%, and during the dry and rainy seasons it ranged from 41 up to 82%. The classification using Sentinel 2A images during the dry season resulted in the highest overall accuracy and kappa values, followed by the classification that used images from all sensors during the dry and rainy season. Optical images during the dry season were sufficient to map the different types of vegetation in our study area.

2.1   Introduction

The Cerrado biome is considered as being among the most extensive and diverse ecosystems in the Neotropics and is a hotspot in the context of biodiversity (Myers et al. 2000). It is also one of the most threatened ecosystems in South America, with over 40% of the biome converted to agriculture and the remainder highly fragmented (Klink and Machado 2005). Despite the threat to the Brazilian Cerrado, studies on this ecosystem are few and recent.

The Cerrado biome is the second largest complex vegetation present in Brazil and occupies about 200 million hectares, of which the largest territory is in the state of Mato Grosso (IBGE 2004). This large distribution of the Cerrado biome in Brazil covers three main vegetation types: grassland, savannas, and forest formations, which results in indeterminate boundary and a gradient of biomass, height, and tree cover. This large variance in different types of vegetation in the Cerrado is responsible for the high biodiversity in this biome. The three areas of biodiversity in Cerrado, the South–Southeast, Central Plateau, and Northeast areas are mainly separated by the altitude and latitude (Castro 1994). The heterogeneity of the vegetation types is also seen in the microclimate variability and in different types of soils, e.g., mostly latosol, red-yellow latosol, red latosol, quartz-neosols, and argisols (EMBRAPA 1999; Sano et al. 2007a; Walter 2006). In addition, the amount of biomass and carbon storage is differently distributed in the biome, depending on the vegetation type and soil (Fearnside 2005; Fearnside et al. 2009; Felfili 2008). This large biodiversity and floristic heterogeneity in Cerrado was and is decreasing due to deforestation since the 1980s, which can lead to a loss or decrease in ecosystem services (Silva Junior et al. 2018).

Cerrado is the most deforested biome in Brazil due to the high agricultural impact, particularly caused by the world market-oriented production of soy, cotton, and sugarcane. Deforestation is facilitated by its flat topography, easy management of the soil for agricultural activities, and high mechanization (Ramankutty et al. 2002). For pasture and agricultural activities, Cerrado has become a more viable alternative to the Amazon despite its poor soil quality. Despite a lack of consistent deforestation records, a few studies have looked at rates of deforestation in the Cerrado biome. Machado et al. (2004) analyzed the deforestation rates from two different sources. They found that from 1985 to 1993, Cerrado lost 1.5% of its total vegetation area annually. From 1993 to 2002, the rate of deforestation per year decreased to 0.67%. Starting from 2002, several Brazilians institutes, such as the Instituto Brasileiro do Meio Ambiente e dos Recursos Naturais Renováveis (IBAMA) and National Institute for Space Research (INPE), started to monitor the rate of deforestation in the Cerrado biome. From 2002 to 2017, Cerrado lost around 0.8% of its total vegetation area per year. The ease of

deforesting in the Cerrado biome created a hotspot region for deforestation at the boundary with Amazon biomes.

Current regulation and restrictions in ecosystem preservation have driven deforestation and cover changes into the forest–savanna transition zone, as in West Africa (Janssen et al. 2018) and South America (Hirota et al. 2010). Janssen et al. (2018) projected an increase of tree cover losses from 20 to 85% in Ghana. In South America, the transitional zone is known as "arc of the deforestation" (AOD). The AOD is located in the frontier states of Mato Grosso, Pará, and Rondônia, and it accounts for 85% of the areas that were deforested between 1996 to 2005 (Macedo et al. 2012; INPE 2011). In these transition areas, the laws that support the protection of forests are even weaker and unmanaged. One example is the environmental legislation that defines the amount of natural vegetation that has to be preserved (80% in the Amazon, 20% in the Cerrado biome) (Soares-Filho et al. 2014). Additionally, this forest–savanna boundary comprises a mixture of floristic characteristics from both adjacent regions, which increases the complexity in mapping the ecotone between the Amazon and Cerrado. Marques et al. (2019) showed that the official boundary between Cerrado and Amazon conducted by the Brazilian Institute of Geography and Statistics (IBGE) is not accurate, and in some areas, the length of the transition zone was miscalculated by 245.5%. This problem is likely to misinterpret the mapping of land use and consequently decrease the accuracy of vegetation classification. Moreover, the problem of low accuracy in the mapping of the boundary between Cerrado and Amazon affects the calculation of wood density, and therefore biomass estimation as well (Nogueira et al. 2007). To overcome these problems, Brazil needs to improve the monitoring system of deforestation and land use change (LUC), especially for the Cerrado biome.

The field monitoring of Cerrado is a time-consuming challenge, given the large size of the biome. Hence, the use of remote sensing facilitates the monitoring of the status and changes in land cover and land use at large scales. Most studies with remote sensing to monitor the differentiation of the vegetation types in Cerrado use optical sensors, mainly in the savanna and grassland formations where there is low signal saturation. These studies mostly use the Normalized Difference Vegetation Index (NDVI) (Bitencourt et al. 2007; Liesenberg et al. 2007; Nascimento and Sano 2010), Spectral Linear Mixture Model (SLMM) (Ferreira et al. 2007; Girolamo Neto et al. 2017), and phenological profiles (Schwieder et al. 2016). Additionally, Müller et al. (2015) demonstrated the challenges in mapping land use in Cerrado, essentially a result of its high diversity. The study showed a considerable uncertainty in the classification of cropland and pastures areas. The same problem was reported by Sano et al. (2010), whose study reports a spectral similarity between cropland, pasture, and natural savanna vegetation, which can increase the uncertainty when mapping. Moreover, Ministry of the Environment (MMA) (MMA 2015) mapped the land use in the whole Cerrado biome and the study showed that one of the

biggest challenges for this area was to map the different types of vegetation, due to the strong seasonality of natural vegetation. However, the optical sensors can extract the information from the canopy, but arboreal vegetation types have differences in vertical structure and tree cover, so that with optical sensors, uncertainties in the identification of forest savanna vegetation types increase. Additionally, optical images are affected by weather conditions (cloud cover).

Radar sensors have an important advantage compared to optical sensors: the ability of radiation to penetrate through cloud cover and considerable parts of the canopy of trees/forest stands due to the higher wavelengths compared to optical sensors. Thus, the resulting radar signals (amplitude/backscatter and, if available, coherence) provide information that can be used to describe the vertical structure of vegetation stands. This information can be used to better estimate forest structure variables such as canopy cover, tree density, tree height or others, as well as to stratify vegetation (e.g., different types of forest). The longer the wavelength, the deeper radar Bands penetrate dense vegetation, which increases its sensibility to perceive the differences that improve discrimination of vegetation types. Almeida and Shimabukuro (2000) demonstrated that the L Band from the JERS-1 synthetic-aperture radar (SAR) can be used to detect cover changes in forested and non-forested areas in the Cerrado biome. Evans and Costa (2013) also mapped six vegetation habitats in Brazil using L and C Bands using the backscattering information from the surface. In the same country, Saatchi et al. (2010) mapped five land cover types using the JERS-1 mosaic, using texture measurement. Santos et al. (1998), Sano et al. (2001), and Mesquita JR et al. (2001) had satisfactory results using radar images to discriminate the vegetation types in the Cerrado biome, especially with the L Band. The sensitivity of the radar sensor to perceive the differences in vegetation structures makes it useful for mapping different types of forests.

The savanna vegetation has one of the largest forest diversities. In this case, the combination of different satellite images (optical and radar) and spatial resolution (low, medium, and high) may help to improve the quality of satellite based monitoring concepts (Saatchi et al. 2010). However, there is little information about how the synergy of different data can contribute to map forest vegetation types in Cerrado. Yet, the free availability and the development of new optical and radar sensors, such as Sentinel 2A, Sentinel 1A (both free) or ALOS2 and TanDEM-X, are increasing the use of both sensors (radar and optical) for vegetation mapping. Recent studies have shown that the synergy of radar and optical images improved vegetation type discrimination, especially in the Cerrado biome, where the greenness seasonality had a huge influence during the year (Bitencourt et al. 2007; Carvalho et al. 2010; Sano et al. 2005).

The aforementioned studies concentrate on parts of Cerrado where the vegetation cover is mostly homogeneous and that are not located in transitional areas such as the Arc of Deforestation. However,

most of the deforestation and expansion of agricultural and pasture areas are concentrated in this region. Additionally, these regions have a mixture of vegetation type and species from Cerrado and Amazon, which makes the study in this area more complex. The few studies in this area are related to the land use and not the mapping of vegetation type, as in Zaiatz et al. (2018) who evaluated the spatial and temporal dynamics of land use and cover of the Upper Teles Pires River Basin from 1986 to 2014. In order to overcome the lack of studies using both sensors to discriminate vegetation types, the aim of this study is to evaluate the use of optical and radar remote sensing for mapping the different types of vegetation in the transitional area between the Cerrado and Amazon biomes.

2.2 Materials and Methods

2.2.1 Study Sites

The study area was the result of an overlap between the satellite images selected for this study and it is located around the city of Nova Mutum, Mato Grosso, which includes the Cerrado and Amazon biomes. Nova Mutum is located in the north of Mato Grosso, Brazil, and it is part of the Alto Teles Pires River Basin (Figure 2.1). Its climate is classified as Aw (after the Köppen climate classification), with a clear seasonality of rainy season (October to April) and dry season (May to September). The annual average temperature is 24 °C and annual precipitation is approximately 2200 mm (Goedert 1986). The topography is flat with maximum slopes of 3%. The soils in the area are Oxisols (80%) and Entisols (20%) (IBGE 2001).
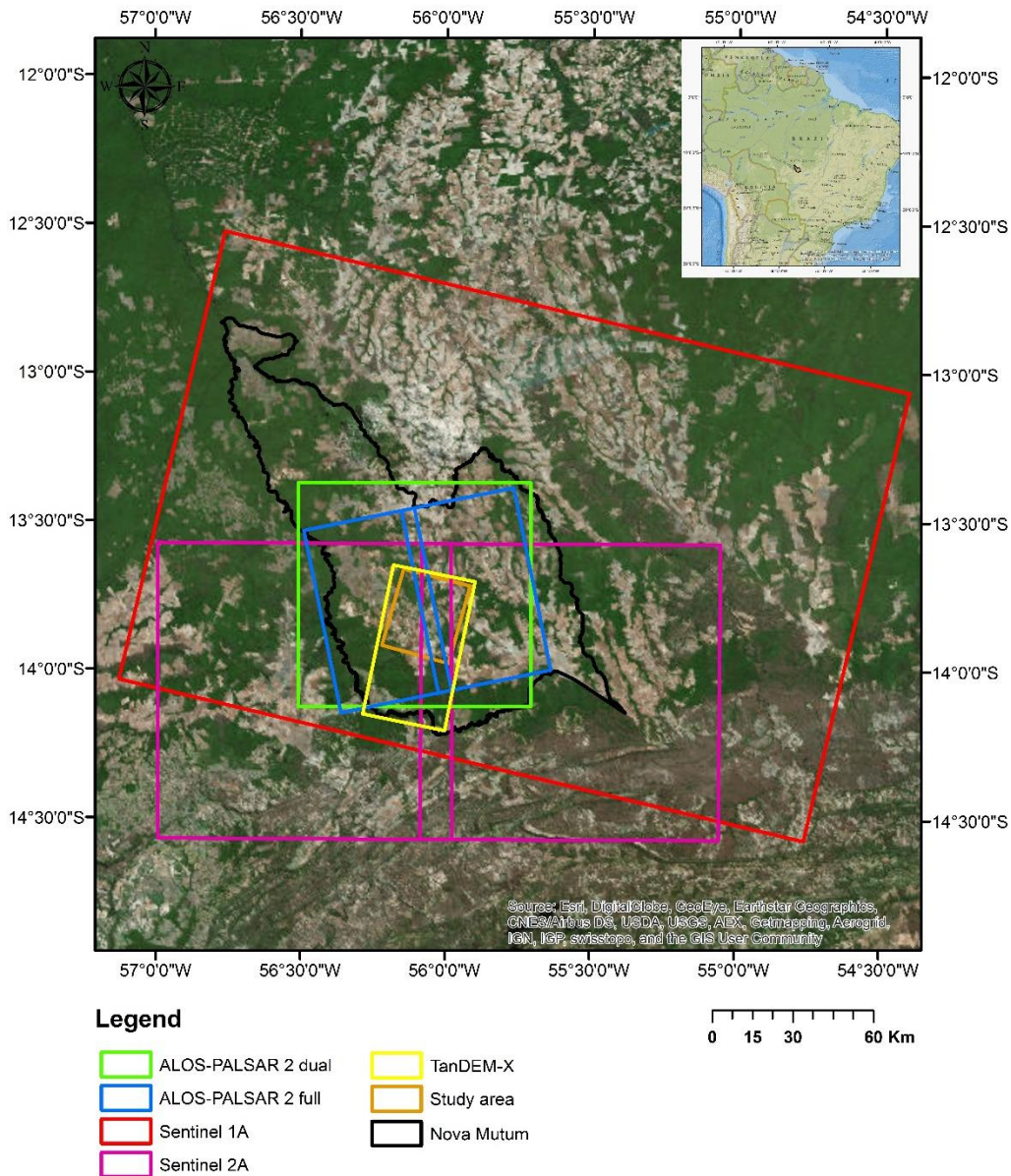
Figure 2.1. Location of the study area within the South America context. The scene footprint of different satellites are shown on top of a Google Earth image.

Nova Mutum is located in the AOD; this area covers 256 municipalities with the most intensive deforestation activities in an area of approximately 1,700,000 km² and it plays an important role in the context of deforestation in the frontier of Amazon and Cerrado. The AOD accounts for 75% of the deforestation in the Brazilian Amazon and the largest agricultural area (INPE 2011). Legislation, soil, relief, climate conditions, and the subsidies offered by the government have encouraged agricultural activity since 1970. Recently, the Brazilian government has established policies to decrease the rates of deforestation in these areas, such as the "Soy Moratorium" (Rudorff et al. 2012), which was an agreement with the major soybean traders not to purchase soybean that was planted in deforested areas after July 2006 in the Brazilian Amazon biome.

In general, the vegetation of Cerrado in Brazil covers three main different vegetation types: grassland, savannas, and forest formations. The forest formations consist of arboreal species in a continuous canopy and include the Gallery, Dry, and Open Forest. The savanna formation is characterized by a discontinuous herbaceous-shrub and tree canopy. The seven types of savanna formation are Dense Woodland, Woodland, Open Woodland, Park Woodland, Palm, Vereda, and Stone Woodland. The grassland formations include three vegetation types: Stone Grassland, Shrub Savanna, and Grassland. The first two types of grasslands are characterized by the large presence of shrubs with different types of soils. Figure 2.2 summarizes the distribution of the three different vegetation formations in the Cerrado biome. Each of these types has a high diversity, which is a consequence of the high variability of the soil and microclimates as well as the floristic evolution with plants from different Brazilian biomes (Walter 2006).
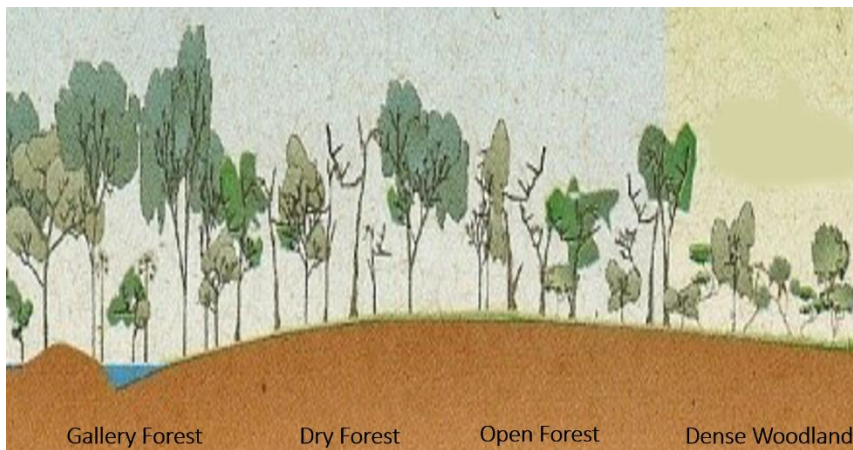
Figure 2.2 Cerrado biome phytophysiognomies. The graphic depicts two vegetation formations and their subdivisions in the study area, except the Dry Forest. Source: Adapted from Ribeiro and Walter (1998).

In our study, we mapped the four dominating vegetation types in Nova Mutum, Cerradão (Open Forest), Cerrado denso (Dense Woodland), gallery forest, and secondary forest. Cerradão and Cerrado denso are located within the transition area of the Amazon and Cerrado biomes. As mentioned before, this area has a high deforestation rate, which can explain the presence of secondary forest. Cerradão has a crown cover between 50 and 90% and the height of the trees varies from 8 to 15 meters. In general, the soils of Cerradão are well drained, deep, and have medium–low fertility. Cerrado denso has a crown cover between 5 to 70% and tree height varies from 5 to 8 meters. The layers of shrubs and herbs are less dense compared to Cerradão. In general, the soils of Cerrado denso have medium to very clayey texture and are middle-well drained. The gallery forest has a crown cover between 70 to 95% and the height of the trees varies from 20 to 30 meters. Secondary forests are formed after clear-cutting and have different structures, depending on the age of the succession. At the beginning of its succession time, these secondary forests are poor in biodiversity and have a simple structure, whereas

in the next succession time, its structure depends on environmental factors such as soil, climate, and management (Ferreira 1997).

2.2.2   Satellite Data

In order to analyze the use of optical and radar sensors to map the vegetation type in Cerrado, we used a set of images from four sensors (3 SARs and 1 optical). The PALSAR-2 aboard ALOS-2 from the Japan Aerospace Exploration Agency (JAXA); TanDEM-X (TerraSAR-X add-on for Digital Elevation Measurement) from the German Aerospace Center, DLR, and Astrium GmbH; Sentinel 1A and the optical Sentinel 2A from the European Union's Copernicus programme. Figure 2.3 shows the temporal coverage of each satellite image used in our analysis.
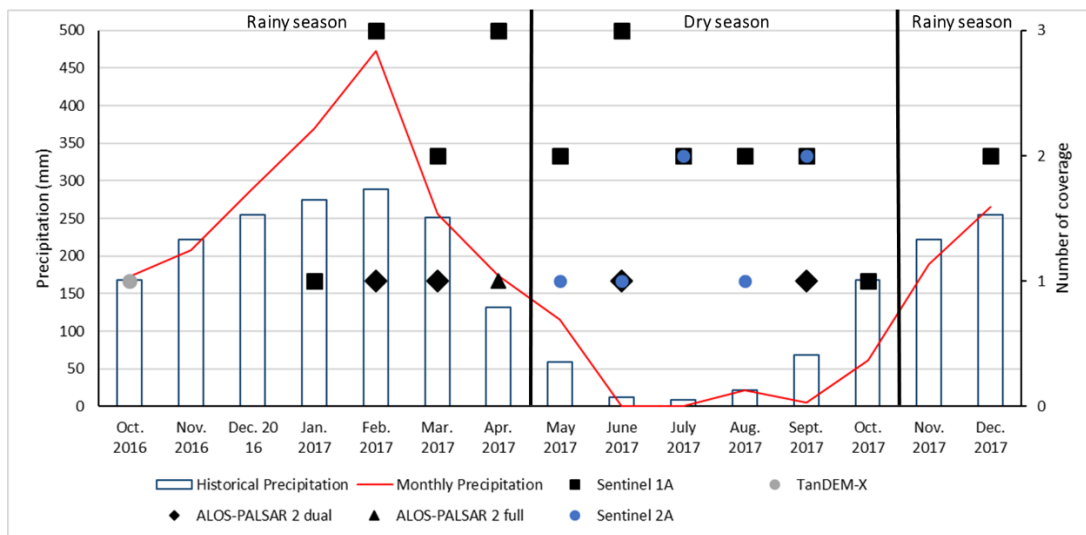
Figure 2.3 Historical (1961–2017) and Monthly (2016–2017) precipitation values and acquisition dates of Sentinel 2A, ALOS PALSAR 2 full, ALOS PALSAR 2 dual, TanDEM-X and Sentinel 1A. Precipitation data were collected from the Diamatino fluviometric station located near to the study area.

We selected the satellite image data following some criteria. First, we selected images from 2017 since the field data were collected in 2017, except for the TanDEM-X image. Secondly, we selected the radar images on the dates of low precipitation, prior to the date of acquisition. Table 2.1 shows the date, polarization, orbit, and accumulated precipitation values three days before the acquisitions.

Table 2.1. Characteristics of the selected satellite images and the accumulated precipitation values three days before Radar acquisition.

Sensor	Date	Polarization	Orbit	Accumulated Precipitation Values 3 Days Before Radar Acquisition (mm)
Sentinel 1A	08.01.2017 01.02.2017	Dual—VH and VV	Descending	3.3 11.5

	13.02.2017			58.3
	25.02.2017			30.2
	09.03.2017			27.2
	21.03.2017			24.0
	02.04.2017			16.8
	14.04.2017			0
	26.04.2017			33.3
	08.05.2017			0
	20.05.2017			0
	01.06.2017			0
	13.06.2017			0
	25.06.2017			0
	19.07.2017			0
	31.07.2017			0
	12.08.2017			0
	24.08.2017			0
	05.09.2017			0
	17.09.2017			0
	11.10.2017			0
	10.12.2017			88.7
	22.12.2017			0
TanDEM-X	20.10.2016	Single – HH		8.1
	01.02.2017		Ascending	11.5
ALOS-PALSAR 2 dual	26.03.2017	Dual – HH and HV	Descending	35.7
	04.06.2017			0
	13.09.2017		Ascending	0
ALOS-PALSAR 2 full	13.04.2017	Full	Ascending	0
	27.04.2017			0
	07.05.2017			0
	16.06.2017			0
	06.07.2017			0
Sentinel 2A	26.07.2017	-	-	0
	15.08.2017			19.2
	04.09.2017			0
	24.09.2017			0

2.2.3 Data Processing

Sentinel 2A

Seven coverages (using nine Bands altogether, from Band 2 to Band 8A, Band 11, and Band 12) of the Multispectral Instrument (MSI) on-board Sentinel-2A were processed using the ESA's Sentinel-2 toolbox in the ESA Sentinel Application Platform (SNAP). First, we applied atmospheric correction using Sen2cor, which is a L2A-processor for Sentinel-2 data that creates Bottom-Of-Atmosphere (BOA) reflectance images using Top-Of-Atmosphere (TOA) data (Louis et al. 2016). Secondly, we resampled all the bands to a 10-m spatial resolution based on the geolocations obtained from Level-1C metadata. For the last step, we created a subset of our study area to speed up processing time, and lastly we mosaicked the images, as our study area was between two different orbits of the Sentinel 2A.

During the final step, we reduced the number of features by applying principal component analysis (PCA) on the spectral dataset due to the fact that some classification algorithms, such as Random Forest, cannot work well with high correlation data. Principal component analysis is a mathematical procedure that reduces a large amount of variables into principal components. The primary function of the PCA is to determine the extent of the correlation between multispectral bands and to remove it through an appropriate mathematical transformation (Sabins 1999). We used the first principal component (PC1) of each one of the ten bands to aggregate only information that was essential to the classification process, as it explained most of the variance, e.g., PC1 of Band 2, PC1 of Band 3, and PC1 of Band 4. Overall, this resulted in a set of ten variables as input for classification for the dry season, and the dry and rainy season, respectively.

Sentinel 1A

Twenty-three coverages from Sentinel-1A IW Ground Range Detected (GRD) Level-1 product were processed using the ESA Sentinel Application Platform toolbox. First, each image was radiometrically calibrated to radar brightness values (β^0) (Rosich and Meadows 2004). Secondly, we applied the terrain flattening to correct any terrain variations in the images. Terrain flattering is an important step for the mapping of land use. Without the terrain flattening, an additional error into the coherency and covariance measurement could be created, due to the difference in the terrain and subsequently the brightness of the radar return (Small 2011). During the third step, we coregistered the 23 images based on the cross-correlation technique to guarantee that every pixel was correctly located in the same target of all images (Yague-Martinez et al. 2017). Once we had the images from the co-registration process, we separated them into two sub-processes. During the first process, we applied the grey level co-occurrence matrix (GLCM) to extract second order statistical textures features. The GLCMs were extracted separately from every single date and polarization (VV and VH). These textures can be useful

to improve land use classification in that it extracts intensity variations from the image involving the information of the neighbor pixels to identify specific clusters or objects (Haralick et al. 1973). Additionally, we applied the Refined Lee speckle filter (window size 5 × 5), after GLCMs extraction. This process is necessary to reduce the noise caused by random constructive and destructive interference from the radar signal (Lee and Pottier 2009). For the second branch of processing, we only applied the Refined Lee speckle filter on the backscatter images. We applied the Range Doppler terrain correction in the last step. This process is necessary to geocode and correct the distortions in the image, which are caused by the topographical variations and the tilt of the sensor (Schreier 1993). The entire process is illustrated in Figure 2.4.
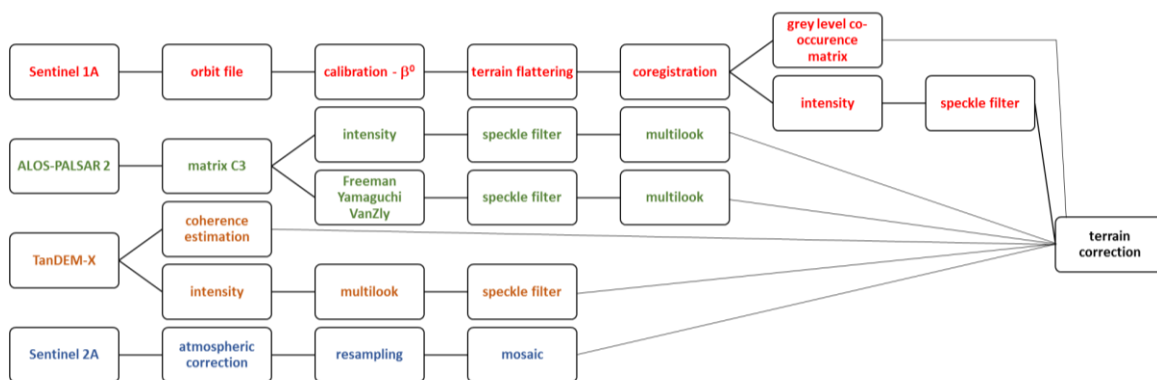
Figure 2.4. Flowchart of the proposal methodology.

We applied the PCA to reduce the number of features in the same way as explained above for Sentinel 2A. In the backscattering images, we applied the PCA for the two different seasons and two polarizations, which resulted in four PCs: a) images of VV polarization in the rain and dry season; b) images of VH polarization in the rain and dry season; c) images of VV polarization during the dry season; and d) images of VH polarization during the dry season. The same was applied for the texture images (ten textures: ASM, contrast, correlation, dissimilarity, energy, entropy, homogeneity, MAX, mean, variance. This resulted in a set of twenty two inputs in the dry season (one PC of VV, one PC of VH, ten PCs of VV textures, and ten PCs of VH textures) and a set of fourth four inputs in the rainy and dry season (one PC of VV in the dry season; one PC of VV in the rainy and dry season; one PC of VH in the dry season; one PC of VH in the rainy and dry season; ten PCs of VV textures in the dry season; ten PCs of VV in the rainy and dry season; ten PCs of VH textures in the dry season; ten PCs of VH in the rainy and dry season).

ALOS-PALSAR 2 (Dual and Full Polarimetric)

Four coverages of the dual polarization images were converted to covariance matrix C2 and one coverage of the full polarization images was converted to C3 matrix (Pottier et al. 2007). In this step,

34

multilook with 4 looks in azimuth and 1 in range was applied to convert the image from single look complex to ground range detected. We applied the speckle filter on all images to reduce speckle noise. For that we used the Refined Lee adaptive filter (5 × 5 window), which is more efficient and whose results have less destructive averaging, having been largely used in the radar studies (Lee and Pottier 2009; Schreier 1993; Pottier et al. 2007; Pereira et al. 2018). Here, we separated the images into two subprocesses. For the first, we kept the backscattering images. For the second, we calculated polarimetric decompositions. Polarimetric SAR decomposition is a useful method to map and discriminate the different targets on the surface, especially due to the signal of the target, which is a combination of speckle noise and random vector scattering effects (Cloude and Pottier 1996). In our study, we chose the Freeman–Durden, Yamaguchi, and VanZyl polarimetric decompositions. In general, these three decompositions are based on the covariance matrix that is divided into three scattering mechanism: volume, double bounce and surface scatter (Cloude and Pottier 1996). Additionally, polarimetric compositions have been used before in mapping of vegetation showing the improvement in the vegetation classification in the Amazon and Cerrado (Furtado et al. 2016). We applied the Range Doppler terrain correction in all images.

Following the same process of the other images, we applied the PCA to reduce the number of features and consequently facilitated the further classification process. This resulted in a set of ten PCs, resulting in four of the dual polarimetric, PC1 of backscattering in each polarization (HH and VH) and each orbit (ascending and descending) and six of the full polarimetric: PC1 of backscattering in each polarization (HH, VV and VH) and PC1 of each scattering mechanism (volume, double bounce and surface scatter).

TanDEM-X

The TanDEM-X mission operates two X-Band satellites flying in close formation in order to acquire single-pass interferometric SAR data. The primary mission goal of the TanDEM-X mission was the generation of a global digital elevation model (Krieger et al. 2007). All TanDEM-X acquisitions are available to the science community on request in Coregistered Single look Slant range Complex (CoSSC) format. For the study area, we acquired one TAnDEM-X scene in standard (bistatic) mode with horizontal polarization (HH). The processed data was separated into two different parts. In the first part, we estimated the magnitude of coherence. Coherence describes the degree of correlation between the two complex radar images (Bamler and Hartl 1998). It is a measure of quality of the phase measurement in interferometric SAR analysis and also used as a proxy for soil and vegetation structural parameters.

In the second part, we processed the intensity images. We performed multilook in both images (coherence and intensity) from the first and second part, with 4 looks in azimuth and 3 in range to reduce the noise. Additionally, we applied, as with the other images before, the speckle filter Refined Lee (window 5 × 5). For the last step, we applied the Range Doppler terrain correction. All images were processed to have a final product with spatial resolution of 10 meters. The PCA was not applied for TanDEM-X due to the use of only one single date.

2.2.4 Classification

The process of image classification was separated into two steps. First, a forest mask was generated as a result of a forest/non-forest classification. At the second step, we classified the forest type within this forest mask. The area under investigation is covered by all images used in this study.

We used the RF algorithm implemented in R software for image classification. Random Forests is a supervised classification algorithm that uses multiples decision trees to get an accurate classification and prediction. The N numbers of trees are being built by the classifier, contributing each to the assignment of the most frequent class. This algorithm uses the bagging method to produce random samples of training sets for each random decision tree. Every tree uses a random subset from the original set. This original set was created from training samples, where two-thirds were used to train the classifier and one-third of them were used for validation. Two-thirds of the training sample were the out-of-bag (OOB) data and one-third of the training sample were the OOB error estimate (Breiman 2001). Random Forest can be used for classification and regression and is an efficient tool due to measuring the relative importance of each feature. This variable importance measures the decrease of accuracy when a variable is removed from the classification. The higher a variable is ranked, the more it is contributing to the accuracy. Additionally, it has a lower probability to overfit compared to other models if there are enough trees. This method has many improvements: it does not require any input preparation, it is more stable using big data since it works well with variable non-linearity, it provides a pre-feature selection building the trees, and reduces the time required for the process. For remote sensing analysis, RF showed to be a stable and accurate algorithm, especially when it is applied to different types of sensors and large time series. The achievement of this method can be seen in recent studies such as Breiman; Bradter et al.; Baron and Erasmi (2001; 2011; 2017), which applied RF for vegetation mapping using different types of data. In this study, the RF models consisted of 1000 trees, and 70% of our samples were used for training the classifier and 30% for validation of the classification results.

Forest and Non-Forest

In order to classify the several vegetation types, we first needed to create a map of forest and non-forest areas. For accuracy assessment, we created 100 random points of 3.13 ha each and visually classified them using high-resolution imagery from Google Earth and the sensor Sentinel 2A (Figure 2.5). During the classification process, we used 70% of these points for training the classifier and 30% for validation of the classification results.
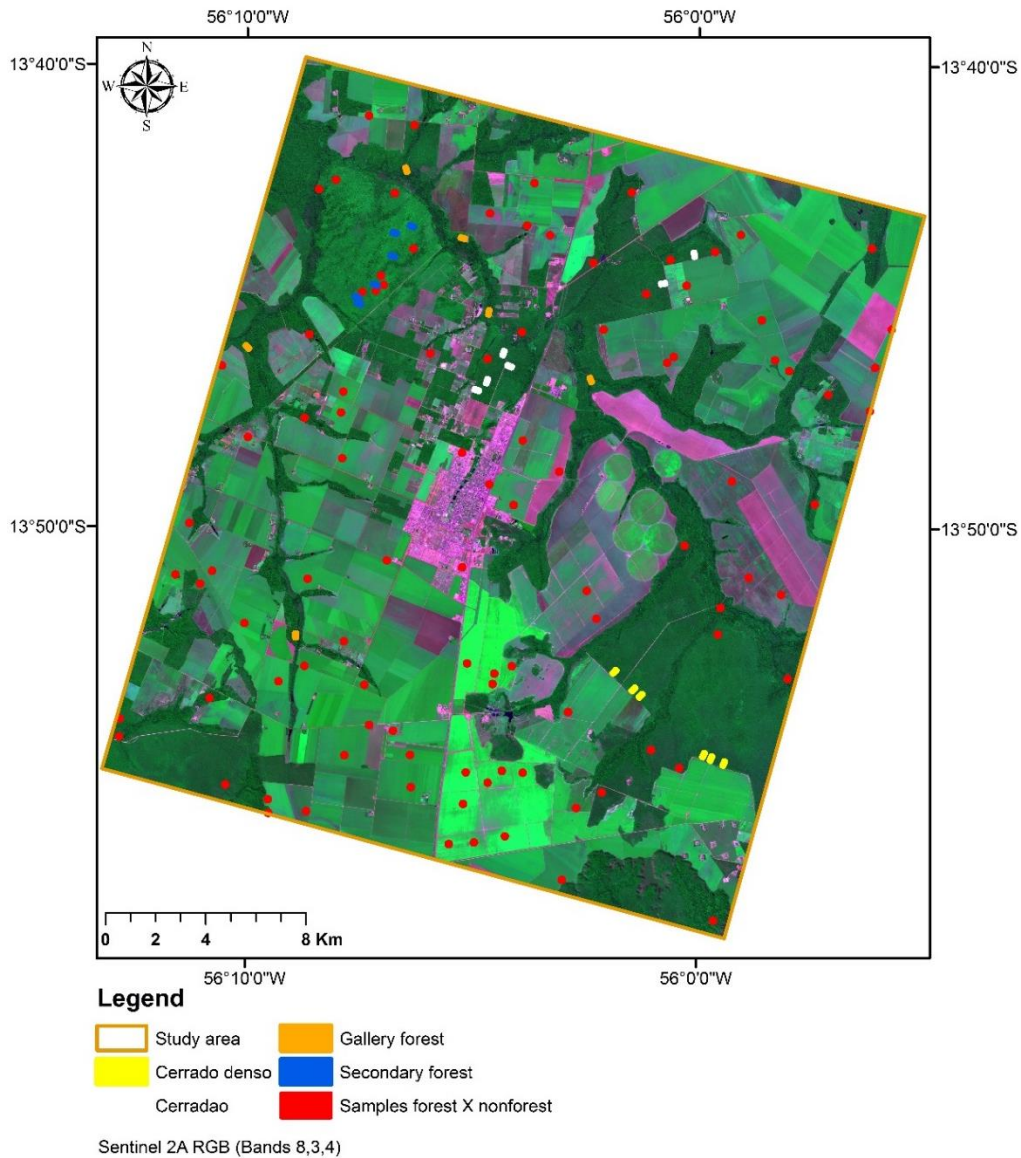
Figure 2.5. Distribution of Random Forest and non-forest samples and forest type samples (4 classes) in the study area, on top of a false color composition of Sentinel 2A Band 3, 4, and 8 (07 July 2017).

Forest Type

Forest-type mapping was only conducted in the areas masked as forests in the previous step. We created 24 reference areas equally distributed into four different vegetation classes (Cerradão, Cerrado denso, gallery, and secondary forest). Each one had an area of 14.265 ha (Figure 5). The polygons were classified based on field data collection (July 2017) and high-resolution imagery from Google Earth and

Sentinel 2A (26 July 2017). During the classification process using RF, we used 70% of the pixels in the 24 references areas for training and 30% for validation.

To analyze the synergy of optical and radar data for mapping Cerrado vegetation types, all possible combinations between optical and radar sensors were tested in two different scenarios, dry season, dry and rainy seasons (Table 2.2). In addition, we used the sensors separately and analyzed the SAR classifications. In total, 23 datasets were processed.

Table 2.2. Classification scheme (number in brackets shows the number of variables per input data).

Dry Season (SAR and Optical)	Rainy+dry seasons (SAR and Optical)	Dry Season (SAR)	Rainy+dry seasons (SAR)
Sentinel 2A (10)	Sentinel 1A (44)	Sentinel 1A+TanDEM-X	Sentinel 1A+TanDEM-X
Sentinel 1A (22)	ALOS2full (6)	Sentinel 1A+ALOS2dual	Sentinel 1A+ALOS2dual
TanDEM-X (3)	Sentinel 2A+Sentinel 1A	Sentinel 1A+ALOS2 full	Sentinel 1A+ALOS2 full
ALOS2dual (4)	Sentinel 2A+ALOS2full	TanDEM-X+ALOS2 full	TanDEM-X+ALOS2 full
Sentinel 2A+Sentinel 1A	All images	ALOS2 dual+ALOS2 full	ALOS2 dual+ALOS2 full
Sentinel 2A+TanDEM-X			
Sentinel 2A+ALOS2dual			
All images			

For the classifications, which combined two or more sensors, e.g., Sentinel 2A and ALOS-PALSAR 2, we did not use all the features of each sensor. In this case, we selected the first three features based on variable importance, which was calculated during RF classification for the single sensor dataset, respectively. Variable importance shows the interaction between the variables/features and inserts them into a hierarchy within a level of contribution and importance for the classification.

For both classifications, forest/non-forest and vegetation type, we used the confusion matrix to analyze the performance of Random Forest classifications. The confusion matrix assesses the accuracy of the classification, showing the relation between classification result and sample site. Column values correspond to the sample site results, rows to the classification results, and diagonal to the correctly classified pixels. The general measurement showed in confusion matrices of q classes is the overall accuracy, which is a result of dividing the total number of pixels and the pixels that were correctly classified. Additionally, the kappa coefficient was largely used to measure the accuracy of the classification. The values of the kappa coefficient range from 0 to 1, where 0 means no relation between the classification results and the sample site results, and 1 means that both are identical (Congalton 1991).

Finally, for detailed analysis, we calculated both the user's and producer's accuracy. User's accuracy (U_i) is obtained considering the number of the correctly identified pixels of a given class (p_{ii}), divided by the total number of pixels of the class in the classified image ($p_{i.}$).

$$U_i = {p_{ii}}/{p_{i.}}, \qquad (1)$$

On the other hand, producer's accuracy (P_j) is the number of correctly identified pixels (p_{jj}) divided by the total number of pixels in the reference image ($p_{.j}$). A detailed description of the classification assessment can be found in the literature (Congalton 1991; Olofsson et al. 2014).

$$P_j = {p_{jj}}/{p_{.j}}, \qquad (2)$$

2.3 Results

2.3.1 Forest and Non-Forest

The two different combinations used for classifications, Sentinel 2A with ALOS-PALSAR2 dual polarimetric and Sentinel 2A with ALOS-PALSAR2 full polarimetric, showed similar high overall accuracy of 0.99 and 1, respectively. The variable importance showed similar results. In both cases, the PC1 of Band 11 and Band 5 of the Sentinel 2A images had the highest contribution for the Random Forest classifier.
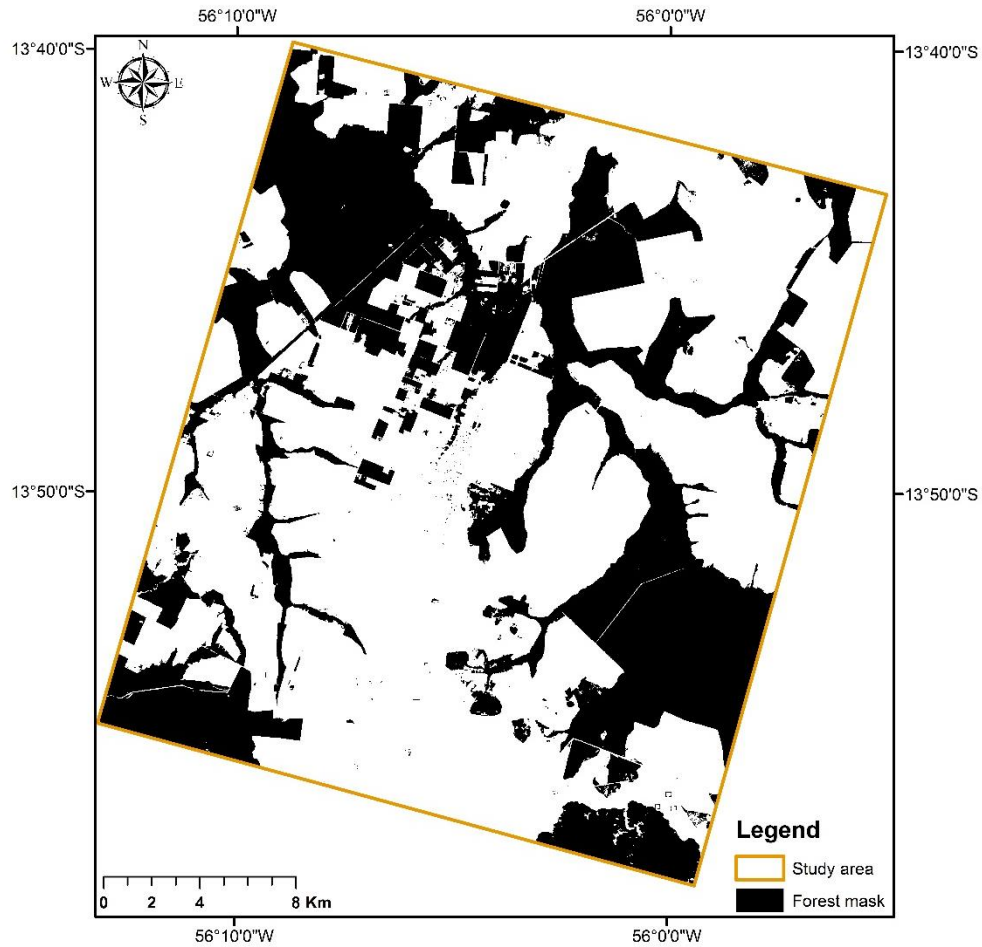
Figure 2.6. Forest mask extracted from the classification of Sentinel 2A with ALOS-PALSAR full polarimetric PC1 images.

Based on this result, we created a mask of forest and non-forest areas, where 34% was forest and 66% was non-forest. (Figure 2.6). This mask was used in the next step for the forest type classification.

2.3.2   Forest Type

Dry Season

The Table 2.3 shows the overall average accuracy (OAA), Kappa, confidence interval (CI) values, and variable importance of the classifications during the dry season.

Table 2.3. Overall accuracy, kappa, confidence interval 95%, overall average accuracy (OAA), and the three most important variables for the classifications based on the Random Forest variable importance for Sentinel 2A (S2), ALOS PALSAR 2 full (A2f), ALOS PALSAR 2 dual (A2d), TanDEM X (TX), and Sentinel 1A (S1). The parameters listed in the variable importance are the PC1 derived from the PCA, except for the images from TanDEM-X, as only one acquisition was available. Only data acquisitions during the dry season were considered.

Dry Season (SAR and Optical)	Overall Accuracy	Kappa	Conf. 95% OAA	Variable

Sentinel 2A	82.60%	0.77	2.29	Bands 11, 12, 5
Sentinel 1A	48.51%	0.31	2.76	Entropy VV, mean VV, variance VH
TanDEM-X	58.22%	0.44	2.78	Coherence, intensity master, intensity slave
ALOS2dual	59.70%	0.46	2.73	HH descending, HV descending, HH ascending
Sentinel 2A+Sentinel 1A	79.90%	0.73	2.08	Bands 12, 11, 5 S2
Sentinel 2A+TanDEM-X	81.91%	0.76	2.14	Band 11 S2, Band 12 S2, coherence HH TX
Sentinel 2A+ALOS2dual	74.91%	0.67	2.53	Band 11 S2, HV descending A2d, HH descending A2d
All images	80.33%	0.74	2.05	Band 11 S2, HV descending A2d, Band 12 S2

Classifications using only a single radar sensor (Sentinel 1A, TanDEM-X and ALOS2 dual) had lower overall accuracy and kappa values compared to the classification that used two or more sensors. Sentinel 2A (S2) had with 82.60 % the highest overall accuracy and kappa values with 0.77. The variable importance shows the PC1 of Bands 11 and 12 were more important during the RF classification, followed by the PC1 of Bands 5, 4 and 2. Figure 2.7 shows the results of the S2 classification. A gradient is visible, with the north mostly comprising of areas of Cerradão, which is closest to the Amazon biome, and whose south Cerrado denso areas are prevailing. Additionally, it illustrates a large area of secondary forest in the northwest of the study area. Based on this map, Cerrado denso covers 34.50% of the Cerrado area, Cerradão 28.70%, gallery forest 28.14% and secondary forest 8.66%.
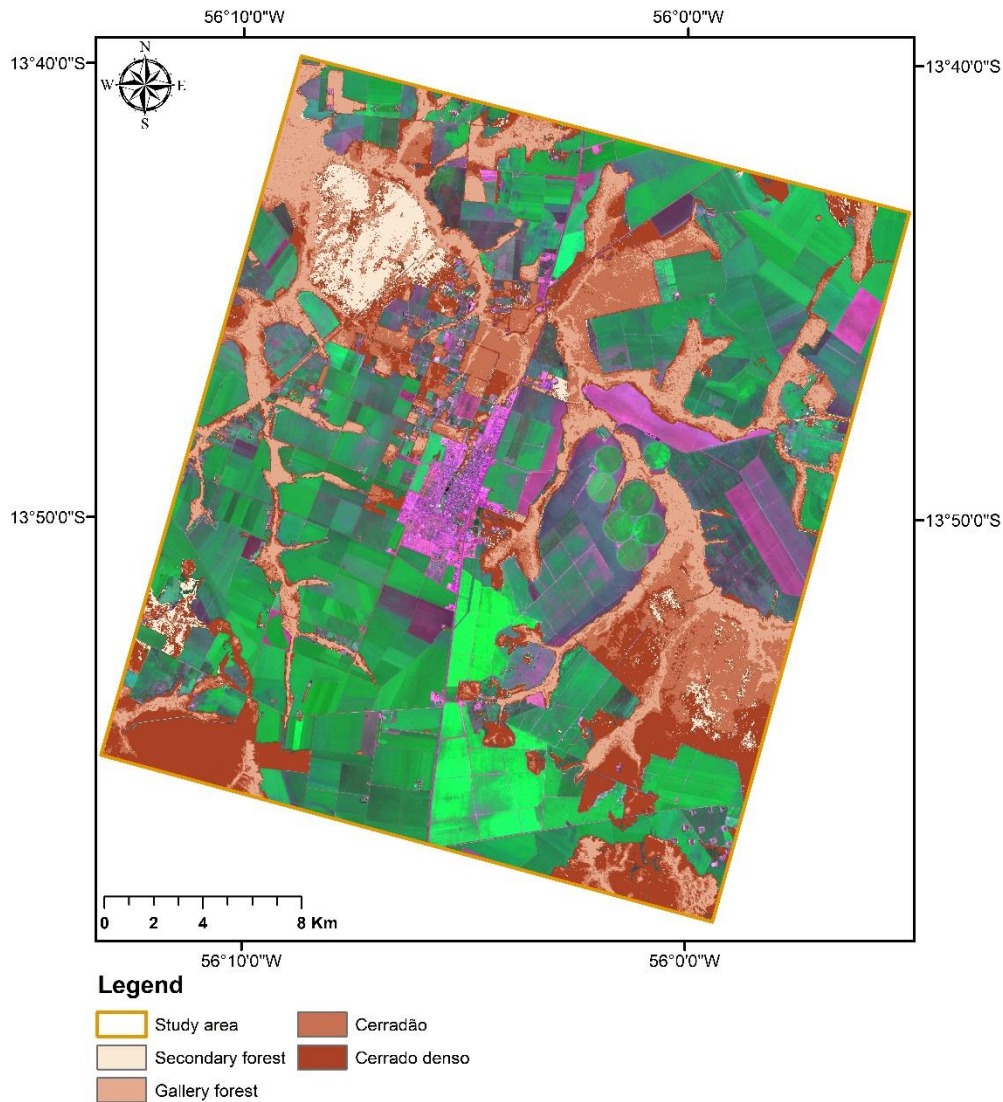
Figure 2.7. Classification results of the spatial distribution of the four Cerrado forest types using Sentinel 2A (dry season) on top of a false color composition of Sentinel 2A, Bands 3, 4, and 8 (07 July 2017).

The overall accuracy and kappa values of the Sentinel 1A (S1) classification had the lowest classification results using only single sensors with an overall accuracy of 48.51% and a kappa value of 0.31. Additionally, the PC1 of entropy and mean images of VV polarization and PC1 of variance image of VH polarization were more important to the RF classifier. The TanDEM-X classification also presented low accuracy and kappa values, 58.22% and 0.44, respectively. The coherence was more important than the intensity. The images from ALOS-PALSAR 2 dual and full polarimetric showed different results in the classification. In our study, the dual polarization images had a higher overall accuracy and kappa values, 59.70% and 0.46, respectively, compared to the full polarimetric images. However, we used four different dates of dual polarimetric images and one of full polarimetric image. This difference in the number of acquisitions from dual and full polarimetric images can cause a better accuracy for the dual polarization images.

42

The combinations of two or more sensors, in general, improved the extraction of the target's information, and consequently, the classification. The classification that used S2 and TanDEM-X showed the highest overall kappa values, 81.91% and 0.76. Variable importance shows the PC1 of Bands 11 and 12 of S2 and the coherence of TanDEM-X were more important to the RF classifier.

The S1 and S2 classifications had an overall accuracy and kappa value of 79.90% and 0.73. PC1 of Bands 11 and 12 of S2 and the PC1 of contrast of VH polarization of S1 had a high ranking in the variable importance. The classification that used all images from the dry season had a similar overall accuracy and kappa values compared to the S2 and TanDEM-X classification. The PC1 of Band 11, PC1 of ALOS-PALSAR 2 dual VH polarization descending orbit, and PC1 Band 12 images had the highest importance.

The highest accuracy for each of the four forest classes was obtained by different classification inputs, the highest producer's accuracy for Cerrado denso class was achieved with S2 and S1 classification and the highest user's accuracy with the classification that used S2 images. The highest producer's accuracy for Cerradão class was reached with the classification that used all images, and the user's accuracy was reached with the S2 and TanDEM-X classification. For the gallery forest, the highest producer's accuracy was obtained with the classification that used S1 images, and the user's accuracy was obtained using S2 images. The highest users' accuracy for secondary forest class was again reached with S2 images. The ALOS-PALSAR 2 dual polarimetric images resulted here in the best producer's accuracy (Figure 2.8).
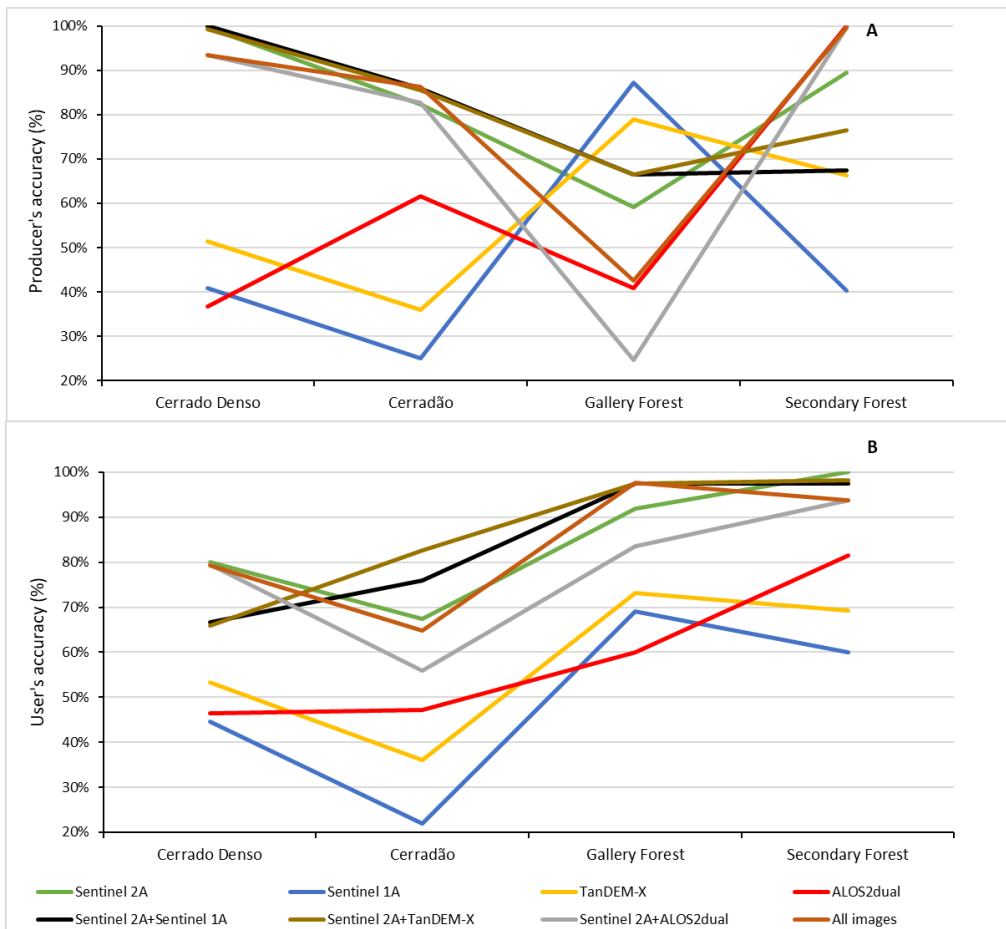
Figure 2.8. Producer's (A) and user's (B) accuracy of classifications based on single-sensor and optical/SAR-combinations for the four Cerrado types. Only data acquisitions during the dry season were considered.

Dry and Rainy Season

Table 2.4 summarizes the results for the classifications during the dry and rainy season. The classification of S1 images during the dry and rainy seasons had higher overall accuracy and kappa values compared to the S1 classification of the dry season, with 16% overall accuracy and a kappa of 33%. This result shows that the use of images combining the dry and rainy seasons improved the classification of S1 images. Here, the PC1 of entropy and of mean images of VV polarization as well as of the VH polarization contrast image were the three most important variables. The ALOS-PALSAR 2 full polarimetric classification showed a lower overall accuracy and kappa values compared to the ALOS-PALSAR 2 dual polarimetric classification during the dry season. Moreover, the volume polarimetric decomposition image was more important to the RF classifier.

Table 2.4. Overall accuracy, kappa values, confidence interval 95% OAA, the three most important variables for the classifications according to Random Forest variable importance for Sentinel 2A (S2), ALOS PALSAR 2 full (A2f), ALOS PALSAR 2 dual (A2d), TanDEM X (TX), and Sentinel 1A (S1). The parameters listed in the variable importance are the PC1 derived from the PCA, except for the images from TanDEM-X, as only one acquisition was available. All data acquisitions during the dry and rainy season were considered.

44

Rainy+dry season	Overall Accuracy	Kappa	Conf. OAA	95%	Variable Importance
Sentinel 1A	56.21%	0.42	2.87		Entropy VV, mean VV, contrast VH
ALOS2full	41.26%	0.22	2.77		Volumetric, C22, C11
Sentinel 2A+Sentinel 1A	81.73%	0.76	2.05		Bands 12 S2, 11 S2, contract VH S1 rainy season
Sentinel 2A+ALOS2full	79.98%	0.73	2.28		Bands 11, 12, 5 S2
All images	81.91%	0.76	1.97		Band 11 S2, HV descending A2d, Band 12 S2

For the dry and rainy season, the classifications that combined radar and optical sensors were more accurate. From each classification, which used more than on sensor, we selected the first three images with highest variable importance, totaling 15 images and used these images as input for all image classifications. This classification had the highest overall accuracy and kappa values (81.91% and 0.76) (Figure 2.9). The PC1 of Band 11 of S2, PC1 of ALOS-PALSAR 2 dual VH polarization at descending orbit and PC1 of Band 12 of S2 were the most important images that contributed to the classification of all images.
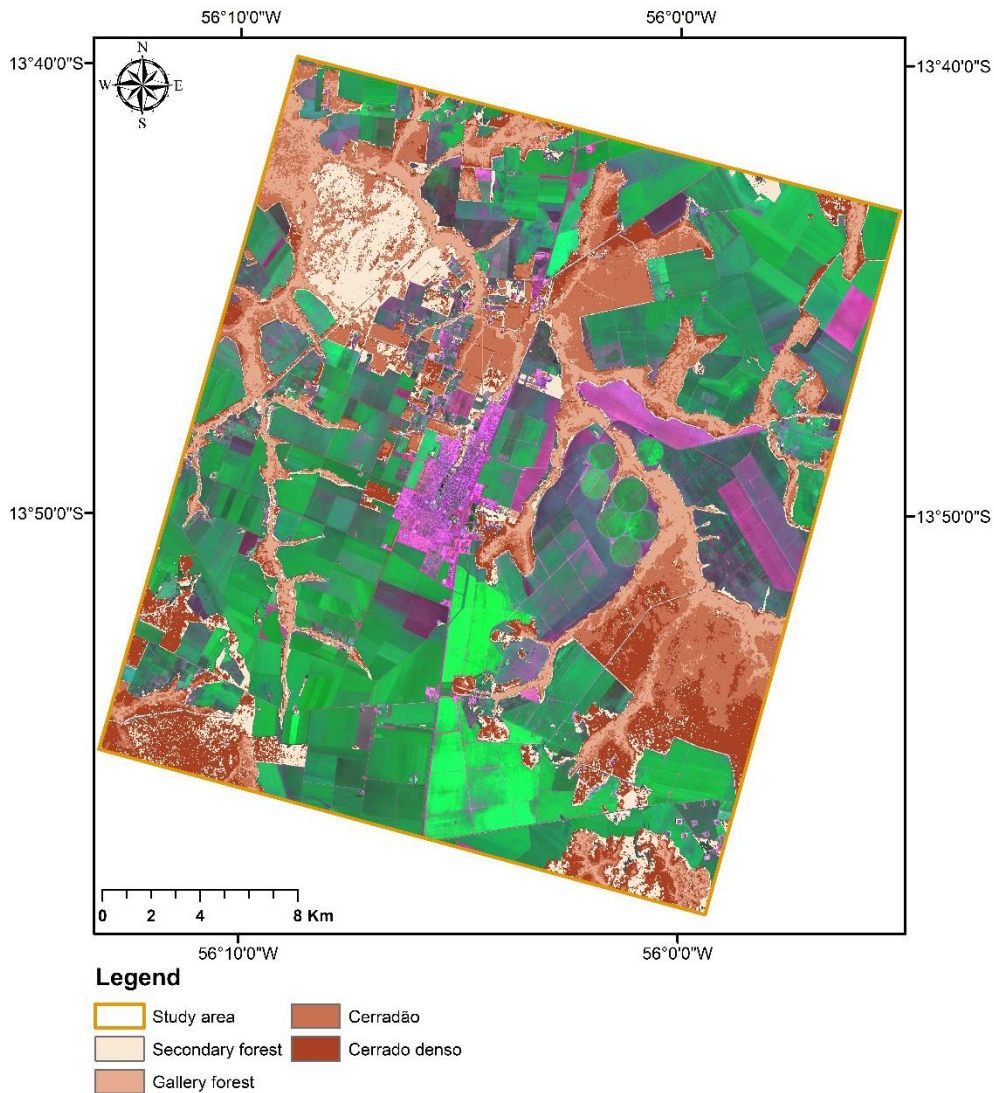
Figure 2.9. Classification of Cerrado forest type using all images from the dry and rainy season on top of a false color composition from Sentinel 2A, Bands 3, 4, and 8 (07 July 2017).

The S2 and S1 classifications showed a higher overall accuracy and kappa values, 81.73% 0.75, compared to the classification during the dry season. Variable importance showed that the PC1 of Bands 12 and 11 of S2 and the PC1 of contrast VH polarization were more important.

The highest producer's accuracy for the Cerrado denso class was achieved with S2 and ALOS-PALSAR 2 full polarimetric classification, and the highest user's accuracy was achieved with the classification that used all images. The highest producer's and user's accuracy for Cerradão class was reached with the classification that used S2 and S1. For the gallery and secondary forest, the highest user's accuracy was obtained using S2 and S1 images. The highest producer's accuracy for the gallery forest was achieved with S1 images and for the secondary forest class with all images (Figure 2.11).
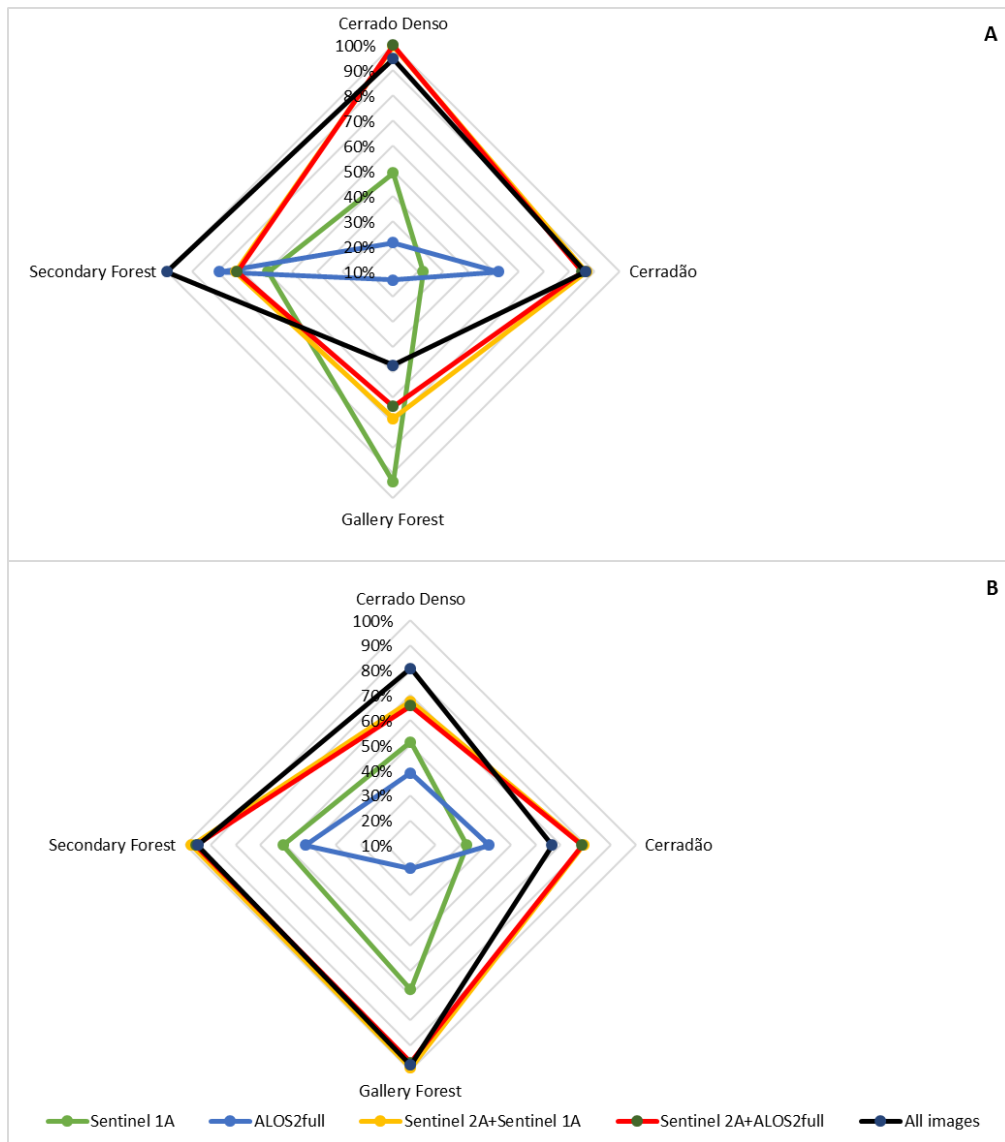
Figure 2.11. Producer's (A) and user's (B) accuracy of classifications based on single-sensor and optical/SAR-combinations for the four Cerrado types. All data acquisitions during the dry and rainy season were considered.

Radar Classification

We separately analyzed the radar classifications of Sentinel 1A, ALOS-PALSAR 2 dual/full polarimetric, and TanDEM-X (C Band, L Band, and X Band, respectively) for both seasons. Table 5 presents the results of these classifications during the dry season. The TanDEM-X in combination with ALOS-PALSAR 2 dual polarimetric classification achieved the highest overall accuracy and kappa values, 66.96% and 0.56. S1, and TanDEM-X had the lowest overall accuracy with 54.46% and 0.39. Furthermore, PC1 of ALOS-PALSAR 2 dual polarimetric VH descending orbit and HH descending orbit and coherence of TanDEM-X images were higher ranked in the variable importance list of Random Forests (Table 2.5).

47

Table 2.5. Overall accuracy, kappa values, confidence interval 95% OAA, and the three most important variables for the classifications based on the Random Forest variable importance for Sentinel 2A (S2), ALOS PALSAR 2 full (A2f), ALOS PALSAR 2 dual (A2d), TanDEM X (TX), and Sentinel 1A (S1). The parameters listed in the variable importance are the PC1 derived from the PCA except for the images from TanDEM-X, as only one acquisition was available.

Dry Season	Overall Accuracy	Kappa	Conf. 95% OAA	Variable Importance
Sentinel 1A +TanDEM-X	54.46%	0.39	2.66	Coherence HH TX, mean VV S1, entropy VV S1
Sentinel1A+ALOS2dual	62.33%	0.50	2.61	HV descending A2d, HH descending A2d, HV ascending A2d
TanDEM-X+ALOS2dual	66.96%	0.56	2.61	HV descending A2d, HH descending A2d, coherence HH TX
Rainy+dry season				
Sentinel 1A+TanDEM-X	64.42%	0.53	0.67	Coherence HH TX, mean VV S1 dry season, entropy VV S1 dry season
Sentinel 1A+ALOS2dual	66.61%	0.55	2.69	HV descending A2d, HH descending A2d, contrast VH S1 rainy season
Sentinel 1A+ALOS2 full	61.10%	0.48	2.78	Volumetric, entropy VV S1 dry seanson, mean VV S1 dry season
TanDEM-X+ALOS2 full	61.01%	0.48	2.81	Coherence HH TX, volumetric A2f, C22 A2f
ALOS2 dual+ALOS2 full	58.30%	0.44	2.81	HV descending A2d, HH descening A2d, HH ascending A2d

Combining the dry and rainy seasons, S1 and ALOS-PALSAR 2 dual polarimetric classification achieved the highest overall accuracy and kappa values, 66.61% and 0.55, respectively. Here, PC1 of ALOS-PALSAR 2 dual polarimetric VH descending orbit, HH descending orbit, and PC1 contrast of VH polarization images were more important. The ALOS-PALSAR 2 dual polarimetric and ALOS-PALSAR 2 full polarimetric classification showed the lowest overall accuracy and kappa values, 58.30% and 0.44, respectively.

Highest producer's and user's accuracy for Cerrado denso and the Cerradão class for the dry season were achieved with TanDEM-X and ALOS-PALSAR 2 dual polarimetric classification. This sensor combination also had the highest user's accuracy and producer's accuracy together with S1 and ALOS-PALSAR 2 dual polarimetric in the secondary forest. For the gallery forest, highest producer's and user's accuracies were achieved with S1 and TanDEM-X classification (Table 2.6). The radar sensors combinations presented a higher overall accuracy and kappa values compared to the single use of these sensors.

Table 2.6. Producer's and user's accuracy of classifications based only on combinations of SAR sensors for the four Cerrado types. Only data acquisitions during the dry season were considered.

Dry Season	Cerrado Denso	Cerradão	Gallery Forest	Secondary Forest
Producer's accuracy				
Sentinel 1A +TanDEM-X	40.21%	28.52%	94.46%	54.04%
Sentinel1A+ALOS2dual	38.11%	34.86%	76.12%	100.00%
TanDEM-X+ALOS2dual	40.91%	59.86%	67.13%	100.00%
User's accuracy				
Sentinel 1A +TanDEM-X	50.88%	24.92%	73.19%	70.00%
Sentinel1A+ALOS2dual	53.96%	34.14%	70.97%	83.33%
TanDEM-X+ALOS2dual	68.02%	47.22%	72.93%	82.37%

The dry and rainy season had similar results. Producer's and user's accuracy were for the gallery forest the highest using S1 and TanDEM-X, too. For Cerrado denso, the best user's accuracy was achieved with S1 and TanDEM-X classification. Highest producer's accuracy was obtained by using S1 and ALOS-PALSAR 2 dual polarimetric images as input for the classification. This combination was also the best for the secondary forest, paired with ALOS-PALSAR 2 dual polarimetric and ALOS-PALSAR 2 full polarimetric. Here, TanDEM-X and ALOS-PALSAR 2 full polarimetric images reached the highest user's accuracies. The highest producer's and user's accuracy for Cerradão class were achieved with ALOS-PALSAR 2 dual polarimetric and ALOS-PALSAR 2 full polarimetric classification (Table 2.7).

Table 2.7. Producer's and user's accuracy of classifications based only on combinations of SAR sensors for the four Cerrado types. All data acquisitions during the dry and rainy seasons were considered.

Rainy+Dry Seasons	Cerrado Denso	Cerradão	Gallery Forest	Secondary Forest
Producer's accuracy				
Sentinel 1A+TanDEM-X	53.85%	40.85%	94.81%	67.72%
Sentinel 1A+ALOS2dual	55.24%	44.72%	66.44%	100.00%
Sentinel 1A+ALOS2 full	47.90%	36.97%	92.04%	67.02%
TanDEM-X+ALOS2 full	43.36%	42.61%	78.89%	78.95%
ALOS2 dual+ALOS2 full	41.96%	51.41%	40.14%	100.00%
User's accuracy				
Sentinel 1A+TanDEM-X	71.96%	37.54%	76.75%	73.11%
Sentinel 1A+ALOS2dual	65.29%	44.88%	76.19%	77.66%
Sentinel 1A+ALOS2 full	59.57%	40.70%	68.56%	71.27%
TanDEM-X+ALOS2 full	56.36%	39.41%	67.66%	80.36%
ALOS2 dual+ALOS2 full	45.63%	46.79%	58.29%	77.03%

Furthermore, the polarization of radar sensors is shown to be an important factor for the Random Forest classification. The intensity of cross-polarized HV polarization PC1 images were one of the most important variables in 60% of the classification, which used radar sensors.

Summary of the Classifications

The three highest overall accuracies and kappa values belonged to S2, S2 with TanDEM-X, and to the combinations of all images for the dry and rainy seasons. Nevertheless, the range of confidence interval shows different results compared to the overall accuracy and kappa values. The three narrowest ranges, which indicate good precision, belong to all images of the dry and rainy season, all images of the dry season and S2 with S1 from the dry and rainy season classifications (Table 2.5).

The variable importance for the classifications that combined optical and radar images showed that PC1 of Bands 11, 12, and 5 from S2, PC1 of ALOS-PALSAR 2 dual polarimetric VH descending orbit, PC1 of ALOS-PALSAR 2 dual polarimetric HH descending orbit, coherence of TanDEM-X, and the PC1 of contrast VH from the rainy season of Sentinel 1A images were the most important variables during the Random Forest classification.

2.4   Discussion

The results showed the importance of integrating satellite images from different sensors to classify the forest and non-forest area. The Program for the Estimation of Amazon Deforestation (PRODES) is the most important project that has been conducting satellite monitoring of deforestation in the Legal Amazon, producing annual deforestation rates in the region, using Landsat images (30 meters spatial resolution). Comparing the data of forest areas from the PRODES project with the results of our work, it is possible to verify a high underestimation in the forest areas, mainly in the classes gallery forest and Cerrado denso. The PRODES estimated an area of 12,702 ha of forest, and our work estimated an area of 27,326 ha. This difference can be associated to the different spatial resolution used in PRODES (30 meters) and in our study (10 meters).

Optical images are largely used to map vegetation types in the Cerrado biome. In our results, S2 classifications showed the highest overall accuracy and kappa values. The application of S2 images to map vegetation types in the Cerrado biome is new. In general, Landsat is the most common sensor used to discriminate vegetation types in the Cerrado. Nascimento and Sano (2010) had 85% overall accuracy for mapping vegetation types in this biome. The authors used Landsat 7 ETM+ images to discriminate the Rupestrian Cerrado (Savanna formation) in the Chapada dos Veadeiros National Park in Goias State, which can be difficult due to the spectral confusion with other types of Cerrado vegetation. The optical

bands located in the red and NIR wavelengths showed high importance and contribution to the discrimination of vegetation type, as was visible in our results (Tables 2.3 and 2.4). Nascimento and Sano (2010) agree on the importance of VIS and NIR regions for characterizing forest areas, as the vegetation has higher reflectance in this wavelength range and is thus more sensitive. Additionally, the number of optical images in ours and other studies helps the increase of discrimination power of different vegetation types, due to the unique spectral signatures of the plant during the year (Hermuche and Sano 2011; Barret et al. 2016). The optical data are certainly useful to map the vegetation type in Cerrado; however, these images are usually not available during the rainy season and the optical data cannot extract information from the structure of the forest (Asner 2001). Moreover, the availability of images in the rainy season would allow for a higher temporal resolution, which is crucial to better discriminate the vegetation types in the Cerrado biome due its high seasonality. Additionally, in dense areas of vegetation, the optical sensor is usually saturated due to the low optical depth penetration through these areas, affecting the mapping of the various vegetation types. There are important projects assessing the land use of the Cerrado biome, such as the TerraClass Cerrado project, which produced a map of the land use of the Cerrado biome. However, the project had great difficulties to discriminate the different types of vegetation, which is important for the preservation of biodiversity in this region. Nevertheless, TerraClass presents another step in the challenge of mapping the different types of vegetation in the Cerrado (MMA 2015).

The use of radar images can be a solution to overcome the lack of image availability in the rainy season and the high saturation of optical images in areas of great biomass density. In our radar, classification results from the dry and rainy seasons, TanDEM-X (X Band) and ALOS-PALSAR 2 (L Band) dual polarimetric classification from the dry season showed the highest overall accuracy and kappa values. The influence of vegetation scattering mechanism dependencies is strongly dependent on the wavelength and polarization of the sensor. In the short/intermediate wavelengths, such as X and C Bands, backscattering represents the radiation interaction of canopy, leaves, branches, secondary branches, and part of volumetric scattering (inside crown). Longer wavelengths, such as the L and P Bands, have the capability for deeper penetration. Bigger vegetation components such as trunks, crown, ground, and branches interact with these lower wavelengths. According to the results for the dry season, L Band dual polarimetric images had the highest overall accuracy and kappa values were comparable to the classifications that used single sensor (X and C Bands). The study area is mostly forested. In these areas, radar signals are more likely to be saturated in the X and C Bands compared to the L Bands (Yu and Saatchi 2016). The polarization controls the types of components that interact with the radiation. In our study, the L Band cross-polarized HV polarization was the most important variable that contributed to the random classifier in the best classification. This agrees with the fact that cross-

polarized images have direct relation with volumetric scattering, and are therefore sensitive to forest structure (Jensen 2014). There are few studies in the Cerrado biome using only radar images. Sano et al. (2001) used the L Band from JERS-1 SAR data to map the different types of vegetation by analyzing the backscattering coefficient values. The study could well separate the grassland, mixed grass/shrub/woodland, and woodland in the state of Distrito Federal.

The results of the CI 95% OAA showed the importance of the fusion between optical and radar data to map vegetation type in the Cerrado biome, since the confidence interval with the narrowest range belonged to the classification that used all images from the dry and rainy seasons, where the narrower the interval, the more accurate the classification. The Cerrado vegetation has one of the largest forest diversities, consequently the combination of different sensors (optical and radar) and spatial resolution (low, medium, and high) results in a great improvement in the accuracy (Saatchi et al. 2010). Of the three classifications that obtained the highest values of accuracy and kappa, two used radar and optical images. This showed the importance of the integration of different sensors in improving the mapping of forest types in Cerrado. A similar result was reported by (Sano et al. 2005), who combined optical and radar images to improve the classification of different vegetation types in the Cerrado biome. The study had a high overall classification accuracy, which used both sensors in regions of savanna and grasslands formations. Sano et al. (2005) used data from the dry and rainy seasons and showed the importance of the time series in improving the classification of different types of vegetation. Additionally, Sano et al. (2005) showed better performance of radar data (JERS-1 SAR) compared to optical data (Landsat). In contrast, our results showed that optical data performed better for classification, compared to the radar data. However, this study used a higher number of radar images using L Band compared to our study, which increased the efficiency of mapping vegetation, due to the sensitivity to identify the various structures of the forest, consequently better distinguishing the type of forest, as reported by Lucas et al. (2000), Garestier et al. (2009) and Santoro et al. (2009). Carvalho et al. (2010) used images from ALOS-PALSAR and Landsat to map the different types of vegetation and the results agree on our findings. The highest overall accuracy and kappa values were from the S2 classification; therefore, in our results, the use of radar images did not reach the highest accuracy and kappa values. Carvalho et al. (2010) showed that the use of radar data did not improve classification accuracy; however, the study used only one data from radar imaging. Concerning GLCM textures, the same study showed similar results. Grey Level Co-occurrence Matrix textures images had a high variable importance during the Random Forest classification, in particular for entropy, which showed the disorder of GLCM elements. This may be related to the differences in the backscattering of the vegetation type classes.

Regarding the user's accuracy, the secondary forest was better classified using optical images, whereas the other three classes were better classified using optical and radar images. The optical bands were the most important variables for the RF classifier. The texture images were the second most important ones. Several authors presented similar results achieved in this study (Schlund et al. 2014; Inglada et al. 2016; Ribeiro and Walter 1998). All mentioned studies showed an improvement in the separability of land cover types employing texture images. The coherence image from TanDEM-X was the third most important variable. Schlund et al. (2014) and Baron and Erasmi (2017) showed an improvement in the discrimination of forest against other classes using coherence as well.

Other studies about classification of vegetation type in the Cerrado biome, such as Mesquita JR et al. (2001) were in regions where the vegetation has a smaller gradient compared to regions within the Arc of Deforestation, such as Distrito Federal, Minas Gerais, and São Paulo. The IBGE and the MMA mapped vegetation types from the whole Cerrado biome. The studies used Landsat images from the year 2004 and scaling of 1:250,000, which is not enough to detect the gradients of the Cerrado biome. The mapping of vegetation types in transition zones is still a challenge, due to these not having a clear border (Ribeiro and Walter 1998). However, these regions play an important role in the conservation of the Amazon and Cerrado biome, wherein 75% of the deforestation in Amazon occurs.

2.5   Conclusion

In this paper, we evaluated the use of optical and radar remote sensing for mapping different types of vegetation in the transitional area between the Cerrado and Amazon biomes. The method described in this study improved the mapping of vegetation type in the Arc of Deforestation in the Cerrado biome and can be applied to create accurate vegetation type maps. We evaluated the use of four different sensors, one optical sensor (Sentinel 2) and three radar sensors (Sentinel 1, ALOS, TanDEM-X), for better vegetation type identification and area discrimination, so that these can be used for better calculations of biomass loss and carbon storage in the high dynamic Arc of Deforestation in Brazil.

When applying a supervised random forest classification, the highest overall accuracy and kappa coefficient were obtained using only the Sentinel 2A for classification. However, of the three classifications that obtained the highest overall accuracy and kappa values, two used radar and optical images. Bands 5, 11, and 12 of Sentinel 2A, texture images from Sentinel 1A cross-polarization, and coherence of TanDEM-X were the most important images in order to separate each class, as calculated by the random forest variable importance. The combination of optical and radar sensor data usually improves the vegetation classification. Nevertheless, in our study, the single use of optical sensors was sufficient to discriminate the four forest classes in the study area: Cerradão (Open Forest), Cerrado

denso (Dense Woodland), gallery forest, and secondary forest classes in a highly fragmented complex vegetation biome. Such information is relevant for the upcoming mapping of vegetation types in the endangered Cerrado/Amazon ecotone.

Author contributions:

Flávia de Souza Mendes – conceptualization, methodology, validation, formal analysis, investigation, writing—original draft preparation, writing—review and editing, visualization

Daniel Baron – formal analysis, writing—review and editing, visualization

Gerhard Gerold – conceptualization, validation, writing—review and editing, visualization

Veraldo Liesenberg – writing—review and editing, visualization

Stefan Erasmi – conceptualization, methodology, validation, writing—review and editing, visualization

3.   Aboveground Biomass and carbon stock in the Cerrado forests, Mato Grosso, Brazil

Abstract

The Cerrado biome represents around 25 % of the land surface of Brazil comprising a high biodiversity and a great proportion of endemic species. The vegetation is characterized by a mosaic of grasslands, savannas and forests. Since the 1970s, the biome is strongly affected by deforestation and degradation along with fragmentation. Within the arc of deforestation four fragments in the Cerradão and two fragments in the Cerrado denso (sensu stricto) were selected to analyze the aboveground biomass (AGB) and carbon stocks in the municipality of Nova Mutum, Mato Grosso, Brazil. To apply appropriate allometric models for AGB estimation and to verify the hypothesis that there exists a gradient of AGB from the border to the center of the fragments, plot analysis along transects (border to center) were launched. For the estimation, the woody components of the tree layer and of the shrub layer were investigated by recording main variables like the diameter at breast height (DBH), the total tree/shrub height, wood density, basal area and the tree species. Finally, the DBH and the total tree/shrub height were the explanatory variables of the allometric model for the Cerradão whereas the DBH and the wood density were the explanatory variables of the allometric model for the Cerrado denso. The estimated tree and shrub AGB of the Cerradão amounted to 93.23 Mg ha-1 with carbon stocks of 46.61 Mg ha-1. The Cerrado denso revealed a total AGB of 56.13 Mg ha-1 and aboveground carbon stocks of 28.07 Mg ha-1. These values are higher compared to similar studies in the Cerrado biome. Moreover, the results showed no significant differences in the quantity and distribution of AGB and aboveground carbon stocks between border and center of the fragments in both vegetation types but a significant difference of the AGB and aboveground carbon stocks between the two investigated vegetation types. Extrapolations of the AGB and carbon stock results mention that for the Cerradão in Mato Grosso total AGB is 0.29 Gt and the AGB for the Cerrado denso is 0.41 Gt. in Mato Grosso. The preservation of the still existing forest areas is not only important for the C-cycle, but also for the regional water cycle and biodiversity.

Keywords: Aboveground biomass and C-stocks, Cerrado Biome, fragmentation, allometric models, Mato Grosso, Brazil

3.1   Introduction

3.1.1   Cerrado vegetation types and deforestation

The savannas of South America that pertains to the neotropical realm, constitute 45 % of the whole land surface (Sankaran et al. 2005; Scholes and Archer 1997). In central Brazil, these neotropical savannas are specified as 'Cerrado'. This unique biome covers above 2 million km2, representing approx. 25 % of the land surface of Brazil and marginal parts of Bolivia and Paraguay. Therefore, the Cerrado is the second largest Brazilian biome after Amazonia. The Cerrado biome, which exhibits a broad range of vegetation formations from grasslands to closed forests with approx. 44 % endemic species (Pfadenhauer and Klötzli 2014; Goodland 1971; Sano et al. 2010). On the southern and southeastern border of the Amazon biome, the Cerrado constitutes a transition zone (ZOT) and conforms with the "arc of deforestation" in Brazil (Figure 3.1), where deforestation is a main process since the 1980s in favour of great cropping fields (soy, cotton, corn) and pastures. Therefore, the transition zone is characterized by a complex mosaic of savanna and forest (Peixoto et al. 2017).

The Cerrado biome is characterized by a semi-humid tropical climate with a rainy season from October-March and a dry season from April-September, with regional variances. Hence, periodic fires and seasonal droughts influence the Cerrado. The annual mean temperature varies regionally from 18 °C to 28 °C and the annual mean precipitation fluctuates from 900 mm to 1,800 mm regionally, whereof the majority falls during the rainy season (Minami et al. 2017; Miranda et al. 2014; Oliveira Filho and Ratter 2013). In the dry season, the monthly precipitation is < 100 mm. The vegetation is developed on acidic, base-poor soils. Therefore, about half of the soils in the Cerrado are Latosols (as defined in the Brazilian system of soil classification), which is equivalent to Ferralsols (WRB) and to Oxisols (USDA-ST). With the dominance of kaolinite clay minerals and high Al-Fe-oxid contents they are nutrient-poor and susceptible to leaching. The predominantly flat relief of the area enables an easy access for deforestation (Miranda et al. 2014; Minami et al. 2017).
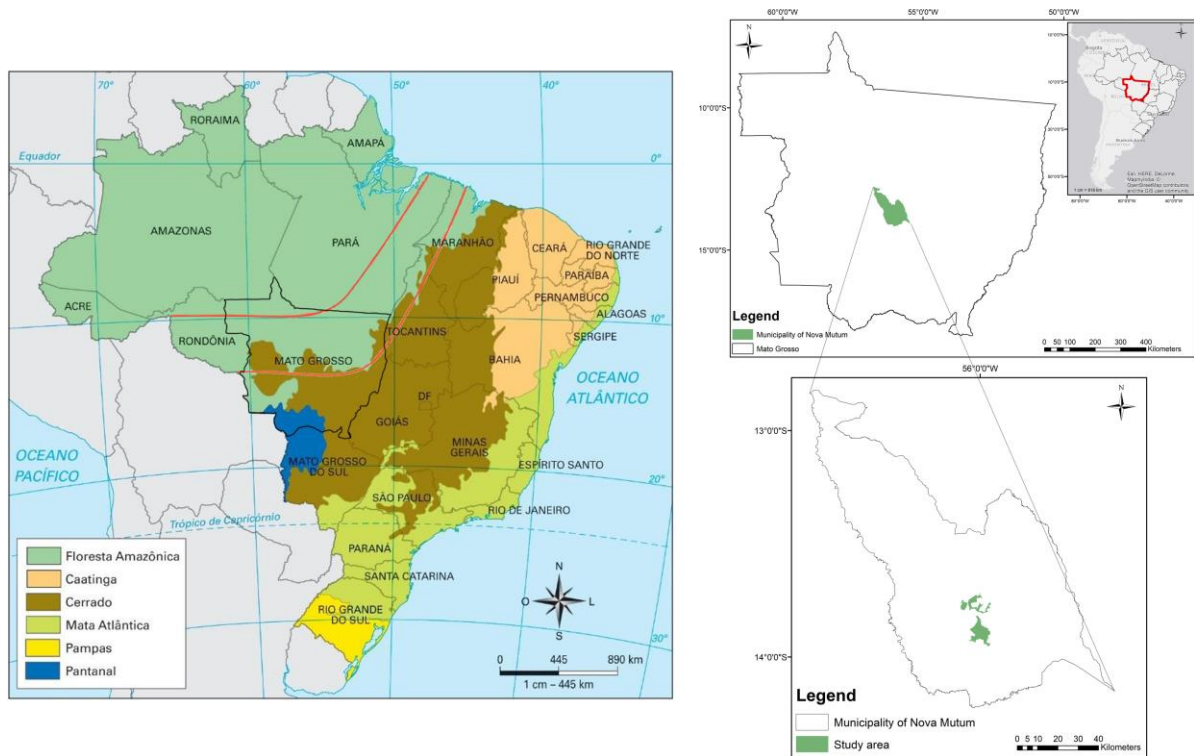
Figure 3.1. The Brazilian biomes, the arc of deforestation (red lines) (left; modified after (Silveira 2015) and the study area (right).

Currently particularly the Amazon biome and the Cerrado biome are exposed to severe human impacts. During the last five decades, vast deforestation and degradation, mainly for agricultural use, caused already a disturbance of 80 % of the Cerrado biome and the irretrievable loss of the primary vegetation cover. During the agro-industrial expansion phase (late 1990s until 2004), large scale expansion of soy and other mechanized crops accompanied by an intensification of cattle production – driven by global market conditions and technological advances – took place in the southeastern part of Amazon (Nepstad et al. 2014). In the state of Mato Grosso, more than half of the forest clearing happened during this phase. The natural vegetation in Mato Grosso is dominated by Cerrado – a semi-arid sclerophyllous shrub vegetation intersected with narrow strips of gallery forest buffers along streams. The state promotes high rates of Cerrado conversion in vast areas of its territory in order to maintain its leading position in soybean and cattle production (27 % of the national soybean production and 14 % of the "the nation's total livestock" of 2010) (DeFries et al. 2013). Approximately 50 % of the original 2 million km2 of the Cerrado area is under agricultural use (Beuchle et al. 2015), compromising about 80 % of the primary Cerrado vegetation. The conversion of Cerrado vegetation is likely to continue as a dominant process of land use change in this region (Lapola et al. 2014). Most of the former Cerrado pasture areas were established after the 1970s (Lilienfein et al. 2003).

The Cerrado contains a significant biodiversity with several species, varying from 300-400 ha-1, including about 3,000-7,000 vascular plant species. The distinctive flora consists of > 1,000 tree species,

> 2,500 herbs and > 250 grass species (Castro and Kauffmann 1998; Oliveira Filho and Ratter 2013). The vegetation period starts in mid-September to the end of October, with the onset of the rainy season and ceases with the onset of the dry season (Arantes et al. 2016). The trees are predominantly indeciduous and its foliage is sclerophyll, i.e. the leaves are thick and leathery. Thereby the foliage is drought-resistant. During the dry season, which is coincident with the flowering, indeciduous trees require sufficient moisture in the deeper soil layers to perpetuate its vitality. The trees of the Cerrado biome exhibit a dimorphic root system, consisting of profound taproots to obtain the water reserves stored in the deeper soil layers and shallow lateral roots, which are connected with the roots of the layer of grass. Consequently, the root system of the Cerrado trees is capable of harnessing either groundwater or surface water or even both coincident (Pfadenhauer and Klötzli 2014). Furthermore, the root system is characterized by the phenomenon of the 'hydraulic lift', i.e. the roots can redistribute the water both from the bottom up and from top to bottom. In general, the Cerrado is a heterogeneous, fire-resistant biome with different vegetation types ranging from the grassland formation over the savanna formation to the forest formation (Figure 3.2). Therefore, it exhibits significant variations in structure, fire frequency and biomass (Delitti et al. 2006).
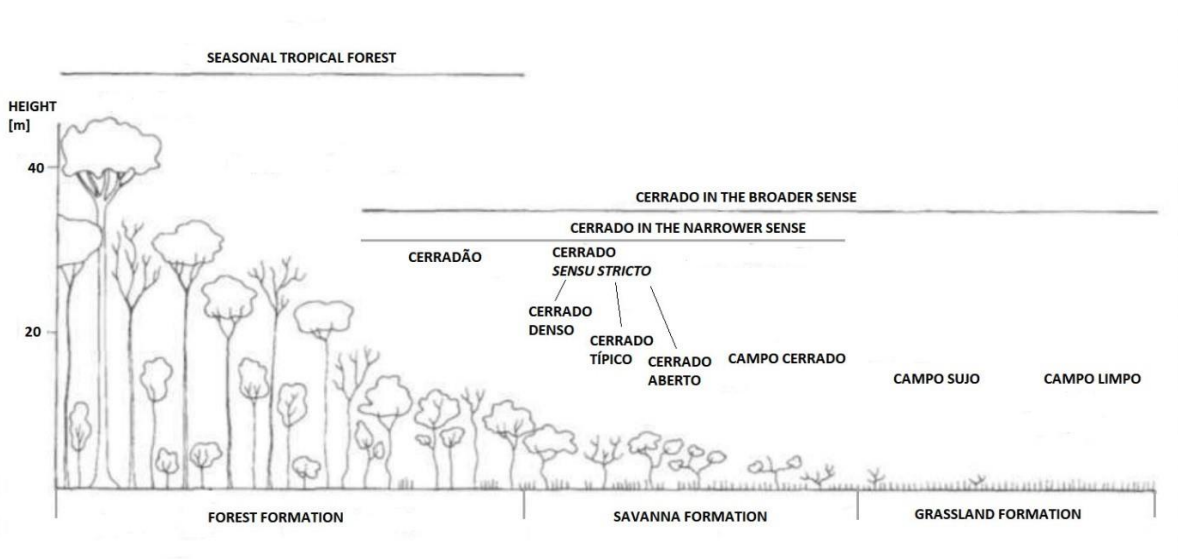
Figure 3.2. Vegetation physiognomy of the Cerrado biome (modified after Coutinho (2007).

In the narrower sense (sensu stricto), the Cerrado types range from the Campo cerrado to the Cerradão (Figgure 3. 2). This narrow section has a deep water table and seasonal water deficits at the topsoil-level. Furthermore, soils of low fertility are common, i.e. latosols are dominating. The trees and shrubs are commonly 3-8 m tall with > 30 % of treetop coverage. Thus, there is a pronounced herbaceous layer, which is 1.0-1.5 m high (Oliveira Filho and Ratter 2013; Felfili 2005). The Cerrado sensu stricto (Figure 3.2) is a biodiverse open woodland with a predominance of trees and scattered shrubs from 8 m up to 10 m as well as a grass understorey (Oliveira Filho and Ratter 2013; Kauffman et

al. 1994). It is divided into the Cerrado aberto alias Cerrado ralo, the Cerrado típico and the Cerrado denso. Compared to the Cerrado típico and the Cerrado denso, the Cerrado aberto has a more open canopy. The Cerrado típico has a treetop coverage of 20-50 % and a tree height of 3-6 m (Ribeiro et al. 2011; Castro and Kauffmann 1998; Oliveira Filho and Ratter 2013).

With the land use change (LUC) from forest (Cerrado) to young pasture or crop-field (≤ 10 yr), soil carbon stocks decrease on Ferralsols by 15 Mg ha-1 and by 13 Mg ha-1 on Acrisols (Göpel et al. 2018). Nevertheless, the main loss is given by deforestation with aboveground biomass burning, which reaches 200-230 Mg ha-1 loss of carbon stored by LUC into young pasture or crop field in Amazon rainforest (Boy et al. 2018). Thus, conservation of remaining natural Cerrado areas is an important issue for biodiversity and carbon storage. But studies on aboveground and belowground biomass (ABG and BGB) for the Cerrado vegetation types are rare, whereas Amazonia is one of the most studied biomes, especially related to carbon fluxes (Ribeiro et al. 2011). (Fearnside 2018) reports on biomass studies of Brazilian savanna woodlands (mostly Cerrado), including those in Amazonia, which have recently been reviewed by Miranda et al. (2014). These authors review 26 studies at 170 sites and emphasize the contrast between the amount of available data and what has been used in global carbon computations, pointing out that the estimate by Saatchi et al. (2011) used only one study at two savanna woodland sites in Brazil. For Brazil as a whole, the review by Miranda et al. (2014) calculates an average aboveground carbon stock of 37.4 Mg C ha-1 in savanna woodlands classified as ''forestland'' (34.4 % of the total savanna woodland area), and 11.5 Mg C ha-1 in those classified as ''shrublands'' (65.6 % of the area), giving a weighted average of 20.4 Mg C ha-1. For grasslands, aboveground biomass averaged 7.2 Mg ha-1 [i.e., roughly 3.6 Mg C ha-1].

However, the Cerrado has only a legal protection status of < 10 % of its area, around 1.7 million ha of shrubland, 764,000 ha of forestland and 413,000 ha of grassland are protected. Amazonia, by contrast, has a legal protection status of > 25 % of its area (IBGE 2015; Sano et al. 2010). Based on land use in 2010 for whole Mato Grosso and emission factors, estimated in the frame of the carbiocial project (see www.carbiocial.de) CO_2-emissions from old cropland amount to 108 Mt of N_2O for cropland and for pasture to 0.03 Mt (Göpel et al. 2018). In 2006/2007 (one year), when the deforestation rate was much higher, Fearnside et al. (2009) calculated an amount of 30.9 106 Mg for forest and 0.6 106 Mg CO2-C-eq. emissions for Mato Grosso, which correspond to 40 % of total fossil-fuel combustion in Brazil. With the deforestation in Amazonia Legal, Nogueira et al. (2018) had estimated an amount of 0.7 109 Mg carbon loss. The mainly anthropogenic disturbances in the Cerrado biome such as deforestation and intensive agriculture, which trigger fragmentation and land degradation, result in losses of AGB and aboveground carbon stocks, so that the area belongs to the "hot spot of climate change" worldwide (Steffen et al. 2018).

As the carbon sequestration capacity is little studied in the Cerrado, the quantification of the AGB and the aboveground carbon stocks is necessary. The aim is, to estimate the AGB as well as the aboveground carbon stocks of the fragmented woody vegetation of the Cerradão and the Cerrado denso in Nova Mutum, Mato Grosso. These estimates will be compared with existing studies about the Cerrado or similar ecosystems, to investigate the importance of these vegetation formations for the regional and global carbon cycle.

The research objectives concerning the Cerradão and the Cerrado denso, in Nova Mutum, Mato Grosso are:

(1) to investigate the impacts of fragmentation on the AGB and the aboveground carbon storage capacity

(2) to identify differences of the AGB and the aboveground carbon stocks between the border and the center of each fragment

3.2   Study Area

The study area was defined using satellite images from Landsat 7 Annual TOA Percentile Composites, Landsat 5 TM 32Day TOA Reflectance Composites and Landsat 8 32Day TOA Reflectance Composites. Two classes were created with Forest and Non Forest using four types of classifiers: Random Forests, CART, Margin SVM and Voting. The mapping of deforested areas was carried out between 1985-2015. From 1985 on there was a large increase of Non Forest with deforestation, after 2010 the Non Forest area grew only by 3.6 %. The potential of Sentinel 1A-C-band radar images to map the fragmented vegetation of the study area was also tested using the interferometry process. Two images with different date were used: July 30 and August 23, 2015. The digital image processing is described in detail in de Souza Mendes, F. de (2016).
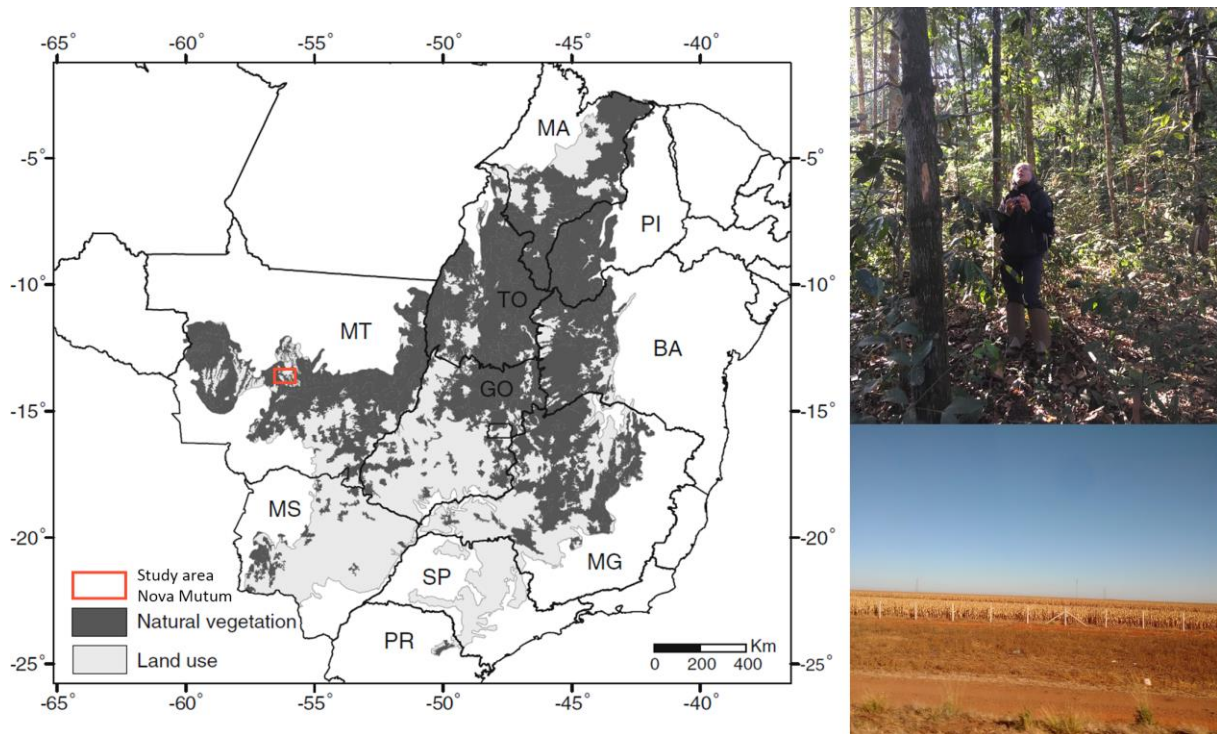
Figure 3.3. Mosaic of natural vegetation and land use that represents mainly intensive agriculture (left, Sano et al. 2010) as well as shots of a Cerradão and of a cornfield in Nova Mutum (right).

The defined area encompasses three main cities: Nova Mutum, São Lucas do Rio Verde and Diamantino. A large portion of this region is dominated by Cerrado denso, a subtype of vegetation of savanna formations, representing 73 % of the vegetation of Cerrado vegetation types present in the state of Mato Grosso (Sano et al. 2007b) Further, Nova Mutum is an important city in the context of deforestation and soybean production in Brazil. In 2014, Nova Mutum had the second largest soybean planted area in Mato Grosso (IBGE 2015) and was on the list of the top 20 cities of mostly deforested natural vegetation between 2002 and 2010 (MMA 2014). Furthermore, the municipality is partially located in the ZOT and is consequently characterized by a mosaic of forest and savanna, whereof the savanna vegetation accounts for approx. 92 % and the forest vegetation accounts for approx. 8 % (Minami et al. 2017). This mosaic is disturbed by grave deforestation mainly for a rapid development of intensive agriculture (Figure 3.3). Thus, the degradation and fragmentation in this region are high. The study area is constituted of six Cerradão fragments and of two Cerrado denso fragments that vary in size (Table 3.1) and isolation, located northerly, northeasterly and southeasterly of the downtown area within a distance of < 30 km (Figure 3.5). The annual mean temperature in Nova Mutum is 24.6 °C and the annual sum of precipitation is 1,934 mm at an altitude of 470 m a.s.l. (Figure 3.4; Minami et al. 2017). The rainy season last from October until April (Figure 3.4).
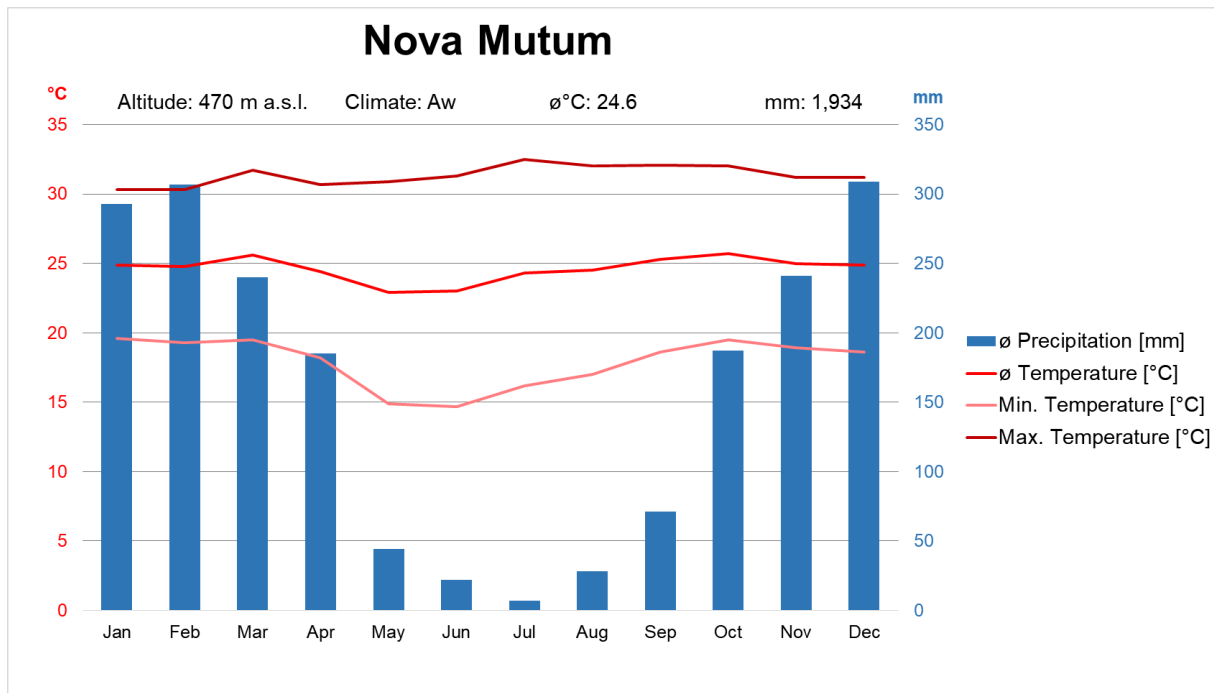
Figure 3.4. Climate graph of Nova Mutum (Mato Grosso, Brazil) (own design; data originate from Climate data and Openstreemap org (2012).

The fragments A-D and G-H are within the Cerradão area (Figure 5). This vegetation type consists of a mixture of forest and savanna tree species. Therefore, depending on the species composition, the Cerradão is considered as a dense to closed woodland or a forest savanna (Miguel et al. 2017a; Eiten 1973; Torello-Raventos et al. 2013; Miguel et al. 2017b). In this study, the Cerradão is classified as part of the forest formation (Figure 3.2).

The Cerradão study area completely presents dystrophic facies with indicator plants like Emmotum nitens or Hirtella glandulosa (Oliveira Filho and Ratter 2013). The trees and shrubs of this predominantly indeciduous broadleaf forest and woodland, respectively, reach heights of 7-15 m and the closed or slightly open canopies exhibit a cover that ranges from 50-90 % (Fearnside et al. 2009). In general, trees and shrubs prevail in the Cerradão, thus it exhibits a greater AGB production as well as higher aboveground carbon stocks as contrasted to other Cerrado vegetation types. Furthermore, the Cerradão has a higher tree density and higher diameters at breast height (DBH1.30) (Morais et al. 2013; Goodland 1971). Because of the high treetop coverage, the herbaceous layer is strongly shadowed and therefore reduced, i.e. the ground is often bare or covered with litter (Pfadenhauer and Klötzli 2014; Oliveira Filho and Ratter 2013). Compared to Amazonian woodland vegetation, the Cerradão has a lower tree density and a more open canopy and partially overlapping treetops (Hoffmann et al. 2009). It is the most closed vegetation type in the Cerrado biome, constituting a transition zone from the savanna (Cerrado sensu stricto) to dry forests (Delitti et al. 2006; Ratter et al. 1973). Moreover, the Cerradão connects the Amazon and the Cerrado biome. Its surface area in Mato Grosso is approx.

31,495.29 km2 (3,149,529.27 ha) and 101,879.85 km2 (10,187,984.73 ha) in the entire Cerrado, dependent upon the Cerradão definition (MMA 2006, 2002; Sano et al. 2007a).
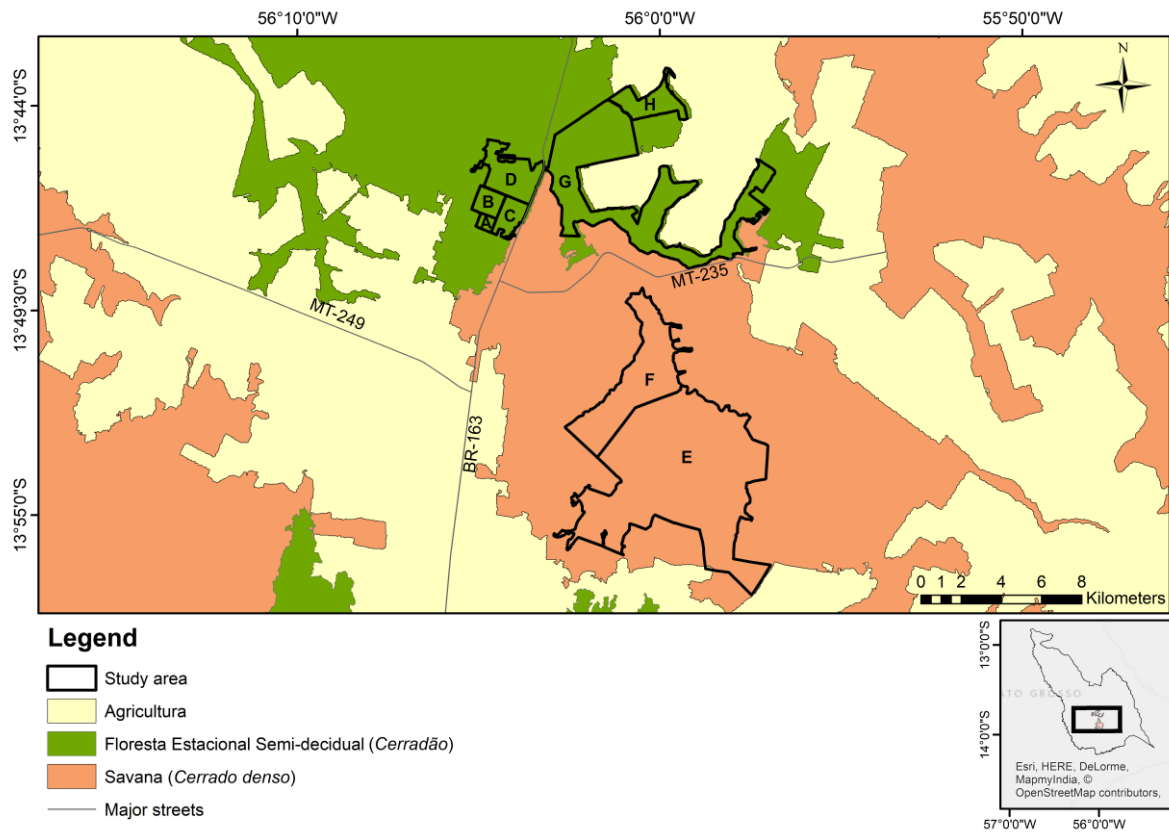
Figure 3.5. Localization of the investigated fragments in the Cerradão (A-D, G-H) and in the Cerrado denso (E-F).

Table 3.1. The size of each fragment [ha].

Fragment	Area [ha]
A	59.9
B	169.4
C	218.3
D	398.8
E	2741.8
F	1572.6
G	5313.2
H	554.2

The fragments E-F are within the Cerrado denso area (Figure 3.5). This vegetation type can be defined as a dense woodland savanna, featuring trees of 5-8 m height and a canopy cover of approx. 50-70 % (Dodonov et al. 2013) and an understorey of shrubs and grasses (Giambelluca et al. 2009).

Compared to the Cerrado típico and the Cerrado aberto, the Cerrado denso has a higher tree density and a more closed canopy (Castro and Kauffmann 1998). Furthermore, it has higher biodiversity in common with the Cerradão (Maracahipes Santos et al. 2015). Since the Cerrado denso area is located in the ZOT just as the Cerradão study area, it is also affected by degradation and fragmentation. Its surface area is approx. 73,121.62 km2 (7,312,161.94 ha) in Mato Grosso and around 245,643.60 km2 (24,564,359.97 ha) in the whole Cerrado (MMA 2006, 2002; Sano et al. 2007a).

3.3   Material and Methods

The field survey took place from mid-July to the beginning of August 2017, i.e. during the dry season. The accessibility to the selected fragments was proved in advance. In general, the selection of the study area was dependent on its homogeneity (e.g. soil type, relief) as well as on a minimum distance of > 100 m of each fragment to rivers. In the field, the access authorization by the landowners to the fragments was finally crucial and restricted the selection on eight fragments with different extents (Table 1; Figure 5). The overall aim of the field survey was the estimation of the AGB and the aboveground carbon stocks (AGC) of each fragment by indirect measurements, i.e. non-destructive and by applying appropriate allometric biomass models. Therefore, the total height and the DBH were determined for trees and shrubs in several defined plots and subplots, respectively. Additionally, the treetop coverage per tree was measured and each tree species was identified. For the survey, trees and shrubs were distinguished as follows: trees are defined as "woody plants higher than 5 m" (Di Gregorio 2005) and in contrast, woody plants lower than 5 m are classified as shrubs (clear tree physiognomy with an altitude higher than 2 m forms an exception). Measurements of trees with a $DBH1.30 \leq 10$ cm as well as the herbaceous layer were neglected in this study, because they contribute just slightly to the aboveground carbon storage and would otherwise bias the results (Chave et al. 2014). Based on the identified species, the measured values of the DBH1.30/DBH0.30, the tree/shrub height and the treetop coverage, the AGB can be determined with an appropriate allometric biomass model.

3.3.1   Sample design

After defining the preselection of the study area, the selection of the fragments in the field was mainly dependent on the access authorization by the landowners. In the end, the study area was constituted of four Cerradão fragments close to the midtown of Nova Mutum, two additional Cerradão fragments in the northeast and two Cerrado denso fragments in the southeast of Nova Mutum (Figure 3.5). The fragment sizes ranged from surfaces > 59 ha to surfaces < 5314 ha (Table 3.1) with varying

degrees of fragmentation. The sampling was executed on four plots along a transect from the edge of each fragment towards its center (Figure 6). Therefore, 32 plots were investigated in total. The location of the transect was predominantly defined in the middle of the fragment edge, closest to the next road and – as possible – without further border influences, e.g. by crossroads. The plot sampling started at a distance of 20 m from the edge of the forest or savanna fragment. The other three plots were constructed after a horizontal distance of 80 m from center to center of each plot (Figure 3.6). Finally, the transect reached up to a horizontal distance of 260 m towards the center of the fragment.
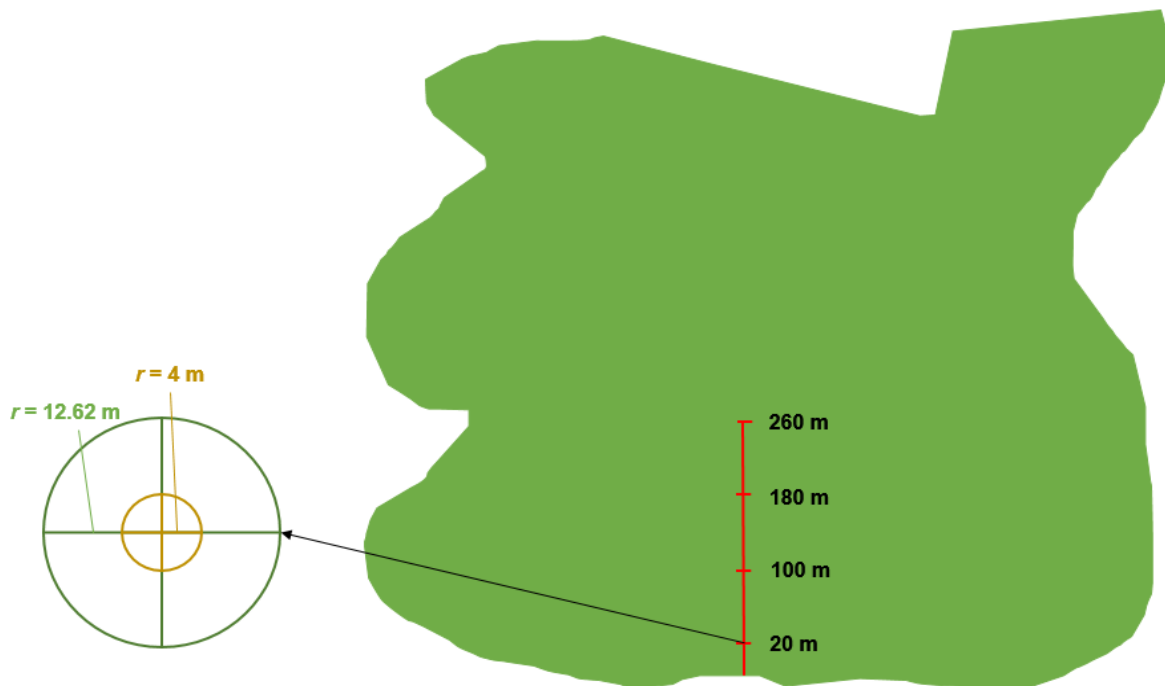
Figure 3.6. Sample design within each fragment (green background) with the transect (red line) from the edge of the fragment towards the center. The red dashes indicate the position of each plot/subplot (circles on the left side).

Based on values of other comparable studies found in the literature (Paula et al. 2011; Laurance et al. 2000; Nascimento and Laurance 2004, 2006). According to these studies, edge effects and fragmentation impacts are greatest within the first hundred meters from edges. The tree mortality is distinctive up to approx. 100 m from the fragment edge, causing long-term carbon losses (Ferreira and Laurance 1997). Besides, the pronounced tree mortality close to the fragment edges induces physiognomic tree alterations and increasing pioneer species communities as well as carbon releases to the atmosphere through decomposition, particularly in fragments < 25 ha (Pütz et al. 2014; Chaplin-Kramer et al. 2015). These incidents effect a biomass decline within the first 100 m of the fragment edge in relation to the fragment interior (Laurance et al. 1997). By contrast, Nascimento and Laurance (2004, 2006) observed biomass and density increments of trees < 10 cm DBH1.30 from tree growth and

recovery within the first 300 m. Nonetheless, these trees are susceptible to windthrow and physiological stress at the fragment edges (Paula et al. 2011).

The shape of all plots was a circle with a radius of 12.62 m and a surface area of approx. 500 m2 and 0.05 ha, respectively (Figure 6). The chosen size of the circle plot arose from empirical values. Thus, the tree layer should exhibit a representative size between 100-500 m2 (Steubing and Fangmeier 1992). The concept in each plot was to gather AGB information of all trees by measuring all living trees with a DBH1.30 ≥ 10 cm in total height, DBH1.30 and treetop coverage. To avoid double measurements and to do not forget the inclusion of sample trees, all relevant trees were counted and marked. A Brazilian botanist – specialized in Cerrado vegetation – determined each tree species. Each plot was located by recording the coordinates with a GPSMap 60CSx GARMIN hand tool in the plot center and geolocation of the smartphone. Additionally, a 360° photo was taken with a RICOH-THETA S camera. To include the shrub layer to the field survey, a subplot with a radius of 4 m and a surface area of approx. 50 m2 was established as a part of the center of the plot. Within this subplot, the number of shrubs was estimated and approx. 30 % of the estimated number of shrubs were measured in DBH0.30 and total height.

3.3.2 Data Collection

The data collection in the field was implemented by indirect, i.e. non-destructive methods, which are based on different wood variables and their mathematical evaluation as opposed to direct methods, where selected trees and shrubs are cut down and weighted. Regarding an allometric appraisal, the most important variables for the estimation of the AGB and the carbon stocks in the field survey are the DBH, the total height and the wood density of the woody components. These variables refer to the bole that accounts for the majority of aboveground woody biomass (Ribeiro et al. 2011). Further crucial variables are the treetop coverage, the tree species and the total basal area. The tree species, the DBH and the total height of trees and shrubs as well as the treetop coverage were directly identified or measured in the field, whereas the wood density and the basal area were determined afterwards. Shrubs, i.e. woody plants lower than 5 m were investigated in the same way as trees but only in the subplot. The number of trees and stems in the study area differed because the trees are frequently multi-stemmed. According to Ribeiro et al. (2011) this feature is common in the Cerrado biome. Therefore, multi-stemmed trees were not only tagged with a number but also with a letter, e.g. a multi-stemmed tree, numbered as 26 had two stems, which were tagged as 26A and 26B. The counting of the trees and stems in each plot enables a determination of the tree and stem density per hectare. For shrub layer measurements and estimates, the number of shrubs within the subplots was determined. The DBH measurements at 1.30 m aboveground were done with a diameter measuring tape (company

WEISS). Many trees exhibited two or partially even three stems. This irregularity modified the DBH appraisal by applying the following equation for multi-stemmed trees:

$$D_x = \sqrt{D1^2 + D2^2 + \cdots + Dn^2} \qquad (1)$$

where Dx is the resulting pooled diameter in cm and D12 to Dn2 are the individual stem diameters of the tree. For their forest inventory in a Cerrado sensu stricto in the state of Minas Gerais, Ribeiro et al. (2011) applied this equation that pools the diameters of multi-stemmed trees. Through the equation (1) by Ribeiro et al. (2011), the biomass of single-stemmed and multi-stemmed trees becomes comparable. Other irregularities like slanting stems, steep slope angles ties or buttress roots did not occur in this field survey. The total height of the trees with a DBH1.30 ≥ 10 cm within the sample plots was measured with the Vertex IV by Haglöf Sweden, a digital altimeter based on ultrasound technique. Within the subplot, the total height of approx. 30 % of the shrubs was primarily measured with a yardstick due to the low heights of the shrubs. The investigation of the treetop coverage was done by using the HabitApp on the smartphone, because of its indirect influence on the development of the subjacent aboveground biomass. Leaf biomass was neglected because it contributes < 5 % to the AGB (Delitti et al. 2006). The basal area is a variable that correlates with biomass and carbon. The basal area is an essential indicator of growth capacity and the tillering density of the stand, including the number of trees within a stand and their DBH (Kershaw et al. 2016). For the multi-stemmed trees, the pooled DBH1.30 value of the stems was squared. The tree's basal area (g) was calculated with:

$$g \; [m^2] = \frac{\pi}{40,000} \times DBH^2 [cm] \qquad (2)$$

Climatic and edaphic factors affect the woody growth and consequently the wood density. Therefore, the wood density is an important variable to indicate diameter growth rates, the successional stage of the particular study area as well as to predict the AGB of the woody components, particularly trees, through an allometric model (Chave et al. 2005; Baker et al. 2004; Fehrmann 2007). In this study, the wood density value for each tree species was obtained by the database of Zanne et al. (2009). The determination of the wood density for each tree species took place after the field survey as the botanist had identified each tree.

3.3.3   Allometric Biomass Models

Allometric biomass models are a favored method to estimate the AGB and carbon stocks of a previously investigated study area (Henry et al. 2013). By multiplying the dry AGB results of each tree by the factor 0.50, carbon mass for dry biomass was estimated (Balderas Torres and Lovett 2013).

According to Chave et al. (2004), the selection of an allometric model is the most significant error source concerning the statistical evaluation of the data. Additional error sources often occur during the field survey regarding uncertainties in the tree and shrub measurement as well as methodological sampling uncertainties with the result that the measuring of the plot area is inaccurate, trees lack, measured twice or standing dead trees are counted as alive (Chave et al. 2004). Furthermore, either the total tree height or the DBH as a sole variable of an allometric model, often causes an overestimation of AGB (Nogueira et al. 2008; Kauffman et al. 2009). There are allometric models for the Cerrado vegetation, so for the Cerradão and the Cerrado denso but the existing models are not directly related to the region around Nova Mutum in Mato Grosso. It is indeterminate which factors mainly influence allometric relationships in the tropics and after Chave et al. (2014), the quality of allometric models to assess AGB is limited (Chave et al. 2014; Malhi et al. 2006). Allometric equations, composed of several variables, often exhibit large differences in AGB estimation (Kauffman et al. 2009). Table 3.2 shows several multi-species allometric models that may fit the area of this study.

Table 3.2. Potential allometric models to estimate the AGB in the study area of the Cerradão and the Cerrado denso. AGB = dry biomass per tree [kg]; DBH = diameter at breast height [cm]; ρ = wood density [g cm-3]; H = total tree height [m].

Reference	Model[b]	Physiognomies
Brown (1997)	$AGB = \exp(-2.134 + 2.530 * \ln(DBH))$	tropical moist forests
Chave et al. (2005)	$AGB = 0.0509 * \rho * DBH^2 * H$	tropical moist forests
Chave et al. (2014)	$AGB = 0.0673 * (\rho * DBH^2 * H)^{0.976}$	pantropical vegetation
Miguel et al. (2017a, b)[c]	$AGB = 0.0123307 * DBH^{1.79393} * H^{1.54701}$	*Cerradão* in Tocantins
Rezende et al. (2006)	$AGB = 0.49129 + 0.02912 * DBH^2 * H$	*Cerrado s.s.* FD
Ribeiro et al. (2011)[a] m₁	$lnAGB = -3.3369 + 2.7635 * lnDBH + 0.4059 * lnH + 1.2439 * ln\rho$	*Cerrado s.s.* MG
Ribeiro et al. (2011)[a] m₂	$lnAGB = -3.1679 + 1.1438 * lnDBH^2 * H + 1.3079 * ln\rho$	*Cerrado s.s.* MG
Ribeiro et al. (2011)[a] m₄	$lnAGB = -3.3520 + 2.9853 * lnDBH + 1.1855 * ln\rho$	*Cerrado s.s.* MG

[a] developed their models after (Loetsch et al. 1973; Chave et al. 2005)

[b] the original symbols of each model were standardized for this study

[c] used a model after (Schumacher & Hall 1933)

The allometric models of Brown; Chave et al.; Chave et al. (1997; 2005; 2014), which base on large and diverse datasets, were developed to estimate the AGB of tropical trees, mainly in old-growth forests. Thus, the allometric equations must encompass a wide span of different and unique trees in tropical South America, Africa and Asia, whose total tree heights and DBH vary greatly in size. Although there is high biodiversity of trees in the study area of the Cerradão and the Cerrado denso in Nova Mutum, the range of the total tree height and the DBH is considerably smaller compared to Amazonia. After conducting initial calculations with these models, the results clarified that the models are not consummate for this study, especially for the Cerradão, assuming an overestimation of AGB values (Table 3.3). The same applies to the allometric models m1 and m2 by Ribeiro et al. (2011), where first calculations show that the AGB values, especially of the Cerradão, are overestimated, presumably due to the application of too many variables (Table 3.2; Table 3.3). The allometric model by Rezende et al. (2006) is adapted to a Cerrado sensu stricto site in Brasília. In general, this model would fit the investigated area of this study but compared to the model m4 by Ribeiro et al. (2011), the latter applied more similar field methods compared to this study, what enhances the comparability. Rezende et al. (2006) measured the DBH of the trees at 0.30 m above the ground, for example, whereas Ribeiro et al. (2011) measured at the common height of 1.30 m above the ground, just as it was conducted during this field survey. The model of Miguel et al.; Miguel et al. (2017a; 2017b) is the best available published model to derive AGB and aboveground carbon stock estimates of the Cerradão study site in Nova Mutum. AGB and aboveground carbon stock estimates of the Cerrado denso are derived from the model m4 of Ribeiro et al. (2011) that is the most appropriate one for this vegetation type. The two models were applied in a Cerradão in Tocantins and a Cerrado sensu stricto in Minas Gerais, respectively, after conducting direct measurements. The investigated sites have similar soil types, annual mean temperatures, altitudes, gradients and precipitation ranges compared to those in Nova Mutum. Furthermore, the field methods of both studies are similar to this study.

Table 3.3. AGB [Mg ha-1] of the investigated study area in Nova Mutum, calculated by different models to test their suitability. The applied models are bold.

Reference	AGB[a] [Mg ha^{-1}]	
	Cerradão	*Cerrado denso*
Brown (1997)	113.13 (± 1.3)	50.34 (± 0.5)
Chave et al. (2005)	117.79 (± 1.3)	32.65 (± 0.5)
Chave et al. (2014)	127.20 (± 1.3)	36.20 (± 0.5)
Miguel et al. (2017a, b)	**86.66 (± 24.4)**	20.27 (± 6.8)
Rezende et al. (2006)	98.55 (± 1.0)	28.30 (± 4.0)
Ribeiro et al. (2011) m_1	195.75 (± 48.1)	56.83 (± 16.4)
Ribeiro et al. (2011) m_2	269.61 (± 3.6)	63.52 (± 1.1)
Ribeiro et al. (2011) m_4	147.05 (± 36.2)	**48.90 (± 12.4)**

[a] included were all trees with a $DBH_{1.30} \geq 10$ cm

3.3.4 Statistical Evaluation

The statistical evaluation of the field data was performed with the graphical user interface RStudio that is meant for the statistical program language R (version 3.4.1) and with the spreadsheet software Microsoft Excel 2013. Thereby the individual plots of the transect within each fragment were regarded in detail mainly based on boxplots with the function boxplot() in RStudio. Besides, the plots were investigated in groups depending on the distance to the fragment border and separated per vegetation type, i.e. all first plots of the Cerradão were analyzed in groups as well as all second plots of the Cerradão were analyzed together. The non-parametric Kruskal-Wallis test – conducted with the kruskal.test() function in RStudio – was used, if there were significant differences within the variable data as well as within the AGB and aboveground carbon stock data from the border of the fragment to the center as well as between the two vegetation types. It was investigated if there were significant differences of the AGB and aboveground carbon stocks between the fragments of one vegetation type to assess whether the fragment size has an impact on the amount of AGB

3.4 Results

3.4.1 Cerradão and Cerrado Denso Characteristics

Overall, 1,182 trees and 1,241 stems were measured within the 32 plots as well as > 3,624 shrubs were recorded within the 32 subplots. Furthermore, the density of these aboveground woody components resulted in 739 tree individuals ha-1, 776 stem individuals ha-1 and > 23,381 shrub individuals ha-1 for both vegetation types together. Figure 3.7 shows the arithmetic means of the number of trees within the Cerradão and the Cerrado denso aggregated by plots. Figure 8 shows the arithmetic means of the number of shrubs within the Cerradão and the Cerrado denso aggregated by

plots. In plot 2 and 3 a higher number of trees exist with more than 40 in the Cerradão and 30 in the Cerrado denso. The arithmetic means of the number of shrubs gently decreased from the border of the fragment to the center in both vegetation types, illustrated in Figure 3.8. It has to be noted that the values of the summarized plot 4 of the Cerradão were computed without the values of the fourth plot in fragment C, because this plot showed strong anomalies, i.e. there were many shrubs that were moreover atypical due to their massive heights.
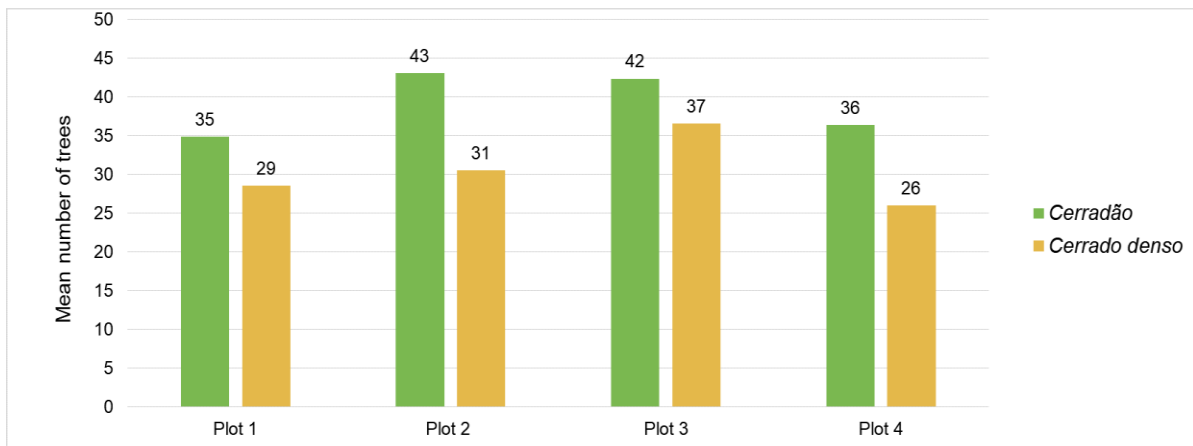
Figure 3.7. Mean number of trees within the study area in Nova Mutum, separated into Cerradão and Cerrado denso site and aggregated by plots.
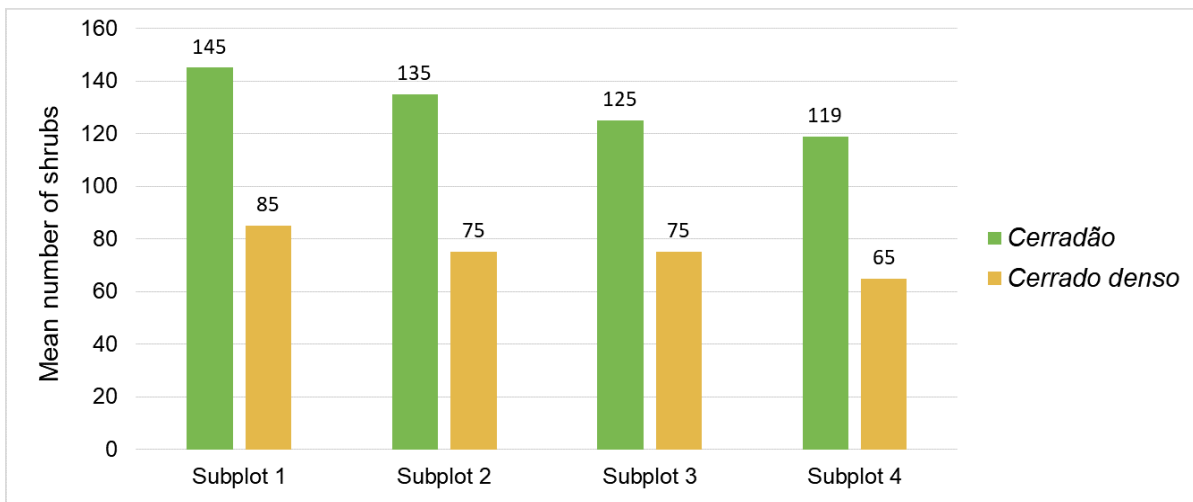
Figure 3.8. Mean number of shrubs within the study area in Nova Mutum, separated into Cerradão and Cerrado denso site and aggregated by subplots.

Comparing the number of trees for the single plots in the fragments A-H (Cerradão), there is a high variance without any trend from the border to the center (see Figure 21 in Kulp (2018) with 27 trees (fragment G) right up to 38 trees (fragment A) at the border and 25 trees (fragment C) right up to 47 trees (fragment H). For the Cerrado denso the tree number at the border (plot 1) is 28 (F) and 29 (E) and for plot 4 (center) 33 (E) and 19 (E).

Cerradão: The DBH as a component of the allometric model was tested for normal distribution (Figure 3.9). Most of the data lies in the smallest class from ≥ 10 - ≤ 15 cm. Boxplots of the DBH-distribution for each fragment show no great differences between the plots of each fragment and the fragment themselves (Figure 3.11). With the Kruskal-Wallis test on a significance level of α = 0.05 no significant differences between the grouped plots (p = 0.06) nor between the fragments (p = 0.17) could be proofed.
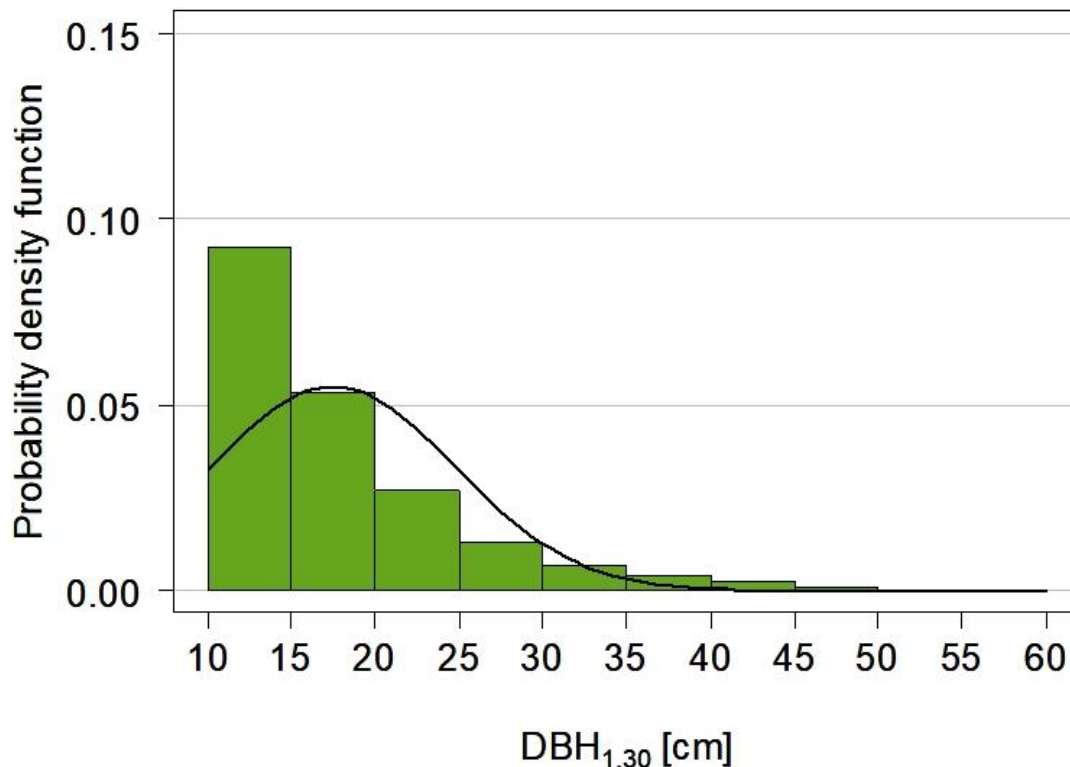
Figure 3.9. DBH classes of the Cerradão plots, represented by a probability density function, where the normal distribution curve is marked.

The total tree height as a further component of the allometric model for estimating the AGB of the Cerradão seems to follow a normal distribution (Figure 3.12), but the total tree height data had a right-skewed distribution. The higher total tree height values did not correspond to the normal distribution, therefore non-parametric statistical test were performed. The boxplots show that the tree height range is similar between the plots in fragment D, G and H (Figure 3.13). The greatest difference exists for fragment A within plot 1 with tree heights between 14.0 and 20.7 m (highest value for the Cerradão). In fragment C the highest trees are in the center (plot 4) with 7.5-20.0 m. The total tree height ranges from 4.5-21.1 m in the whole Cerradão. The significance tests (Kruskal-Wallis) showed no difference between the grouped plots with p = 0.8 (α = 0.05) (no border − center gradient), but across the

fragments exists a significant difference with p = 0.01. The post-hoc Dunn-Bonferroni test shows significant differences between fragment A and B (d = 1.42 after Cohen d-test) as well as for A and D (d = 1.80 after Cohen d-test).
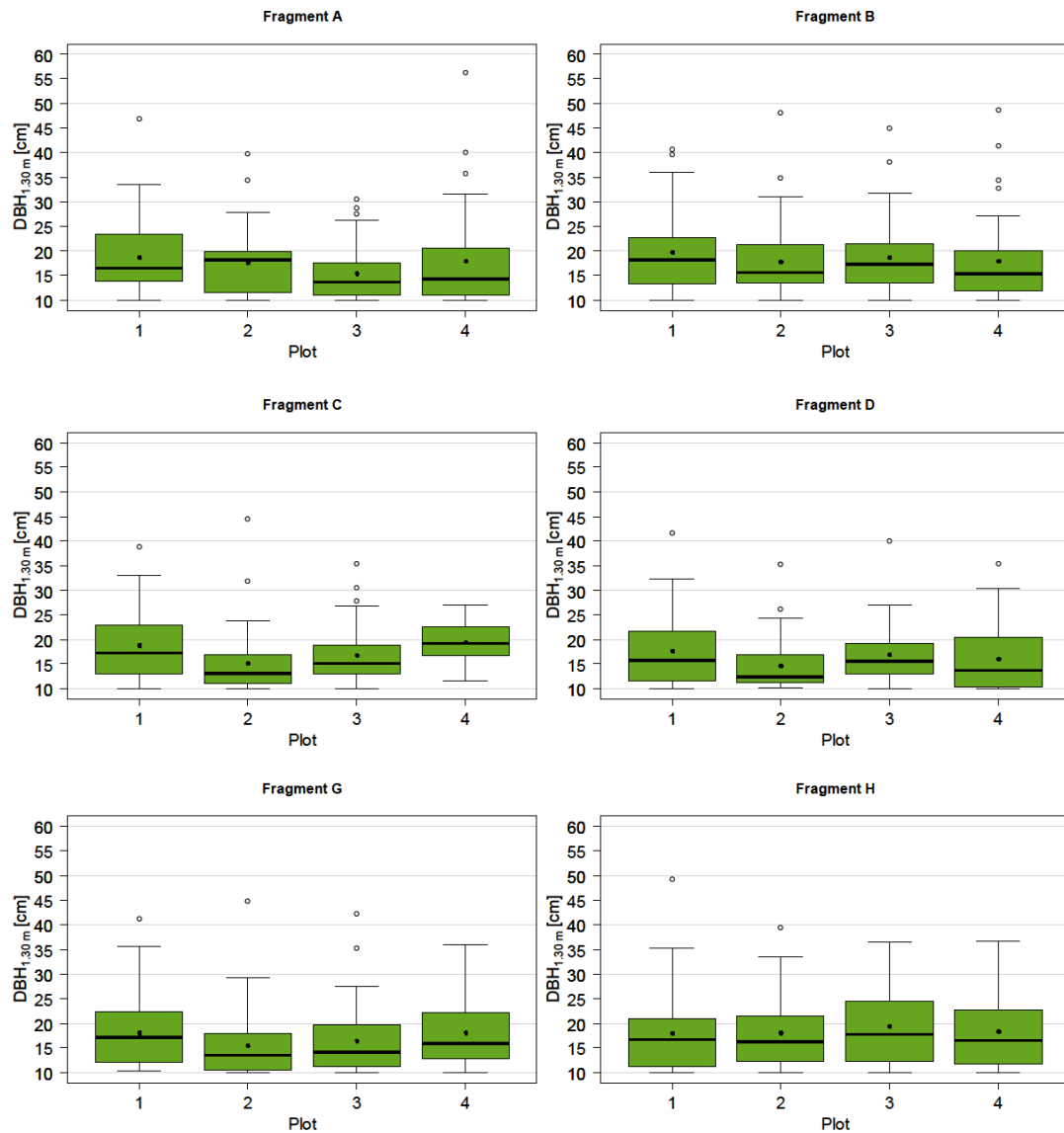
Figure 3.11. Boxplot graphs of the tree DBH1.30 [cm] distribution within the single plots of the investigated fragments (A-D and G-H) of the Cerradão. Outliers are described by white dots. The black dots represent the arithmetic mean of the respective plot.

Cerrado denso: The DBH distribution in the Cerrado denso was similar to the DBH distribution in the Cerradão. In the Cerrado denso most of the data are within the smallest class from $\geq 10 - \leq 15$ cm, the highest DBH value within the Cerrado denso study area was 32 cm (Figure 3.14). The data were not normally distributed. Figure 3.14 does not show significant differences of the tree DBH distribution from the border (plot 1) to the center (plot 4) in every fragment. In both fragments, the DBH range was

highest in plot 1 ranging from 10.0-23.2 cm in fragment E and from 10.0-29.2 cm in fragment F. There were no significant differences of the DBH between the grouped plots. The results showed a p-value = 0.24 (α > 0.05). Besides, the fragments showed no significant difference (p = 0.15, α > 0.05). A comparison of the arithmetic DBH means of both vegetation types based on the Kruskal-Wallis test with equal test conditions as above showed a significant difference with a p-value = 0.02 (α < 0.05). The Cohen d-value of 3.89 shows a large effect.

The total tree height [m] neither points out significant differences between the plots and the two fragments (Figure 3.15). The trees of the Cerrado denso were predominantly smaller compared to the trees of the Cerradão. Thus, the smallest tree within the Cerrado denso was an Eschweilera nana with a total tree height of 2.1 m (in Cerradão 4.5 m) and the highest tree was a Xylopia sericea with a total tree height of 14.3 m.
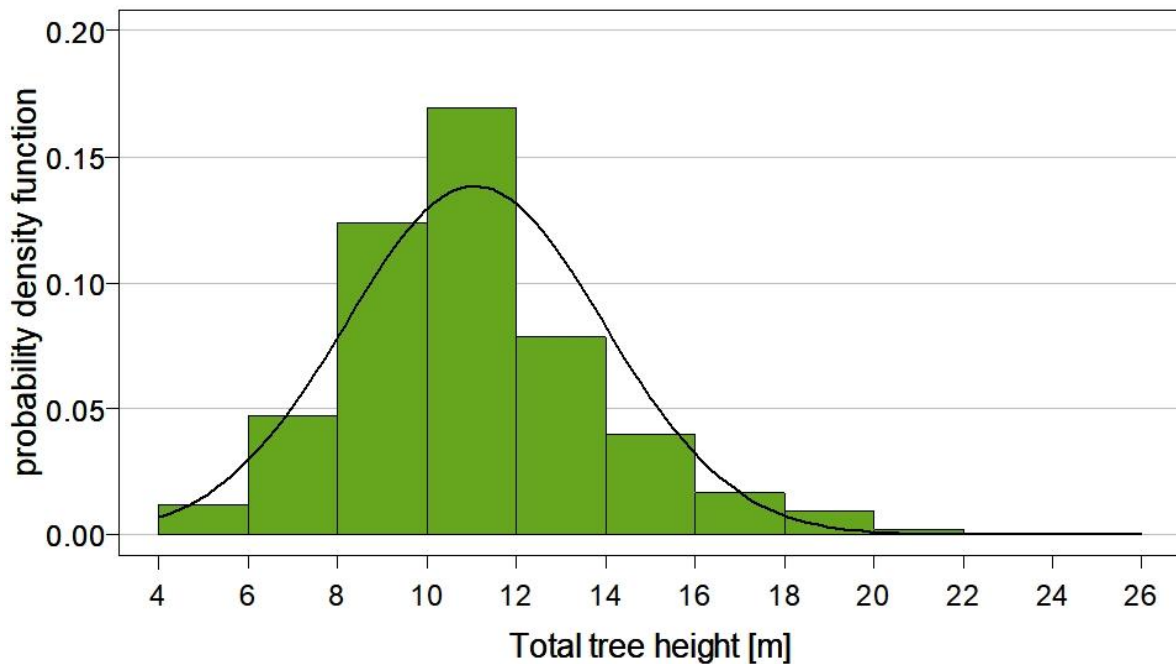
Figure 3.12 Tree height classes of the Cerradão plots, represented by a probability density function, where the normal distribution curve is marked.
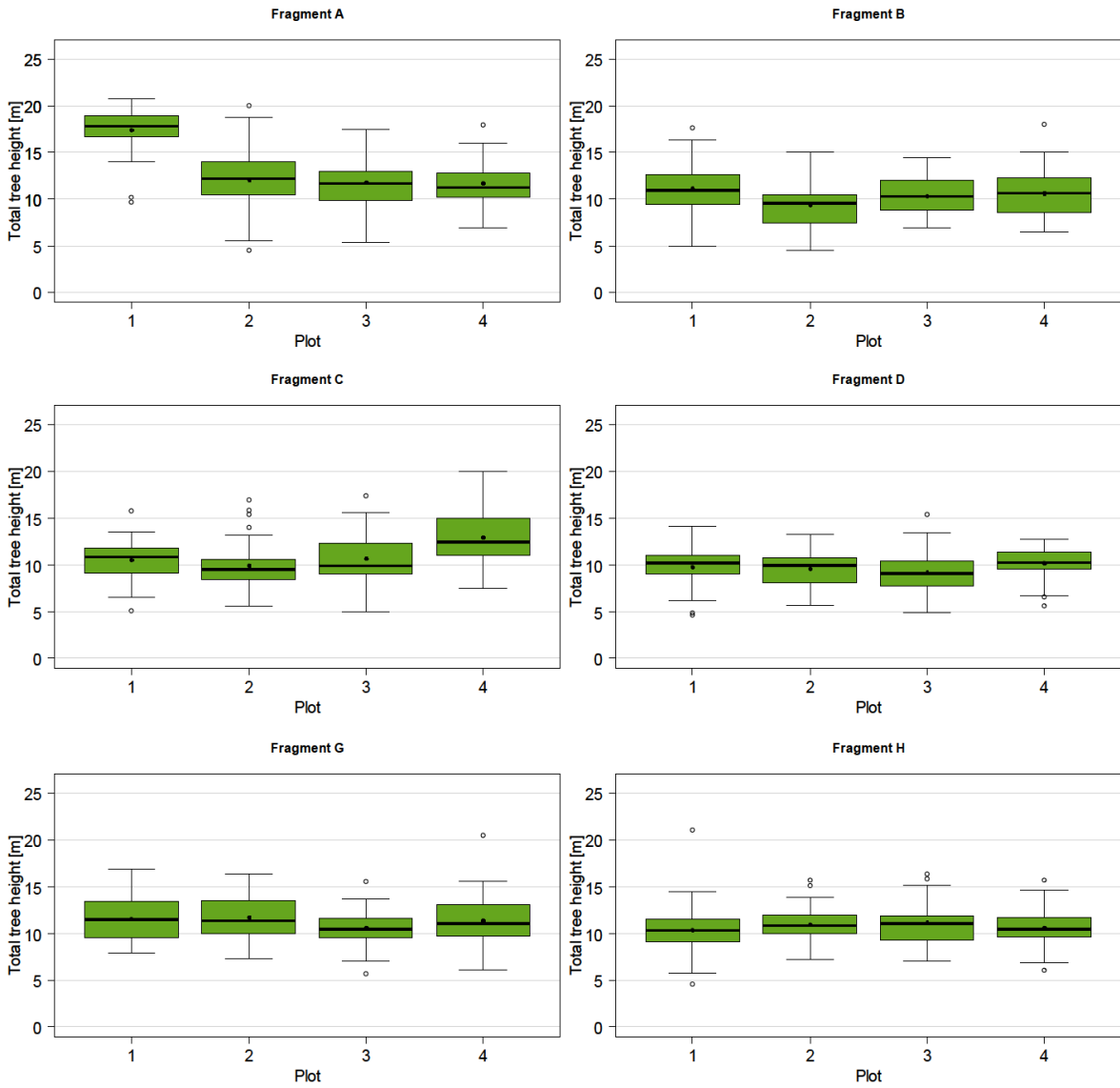
Figure 3.13 Boxplot graphs of the total tree height [m] distribution within the single plots of the investigated fragments (A-D and G-H) of the Cerradão. Outliers are described by white dots. The black dots represent the arithmetic mean of the respective plot.
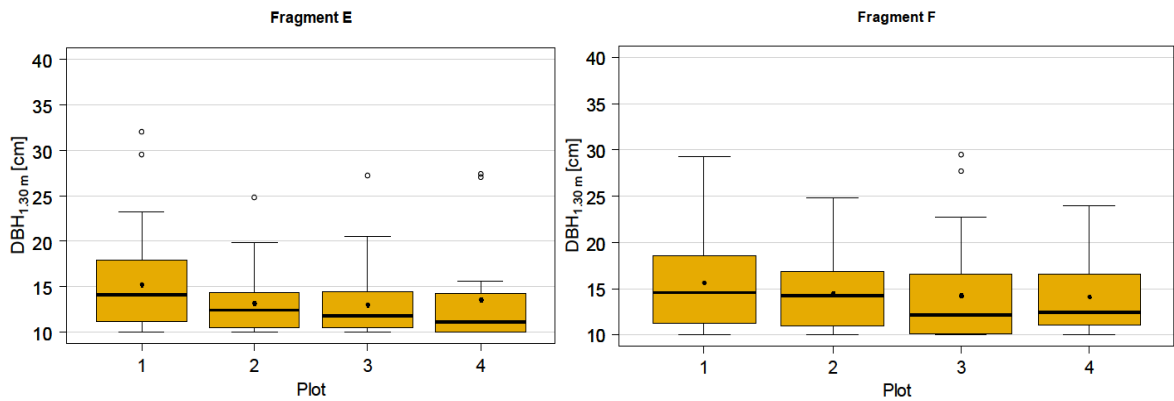
Figure 3.14 Boxplot graphs of the tree DBH1.30 [cm] distribution within the single plots of each investigated fragment (E-F) of the Cerrado denso. Outliers are described by white dots. The black dots represent the arithmetic mean of the respective plot.
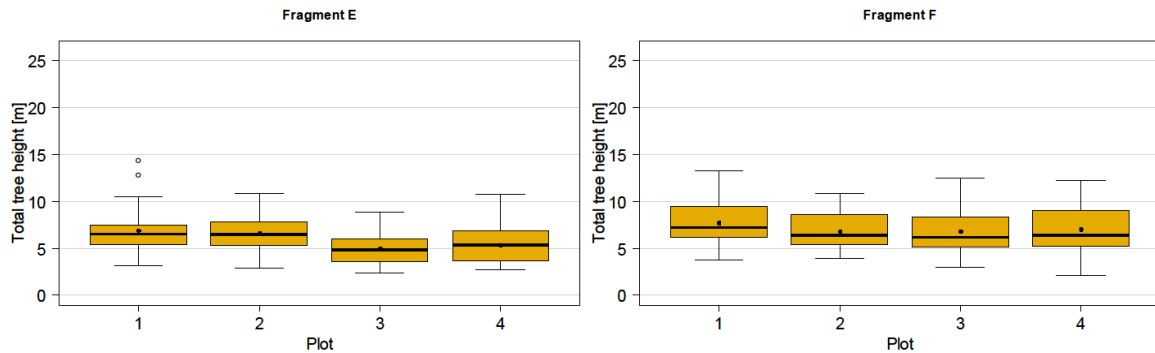
Figure 3.15 Boxplot graphs of the total tree height [m] distribution within the single plots of the investigated fragments (E-F) of the Cerrado denso. Outliers are described by white dots. The black dots represent the arithmetic mean of the respective plot.

3.4.2   Aboveground Biomass and Carbon Stock

To estimate appropriate AGB values for the study site, different models were tested for their suitability (Table 3.2). After conducting initial calculations (Table 3.3), the model of Miguel et al.; Miguel et al. (2017a; 2017b) was selected for the Cerradão calculations, whereas the model m4 by (Ribeiro et al. 2011) was selected for the Cerrado denso calculations (see 3.3). Pooled by plots, the Cerradão showed higher tree AGB means than the Cerrado denso (Figure 3.16). The highest mean was within the first plot in both vegetation types. In the Cerradão the means decreased from plot 1 with 95.05 Mg ha-1 (± 43.06) to plot 3 with 81.65 Mg ha-1 (± 14.11) and reached finally 87.76 Mg ha-1 (± 16.36) in plot 4. The Cerrado denso by contrast showed a decrease from plot 1 with 63.71 Mg ha-1 (± 5.11) to plot 2 with 44.82 Mg ha-1 (± 1.22). The third plot displayed a slight rise of 51.09 Mg ha-1 (± 10.41) and plot 4 had the lowest AGB mean with 35.99 MG ha-1 (± 16.77) (Figure 3.16). Due to lower DBHs and total heights of the shrubs compared to the trees, the arithmetic means of the shrub AGB per subplot were also much lower than the means of the tree AGB (Figure 3.17). In contrast to fragmentation studies (Nascimento and Laurance 2004) subplot 1 – with a distance of 20 m to the border of the fragment – had the lowest AGB within the Cerradão (0.16 Mg ha-1) and within the Cerrado denso with 0.61 Mg ha-1.
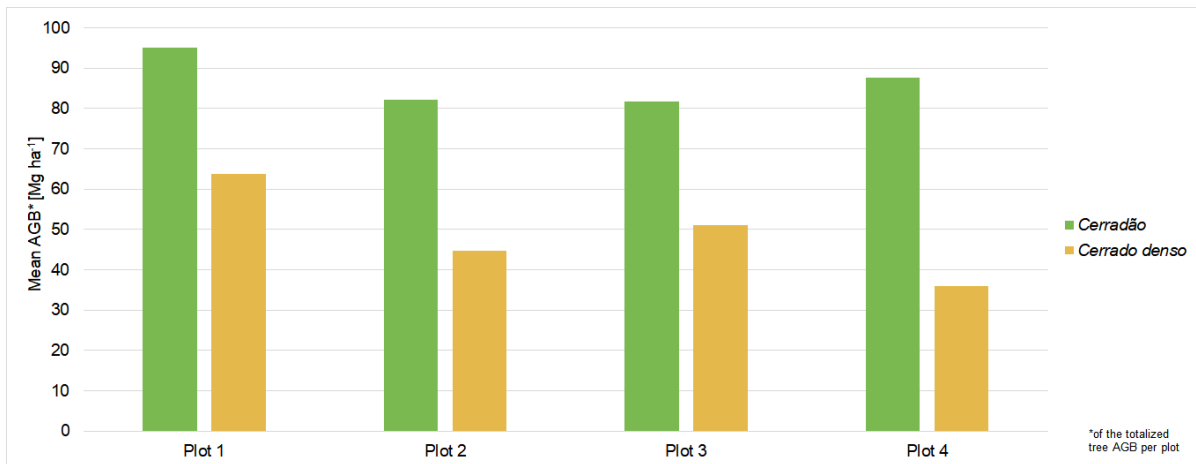
Figure 3.16 Arithmetic mean of the AGB [Mg ha-1] of the totalized tree AGB per plot, separated into Cerradão and Cerrado denso site, grouped by plots.

The distribution of the AGB per tree follows the DBH distribution (Figure 3.9), most of the data lies in the smallest class (0.0 to ≤ 0.1 Mg). The residuals of the tree AGB (Q-Q-plot in Kulp (2018) show that most of the data points are in straight line, but the smallest and highest quantiles differed strongly, so that a normal distribution is not given. As for the DBH boxplot diagrams, the AGB per plot and fragment illustrates the highest variance for fragment A and C, due to extreme outliers with some tree species (Humiria balsamifera 1.33 Mg in plot 1 and Buchenavia grandis with 1.48 Mg in plot 4, fragment A).
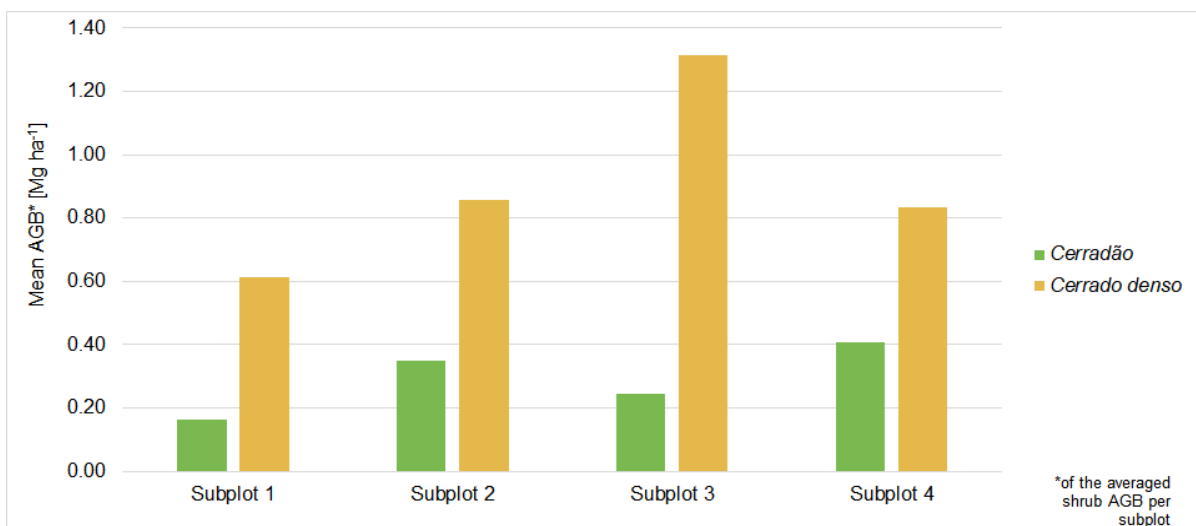
Figure 3.17 Arithmetic mean of the shrub AGB [Mg ha-1] per subplot, separated into Cerradão and Cerrado denso site, grouped by subplots.

The results of tree AGB and therefore of carbon stocks show no clear distribution pattern, concerning fragment differences and plot differences (border to center). The non-parametric Kruskal-Wallis test with $p = 0.54$ ($\alpha = 0.05$) proofs that no significant differences exist between the fragments. Even for the grouped plots with $p = 0.11$ ($\alpha = 0.05$) no significant differences exist. The absolute values

per ha for the plots of all Cerradão fragments have a great variance with 51.52 Mg ha-1 to 177.72 Mg ha-1. Most of the plots exhibit values between 80 and 100 Mg ha-1 (Table 3. 4).

Table 3.4 Sum of the tree AGB and carbon stocks in Mg ha-1 per plot within each fragment in the Cerradão.

Fragment	A				B			
Plot	1	2	3	4	1	2	3	4
AGB [Mg ha^{-1}]	177.72	97.35	96.85	96.31	101.94	70.73	79.81	87.53
C [Mg ha^{-1}]	88.86	48.67	48.43	48.15	50.97	35.36	39.90	43.77
Fragment	C				D			
Plot	1	2	3	4	1	2	3	4
AGB [Mg ha^{-1}]	69.50	74.58	68.13	76.41	73.36	51.52	63.77	62.14
C [Mg ha^{-1}]	34.75	37.29	34.06	38.20	36.68	25.76	31.89	31.07
Fragment	G				H			
Plot	1	2	3	4	1	2	3	4
AGB [Mg ha^{-1}]	60.48	100.80	83.76	96.19	87.28	98.09	97.60	107.96
C [Mg ha^{-1}]	30.24	50.40	41.88	48.10	43.64	49.04	48.80	53.98

3.5 Discussion

3.5.1 Plot Characteristics

With the allometric models and estimated plot parameters DBH, H and ρ (see Table 3.2) the tree AGB for the two vegetation types in Nova Mutum was calculated (Table 3.3). Because of the direct measurements (tree yield method) and comparable environmental conditions in Tocantins (Cerradão, (Miguel et al. 2017a; Miguel et al. 2017b) and Minas Gerais (Cerrado denso, sensu stricto, (Ribeiro et al. 2011) their allometric models were used to discuss the AGB and carbon stocks. The results with different allometric models (Table 3.3) show the great variance within each vegetation type. In the study of Miguel et al.; Miguel et al. (2017a; 2017b) who investigated 54 plots (400 m2 each), the tree density was 1150 ha-1 compared to our study with 783 ha-1. Around 80 % of single trees lies in the DBH-class 10-20 cm whereas the study of Miguel et al.; Miguel et al. (2017a; 2017b) had around 90 % (5-20 cm DBH). The highest biomass portion is given by the DBH-classes 10-20 cm, similar to our study. The AGB (bole and crown) was calculated with 61.7 (± 5.4) Mg ha-1, for Nova Mutum the value is 86.7 (± 24.4) Mg ha-1. The other allometric estimations (Table 3.3) with AGB > 100 Mg ha-1 are too high. The AGB-portion for the DBH-class 5-10 cm in the Cerradão of Tocantins was 10 %. For the dense woodland (forested savanna Sd) Fearnside et al. (2009) indicated 51.2 Mg ha-1, whereas the seasonal forest as a transition to the rainforest had 252 Mg ha-1. For the Cerrado denso in Minas Gerais with 2086 trees ha-1 Ribeiro et al. (2011) calculated the AGB with 62.9 Mg ha-1, for Nova Mutum 48.9 Mg

ha-1 is given with a lower tree density (608 ha-1). The tree density differences may result from different human impacts and that trees > 5 cm DBH were measured (Nova Mutum ≥ 10 cm DBH). The absolute variance of DBH in Ribeiro et al. (2011) was 5-43.9 cm (mean 8.7 cm), in our study 10-29.5 cm (mean 14.1 cm). For the Cerradão in Tocantins the variance of DBH was 5-65 cm (no mean written), for Nova Mutum 10-44.8 cm (one outlier in plot 1, fragment A with 55.3 cm). The basal area with 14.9 m2 ha-1 was higher in Minas Gerais compared with Nova Mutum 10.5 m2 ha-1 (Table 3.5). The shrub biomass cannot be neglected in both vegetation types. For Cerradão shrub AGB is 7 % of total AGB (tree and shrub), for Cerrado denso it amounts to 13 % (Table 3.5). In Ribeiro et al. (2011) the portion is smaller (7.4 %). Because of the more open treetop coverage shrubs are more common in the Cerrado denso then in the Cerradão (Fearnside et al. 2009), but in the Nova Mutum fragments the difference is not so great (Table 3.5), which indicates the logging impact in the Cerradão. Unfortunately, shrub biomass and treetop coverage is not given in Miguel et al.; Miguel et al. (2017a; 2017b).

Table 3.5 Summary of the study results within the Cerradão and the Cerrado denso.

Vegetation type	Investigated area [ha]		Number of				Dominant tree species
	trees	shrubs	trees [ha⁻¹]	stems [ha⁻¹]	shrubs [ha⁻¹]	species	
Cerradão	1.2	0.115	783	811	> 26,296	81	Sacoglottis mattogrossensis
Cerrado denso	0.4	0.04	608	670	> 15,000	52	Tachigali paniculata

Vegetation type	AGB [Mg ha⁻¹]			C [Mg ha⁻¹]			Mean DBH [cm]	
	trees	shrubs	overall	trees	shrubs	overall	trees	shrubs
Cerradão	86.66	6.57	93.23	43.32	3.29	46.61	17.5	2.2
Cerrado denso	48.90	7.23	56.13	24.45	3.62	28.07	14.1	2.9

Vegetation type	Mean total height [m]		Mean TTC [%]	Mean WD [g cm⁻³]	Mean total BA [m² ha⁻¹]
	trees	shrubs			
Cerradão	11.1	2.5	73.7	0.69	22.1
Cerrado denso	6.5	3.2	66.2	0.67	10.5

The Cerradão had a larger number of trees, stems and shrubs per hectare than the Cerrado denso. However, the latter had a greater proportion of multi-stemmed trees. The AGB and aboveground carbon stocks (C) per hectare were almost two times greater in the Cerradão. The AGB and C-stocks in

the shrubs of the Cerrado denso were higher, despite a higher shrub number in the Cerradão. Mean DBH and height was greater in the Cerrado denso (Table 3.5). The mean treetop coverage (TTC), wood density (WD) and basal area (BA) were always larger in the Cerradão, but the wood density values did not differ strongly.

Compared with other studies in the Cerrado biome, the tree density of this study was significantly lower, exhibiting 739 individuals ha-1 pooled for both vegetation types. Especially the tree density of the Cerradão with approx. 783 individuals ha-1 was lower than the tree density of other Cerradão areas in Brazil that varied according to the studies of Miguel et al.; Miguel et al. (2017a; 2017b) and Souza et al. (2010) from 1,172-1,251 individuals ha-1. Rezende et al. (2006), found a density of 681 trees ha-1 in a Cerrado sensu stricto in Brasília, including trees with a DBH1.30 ≥ 5 cm, similar to our study. The high Cerradão tree densities of other studies were predominantly obtained by including trees with a DBH1.30 ≥ 5 cm (Miguel et al. 2017a). Depending on the definition of the woody components, which constitute the AGB, several shrubs in this study would possibly considered as trees in other studies.

The applied allometric models did not include the basal area. The basal area results outlined the tillering density of the study area and stated an indirect insight into the amount of AGB. The mean total basal area of the Cerradão study area amounted to 22.1 m2 ha-1. Consequently, it lies within the range of 17.05-24.90 m2 ha-1 for Cerradão areas (Miguel et al. 2017a). Furthermore, this value is similar to the conclusions of Miranda et al.; Scolforo et al.; Miguel et al. (2014; 2008; 2017a) who had a total basal area of > 20 m2 ha-1 on Cerradão areas scattered across the whole Cerrado biome, 17.58 m2 ha-1 on a Cerradão study site in Minas Gerais and 17.34 m2 ha-1 on a Cerradão site in Tocantins, respectively. A gallery forest in Mato Grosso in contrast, exhibited a total basal area of 33 m2 ha-1 (Holzner 2013). The mean total basal area of the Cerrado denso study area amounted to 10.5 m2 ha-1. This outcome is slightly lower compared to the total basal area determined by Abdala et al. (1998) with 14.5 m2 ha-1 in a Cerrado denso in the Federal District (DF) or compared to the basal area of 14.9 m2 ha-1 detected by Ribeiro et al. (2011) in a Cerrado sensu stricto in Minas Gerais. The calculated value for the Cerrado denso in this study is within the range of other studies. The treetop coverage results are in the given value range of 50-90 % for the Cerradão and of 50-70 % for the Cerrado denso in the whole Cerrado biome (see mean TTC in Table 3.5; Fearnside et al. 2009; Dodonov et al. 2013). The distance to the border of the fragment had no impacts on the treetop coverage.

The mean wood density results of this study are quite high (Table 3.5). Miranda et al. (2014) also determined a high mean wood density value of 0.66 g cm-3 for the shrubs and trees in the whole Cerrado biome. This value was similar to a mean wood density of 0.67 g cm-3 determined in Central Amazonia (Miranda et al. 2014). The high wood density values of the Cerradão study area are caused by the high wood density values of the most common tree species. Thus, Sacoglottis mattogrossensis

with a wood density of 0.77 g cm-3 was the dominating tree species in the Cerradão. The Cerrado denso study area has a relatively high mean wood density due to several tree species with a wood density ≥ 0.90 g cm-3.

The diameter range for the Cerradão trees (10.0-56.3 cm) and for the Cerrado denso trees (10.0-32.0 cm) in this study was similar to the diameter range of Miguel et al.; Miguel et al. (2017a; 2017b) that varied from 5.0 - > 60.0 cm and the pooled diameter range in the study of Ribeiro et al. (2011) that varied from 5.0-43.9 cm. Compared to other studies, the arithmetic mean of the DBH in this study is higher in both vegetation types (Table 3.5), because the DBH of 5 - ≤ 10 cm was not included. The trees of the Cerrado sensu stricto in the study by Ribeiro et al. (2011) revealed an arithmetic DBH mean of 8.7 (± 3.8) cm and the trees of the Cerradão site in Tocantins in the study of Miguel et al. (2017a) showed a mean DBH value of 11.55 (± 6.9) cm. According to Holzner (2013), who investigated gallery forests in Mato Grosso, the arithmetic mean of the DBH amounted to 13.35 (± 9.16) cm. This substantial difference results by the non-consideration of DBH1.30 values < 10 cm, i.e. the mean of the DBH would be lower if smaller trees would have been included. Furthermore, the pooling of the diameters in the case of multi-stemmed trees, triggered partly higher diameter values for these trees. Methods of DBH-estimation from multi-stemmed trees are often not documented.

3.5.2   AGB and C Estimation

Allometric models had been applied that focus mainly on large diameters – like the model by Chave et al. (2005) – so that the AGB for smaller trees and especially for shrubs would have been overestimated (van Breugel et al. 2011). Moreover, according to Delitti et al. (2006) and van Breugel et al. (2011) the inclusion of a second variable to an allometric model improves the AGB estimates significantly on the plot level. In this study, the wood density and the total tree height functioned as the second variable. Nevertheless, the outcomes differ as in Miguel et al.; Miguel et al. (2017a; 2017b) with an AGB value of 61.67 Mg ha-1 in a Cerradão in Tocantins. Despite including dead and alive trees with a DBH1.30 ≥ 5 cm, the AGB per hectare is slightly lower in the study of Miguel et al.; Miguel et al. (2017a; 2017b) compared to this survey (Table 3.5). However, the AGB of 73.97 Mg ha-1 of a Cerrado sensu stricto in Minas Gerais, which was determined by Ribeiro et al. (2011), who included all plants with a DBH1.30 ≥ 5 cm was distinctly higher by contrast with the AGB of the Cerrado denso in this study (Table 3.5). The inclusion of the lower diameter plants could be already crucial for the disparities in AGB. Ribeiro et al. (2011) stated that their findings were relatively large compared to reference values of other Cerrado sensu stricto, probably interrelated with the selection of sample trees. The AGB of shrubs was within the value range presented by other studies (e.g. 4.68 Mg ha-1 by (Ribeiro et al. 2011).

Due to the high quantity of shrubs in this study, the AGB of shrubs was higher both in the Cerradão and in the Cerrado denso (Table 3.5).

The study area is partially located in the ZOT to Amazonia, so that the estimated AGB and its carbon stocks per hectare were higher compared to other Cerradão and Cerrado denso sites in the Cerrado biome. In consideration of the AGB and aboveground carbon stock reference values by different authors, illustrated in Table 3.6, this assumption can be partially confirmed. Thus, the AGB and its carbon stocks in Mg ha-1 of the Cerradão determined by Scolforo et al.; Santos et al.; Morais et al.; Miranda et al. (2008; 2010; 2013; 2014) are lower compared to this study. That also applies to the AGB and aboveground carbon stocks in Mg ha-1 of the Cerrado denso determined by Castro (1995) and Ottmar et al. (2001) (Table 3.6). Similar to this study, Marimon et al. (2014) investigated a protected Cerradão site in the ZOT, i.e. in Nova Xavantina, Mato Grosso. Their analysis, basing on the Cerrado model by Ribeiro et al. (2011) featured an AGB value of 120.2 (± 25.1) Mg ha-1, which is higher than in other investigated Cerradão sites.

By comparing both vegetation types with each other, the DBH and therefore the AGB is significantly different ($p = 0.02$). This can be explained by differing vegetation physiognomies. The DBH1.30 variable and the total tree height variable were also tested for differences between the fragments (Kruskal-Wallis test). There were no significant differences in the DBH values between the fragments, neither in the Cerradão ($p = 0.17$) nor in the Cerrado denso ($p = 0.15$), so it is proved that the fragment size and shape have no influence on the development of the trees DBH. Based on the statistical analysis of the total tree heights between the fragments ($p < 0.05$), it can be assumed that the fragment size as well as the fragment shape could have an influence on the development of the total tree height. (mainly due to plot 1 in fragment A).

Table 3.6 AGB and carbon stock reference values of different study areas from the literature.

Localization	Vegetation type	Measurement criteria	AGB [Mg ha^{-1}]	Carbon stocks [Mg ha^{-1}][c]	Reference
DF, Brazil	*Cerrado sensu stricto*	Height > 2 m (DBH$_{0.30}$ and DBH)	12.8	6.4	Castro & Kauffman (1998)
DF, Brazil	*Cerrado sensu stricto*	DBH$_{0.30}$ ≥ 5 cm	12.4	6.2	Vale et al. (2002)
DF, Brazil	*Cerrado sensu stricto*	DBH$_{0.30}$ ≥ 5 cm	9.85	4.93	Rezende et al. (2006)
MG, Brazil	*Cerrado sensu stricto*	All shrubs and trees in the plot	17.1	8.55	Lilienfein et al. (2001)
MT, Brazil	*Cerrado sensu stricto*	DBH$_{0.30}$ ≥ 2 cm	35.4	17.7	Ottmar et al. (2001)
MT, Brazil	*Cerrado sensu stricto*	All shrubs and trees in the plot	12.4	6.2	Araujo et al. (2001)
Brasília, DF, Brazil	*Cerrado sensu stricto*	All woody plants with a circumference > 6 cm at 30 cm up from the soil level	26.02	13.01	Abdala et al. (1998)
MG, Brazil	*Cerrado sensu stricto*	All plants with a DBH ≥ 5 cm	73.97	36.99	Ribeiro et al. (2011)
Tocantins, Brazil	*Cerradão*	Trees, alive or dead with a DBH ≥ 5 cm	61.67	30.84	Miguel et al. (2017a, b)
Nova Xavantina, MT, Brazil	preserved *Cerradão*	All individuals with a DBH ≥ 5 cm	45.09-54.48	22.55-27.24	Peixoto et al. (2017)
Nova Xavantina, MT, Brazil	regrown *Cerradão*	All individuals with a DBH ≥ 5 cm	24.55-24.71	12.28-12.36	Peixoto et al. (2017)
MG, Brazil	*Cerradão*	All woody plants	47.80	23.90	Scolforo et al. (2008)
MT, Brazil	*Cerradão*	All woody plants	72.30	36.15	Santos et al. (2002)
Nova Xavantina, MT, Brazil	protected *Cerradão*	All plants with a DBH ≥ 10 cm	120.2 (± 25.1)[a]	60.1	Marimon et al. (2014)
MG, Brazil	*Cerradão*	All plants with a DBH ≥ 5 cm	73.56	36.78	Morais et al. (2013)
Cerrado biome	*Cerradão*	All plants with a DBH ≥ 5 cm	79.66 (32.3 %)[b]	39.83	Miranda et al. (2014)
Brasília, DF	*Cerrado denso*	All woody plants	24.94	12.47	Castro (1995)
n/s	*Cerrado denso*	Total AGB	29.90-71.89	14.95-35.95	Bustamante & Ferreira (2010)
MT, Brazil	*Cerrado denso*	All woody plants	47.78	23.89	Ottmar et al. (2001)
Dassari basin, Benin, Africa	Savanna woodland	All woody plants	45.29 (± 2.51)[a]	22.65	Chabi et al. (2016)
Dassari basin, Benin, Africa	Shrub savanna	All woody plants	14.05 (± 0.72)[a]	7.03	Chabi et al. (2016)
Europe	Beech forest (*Fagus sylvatica*)	Tree AGB	238	119	Jandl et al. (2007)
Europe	Oak forest (*Quercus* sp.)	Tree AGB	166	83	Jandl et al. (2007)

n/s: not specified
[a] standard deviation in parentheses
[b] coefficient of variation (%) in parentheses
[c] mainly calculated by multiplying with the factor 0.5

According to Nascimento and Laurance (2004) fragmentation in Amazonia that is primarily induced by deforestation, alters the AGB and carbon stocks essentially, i.e. the fragments are characterized by a general carbon stock decline, mainly because small successional trees and lianas prevail in contrast to old-growth trees. Pütz et al. (2014), who investigated fragmented neotropical forests determined lower carbon stocks in smaller fragments than in larger ones. In general, it was quantified that the global carbon loss rate in fragmented tropical forests ranges between 0.12-0.24 Gt C year-1 (Pütz et al. 2014). According to the second hypothesis, the fragmentation triggers negative edge effects, i.e. the AGB is lower at the border of a fragment compared to its center, a Kruskal-Wallis test showed that the AGB was equal from the fragment border to the center, both in the Cerradão (p = 0.11) and in the Cerrado denso (p = 0.22). Moreover, the components of the AGB, i.e. the DBH and the total tree height also demonstrated that the AGB was equal from the fragment border to its center. The outcomes of this study in the Cerrado demonstrate that fragmentation does neither substantially modify the quantity nor the distribution of AGB in the Cerrado study area in Nova Mutum. A main influencing factor is the age and intensity of human impacts by selective logging, which is not restricted to the fragment border.

3.6   Conclusion

With the surface area of the Cerradão and of the Cerrado denso in Mato Grosso as well as of the whole Cerrado, an estimation of the total AGB and aboveground carbon stocks is possible. The AGB of the Cerradão in Mato Grosso amounted to 0.27 Gt and the aboveground carbon stocks to 0.14 Gt whereas the AGB and the aboveground carbon stocks of the Cerrado denso in Mato Grosso amounted to greater values of 0.36 Gt and 0.18 Gt, respectively. This is due to the greater surface area of the Cerrado denso in Mato Grosso (Table 3.7). The AGB and the aboveground carbon stock results of the Cerrado denso in the whole Cerrado biome amounted to 1.38 Gt and 0.69 Gt, for the Cerradão to 0.95 Gt (0.48 Gt C).

Table 3.7 Extrapolation of the estimated AGB [Gt] and aboveground carbon stocks (C) [Gt] for Mato Grosso and the Cerrado biome.

	Mato Grosso[a]		Cerrado biome[b]	
	AGB [Gt][c]	C [Gt][c]	AGB [Gt][c]	C [Gt][c]
Cerradão	0.29	0.15	0.95	0.48
Cerrado denso	0.41	0.21	1.38	0.69

[a] Surface area of Mato Grosso: around 904,982.33 km^2, approx. 31,495.29 km^2 thereof are *Cerradão* and approx. 73,121.62 km^2 thereof are *Cerrado denso*

[b] Surface area of the Cerrado biome: around 2,000,000 km^2, approx. 101,879.85 km^2 thereof are *Cerradão* and approx. 245,643.60 km^2 thereof are *Cerrado denso*

[c] These values – consisting of tree and shrub results – were generated from the estimated AGB and carbon stock values, which were calculated with two different allometric models

The AGB estimations and therefore the C-stocks for the Cerrado Biome differ to a great amount. Marimon et al. (2014) determined a quite high AGB value of 120.2 Mg ha-1 for a protected Cerradão area, whereas Peixoto et al. (2017) determined considerably smaller AGB values ranging from 45.09-54.48 Mg ha-1 for a preserved Cerradão. Nogueira et al. (2015) emphasized that Mato Grosso has the largest cleared area in the forest and nonforest types with 338,530.22 km2 in Brazil's Legal Amazonia region (status for 2013). The total AGB declined from around 19.05 Gt in the 1970s to approx. 11.77 Gt in 2013, this corresponds to an AGB loss of around 38.2 %. The extrapolations of the AGB and carbon stock results in this study (Table 3.7) mention that the AGB of 0.29 Gt for the Cerradão in Mato Grosso and the AGB of 0.41 Gt for the Cerrado denso in Mato Grosso seem negligible by comparing them with the Brazilian Amazon AGB of 87.6 Gt. Nevertheless it is essential, because it regulates the water and carbon cycle and preserves biodiversity on a regional scale. The deforestation or even selective logging that leads to a decline of AGB, induces aboveground carbon releases and might change regional climatic processes, including the decrease of precipitation with the simultaneous increase of the water deficit in the arc of deforestation (Malhado et al. 2010). After Oliveira et al. (2014) the evapotranspiration (Eta) will decrease with deforestation to pasture or cropland for Cerradão (Eta 1272 ± 364 mm yr-1) and Cerrado sensu stricto denso (Eta 1268 ± 313 mm yr-1) will decrease by 500-550 mm yr-1. Finally, the AGB and the carbon storage capacity are crucial for the regional water and carbon cycle as well as for global energy and water fluxes.

Author contributions:

Larissa Kulp – validation, formal analysis, investigation, data curation, writing—original draft preparation, visualization

Flávia de Souza Mendes – conceptualization, methodology, investigation, resources, writing—review and editing, visualization, supervision, project administration, funding acquisition

Gerhard Gerold – methodology, investigation, resources, writing—review and editing, visualization, supervision, funding acquisition

4. Time series of optical remote sensing to assess the edge effect in fragments of Cerrado biome

In preparation.

Abstract

Deforestation leads to fragmentation and corresponding edge effects, e.g. microclimate deterioration at the forest border, tree mortality and changes in the vegetation structure and productivity. Fragmentation decreases carbon and biomass in the forest. However, most studies about edge effects are focused on temperate and tropical biomes, such as the Amazon. A small number of studies assessed the Cerrado biome, which is considered a hotspot for biodiversity. Furthermore, this biome has a major influence on large river basins' water resources of large basins, such as the Amazon. We evaluated the edge effect in the long-term based on NDVI values of the transitional area between the Cerrado and Amazon biomes. The method described in this study corroborates studies that assessed edge effect on vegetation within the Cerrado and Amazon biomes. In this study, we applied a different approach to investigate possible edge effects using vegetation index from freely available time series satellite images. Our results showed a positive and significant trend (p-value < 0.00005) via the NDVI values in relation to distance from the nearest edge, thus, the closer the vegetation was to the edge, the lower their respective NDVI value. Our results suggest that the NDVI can be used to identify edge effects in the vegetation. Nevertheless, more studies are needed to adequately understand the dynamics of edge effects.

4.1   Introduction

Tropical forests play an important role in the context of the Earth's carbon cycle. Consequently, such areas must be preserved. Yet, deforestation within these areas is increasing. Achard et al. (2014) reported a tropical forest cover loss for 1990s and 2000s of 6.05 million ha yr^{-1} and 5.93 million ha yr^{-1}, respectively, which results in an annual rate of deforestation of 0.49 %. At this alarming deforestation rate, it is essential that measures against deforestation are reevaluated to ensure a sustainable contribution to the Earth's carbon cycle. While deforestation leads to fragmentation, edge effects change forest structure and composition with increasing tree mortality, wildfire susceptibility and carbon emission (Laurance et al., 1997).

Edge effects are a consequence of a forest fragmentation process, which creates edges in these habitats occur mostly in tropical forests, because most deforestation is located in these regions. These effects are in a transition between two ecosystems from the border to the interior of the fragment (Didham et al., 1998). Brinck et al. (2017) analyzed the fragmentation and edge effect within the tropical forests in America, Africa and Asia. Their study showed that 19% of the tropical forests are within a distance of 100 m to the forest edge, in which 84% were anthropogenically created. Similarly, Dantas de Paula et al. (2016) analyzed the dimensions of edge effects in changes of tree cover in large areas across the world's tropical forest using Landsat Tree Cover (LTC) and reported a change in tree cover patterns after five years of fragmentation, thus, the closer a forest boundary is to the edge, the higher the decrease in tree coverage (i.e. between 50 and 100 m). In Brazil, the high deforestation rates lead to further fragmented forest patches in a fragmented tropical forest (Gross, 2017), nevertheless, the fragmentation different effects and trends within each biome. Pütz et al. (2014) assessed the fragmentation and edge effect (carbon loss) in the Amazon and Atlantic Forest biomes. In the Amazon biome, the number of fragments was smaller and sizes were larger than those in the Atlantic forest biome (77,038 fragments and 8,376 ha, 245,173 fragments and 64 ha). In that same study, it was also reported that the Atlantic Forest biome lost about 69 million tons of carbon over a period of 10 years due to forest fragmentation and the Amazon biome lost 599 million tons of carbon during the same period. Cunha (2007) estimated that 82.12% of the fragments in the Cerrado biome in Goiás State were smaller than 1 ha. Similarly, Jorge and Garcia (1997) found a high frequency of small fragments (10 ha) in the region of Sao Paulo. These studies show that two important biomes in Brazil (Amazon and Atlantic Forest) are highly affected by deforestation and fragmentation, which in turn decrease the capacity to store carbon. In addition, these studies can support analysis of other important Biomes that have been destroyed in recent years, such as the Cerrado. With deforestation, edge effects are common in tropical forests. But most studies analyzed single years and compared them after deforestation. Long time

series are rare, and they give new insights into how fragmentation effects change with time when the border is not newly affected by deforestation or fire. Likewise, only a few studies have analyzed the impact of edges and fragmentation on forest structure, composition and productivity in the Cerrado biome.

In contrast to studies that have found edge effects in Amazon and Atlantic forest, some studies in the Cerrado Biome have found no significant edge effects., Queiroga (2001) studied the border effect in Cerrado biome in Maranhao State and did not find differences between the edge distances regarding species distribution, vegetation structure and microclimate. In corroboration, Mendonça et al. (2015) also did not find any abiotic (microclimate) and biotic changes caused by edge effects in the Cerrado biome (in Iaras city in Sao Paulo State). Additionally, Kulp et al. (2018) estimated the above-ground biomass AGB and carbon stocks with transects from the cerradão border to the interior and showed no marked differences between forest border plots (20 m distance) and interior plots (260 m distance). Unlike, Lima-Ribeiro (2008) rather reported a strong influence of edge effects on the vegetation structure and microclimate parameters (SE-Goiano). These findings were based on direct measurement of forest stand parameters at the plot level in the field.

The most common method to assess the edge effects in tropical forest is by direct measururing, which is limited by the replicability, cost of execution and time consuming. Therefore, satellite images may be an alternative in monitoring vegetation cover within the context of the edge effect. Optical sensors are usually used for monitoring vegetation, mainly through the vegetation index (VI), because of its easier image processing compared to synthetic aperture radar (SAR) sensors, costs and long-term availability. To assess vegetation cover, the Normalized Difference Vegetation Index (NDVI) is widely used for detection of forest types (Ferreira and Huete, 2004; Ratana et al., 2005), deforestation (Trancoso et al., 2014; Acerbi Júnior et al., 2015) and deforestation and vegetation dynamics (Bitencourt et al., 2007; Ferreira et al., 2011). Nevertheless, the studies that use vegetation indices to analyze the edge effects in tropical forests are few. Lagos (2017) assessed the edge effect in Atlantic forest biome based on NDVI analysis. The author showed differences of NDVI values from the border to the center of the fragments between 25 and 50 meters ranging from 5 to 200 ha. The NDVI cannot directly estimate the biomass. However, it can be direct proximity to the amount of photosynthesis material (green biomass) and forest productivity. In the short term, the change of the NDVI can be related to the decrease of leaf production, species death and decrease of tree crown cover in the context of edge effect. In the long-term, the differences in forest productivity can be seen in differences in biomass.

There is a consensus that in most regions of the tropical forest edge effects exist, however few studies related to the Cerrado biome show uncertain results. Therefore, this study aims to assess the

long-term edge effects on vegetation that can be correlated to NDVI in forest fragments of the tropical savanna forest (cerradão) in the endangered ecotone Amazon/Cerrado-region of Mato Grosso. The study builds on a time series of seasonal NDVI composites from Landsat-5, -7 and -8 to evaluate the spatial variability and temporal dynamics of vegetation productivity in relation to the forest border.

4.2   Methodology

4.2.1   Study Area

The study area is located in the south central of Nova Mutum city, north of Mato Grosso, Brazil (Figure 1). This region covers two biomes, Amazon and Cerrado, known as the "Arc of Deforestation" (AOD). The climatic condition of the study area is classified as Aw (after Köppen climate classification) with two distinct seasons: dry season, from May to September and a rainy season from October to April. The area records an annual precipitation of about 2200 mm with an annual average temperature of 24 °C (Goedert, 1986). Soil types of the area mainly consist of ~80% Oxisols and ~20% Entisols occurring on a flat topography (maximum slopes of 3%). Due to the characteristics of the soils of the study area, the landscapes encourage deforestation processes and agricultural activity (IBGE, 2001). Therefore, this region plays an important role in the deforestation process, because it holds the highest deforestation rates, around 75%, and the largest agricultural area (INPE, 2011). From 2002, several Brazilian institutes, such as the Instituto Brasileiro do Meio Ambiente e dos Recursos Naturais Renováveis (IBAMA) and National Institute for Space Research (INPE), started monitoring the rate of deforestation in the Cerrado biome. From 2002 to 2017, Cerrado lost around 0.8% of its vegetation per year (F. G. Assis et al. 2019b).
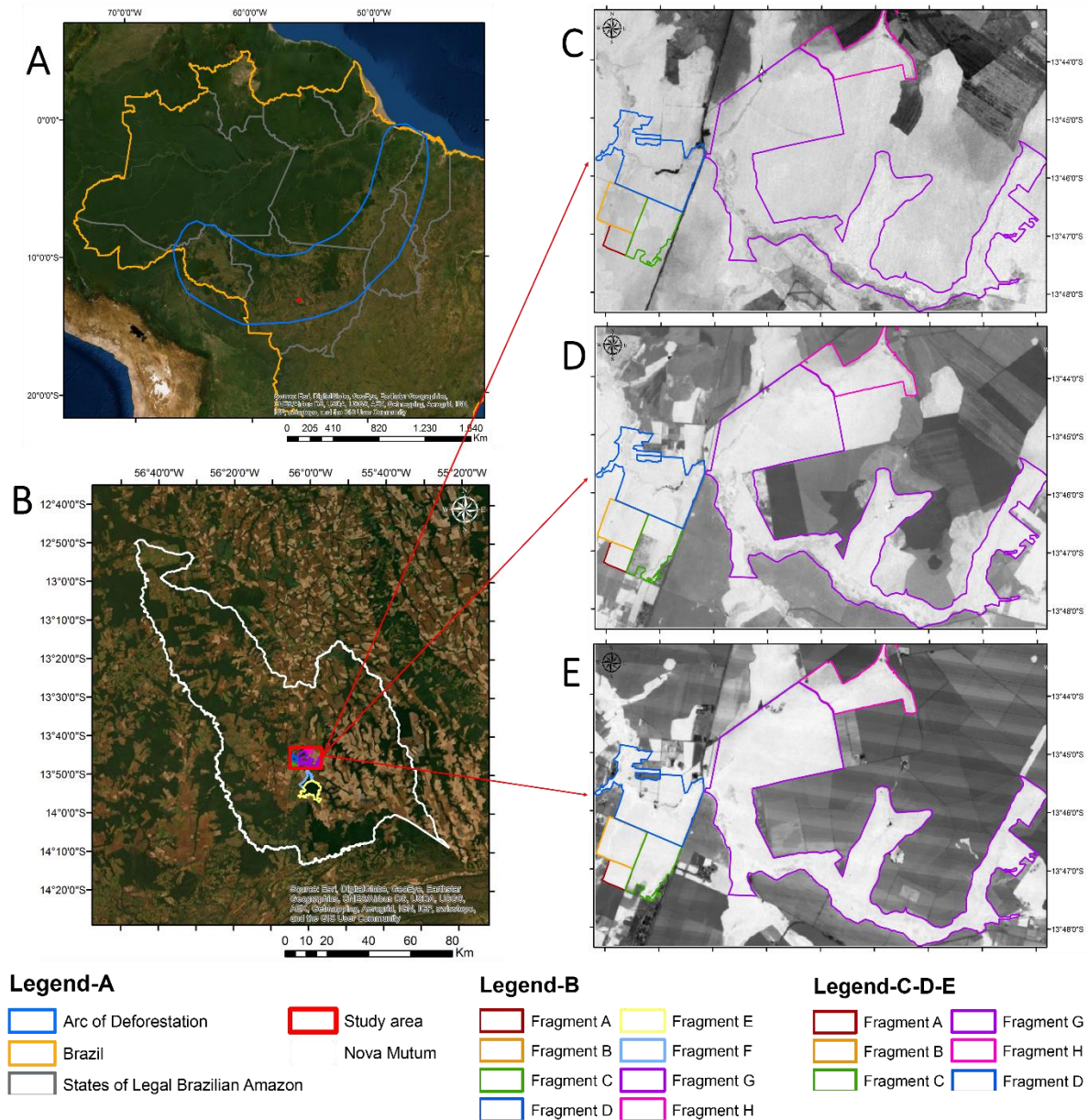
Figure 4.1 Location of the study area in Brazil on top of a Google Earth image (A), in Nova Mutum on top of a Google Earth image, in the exact area of analysis from 1985 (C), 1997 (D) and 2017 (E) on top of a NDVI image.

In general, vegetation cover of the Cerrado consist of three main types, i.e., forest, savannas, and grassland formations (Walter, 2006). The forest formations consist of arboreal species in a continuous canopy and include the Gallery, Dry, and Open Forest while the savanna formation is characterized by a discontinuous herbaceous-shrub and tree canopy. Within the savanna formation are seven distinct types: Dense Woodland, Woodland, Open Woodland, Park Woodland, Palm, Vereda, and Stone Woodland. The grassland formations include three vegetation types: Stone Grassland, Shrub Savanna, and Grassland. The first two types of grasslands are characterized by the large presence of shrubs with different soil types. In our study, we focused on one of the dominant types of vegetation: cerradão (Open Forest). Cerradão is located within the transition area of the Amazon and Cerrado biomes. It is

92

important to stress that this area has a high deforestation rate, which can explain the presence of secondary forest. Cerradão has a crown cover ranging between 50 and 90% and the height of the trees varies from 8 to 15 m. In general, the soils of cerradão are well drained, deep, and have medium–low fertility (mainly Latosols). Because Cerradao is the dominant vegetation type in the study area, we selected fragments of different size in this vegetation type. The fragments were selected according to the similarity of the areas, with same type of soil, precipitation and altitude. Additionally, the fragments are located at least 100 meters from the rivers to avoid contact with gallery forests. To map the fragmentation, we used the image from the Multispectral Instrument (MSI) on-board Sentinel-2A of 26.07.2017. It is important to note that in this work, an area is considered a fragment when there is a distance of 1 pixel (20 meters) between two parallel edges with forest area, therefore, an area is considered a forest fragment when there is a distance of 1 pixel (20 meters) between two parallel edges with forest area. We used the edge density (edge to a per unit area), total edge (an absolute measure of total edge length) and the number of patches (numbers of forest fragments) to support the analysis of this thesis (McGarigal et al., 2002).

The six fragments considered in this study covers a spatial extent of 4,142.49 ha with Fragment A being the smallest and Fragment G being the largest (Table 4.1).

Table 4.1 Characteristics of the fragments.

Fragments	Size (ha)	Vegetation Type	Total Edges (m)	Edge Density (m/ha)
A	59.92	Cerradão	3,086	51.50
B	169.37	Cerradão	5,165	30.50
C	218.30	Cerradão	8,229	37.70
D	554,25	Cerradão	16,817	30.34
G	2741,82	Cerradão	62,768	22.89
H	398.83	Cerradão	13,440	33.70

Fragments A, B, C and D are closer to the city than the fragments, G and H. In this study, we considered the fragments of cerradão vegetation type, which has a length of 109.50 km of external edges. These fragments represent a large part of the study area, as can be seen in Figure 1. With the increase of deforestation, the number increase until 2004. Main deforestation in the study region was from 1984 until 1996 (Figure 4.2).
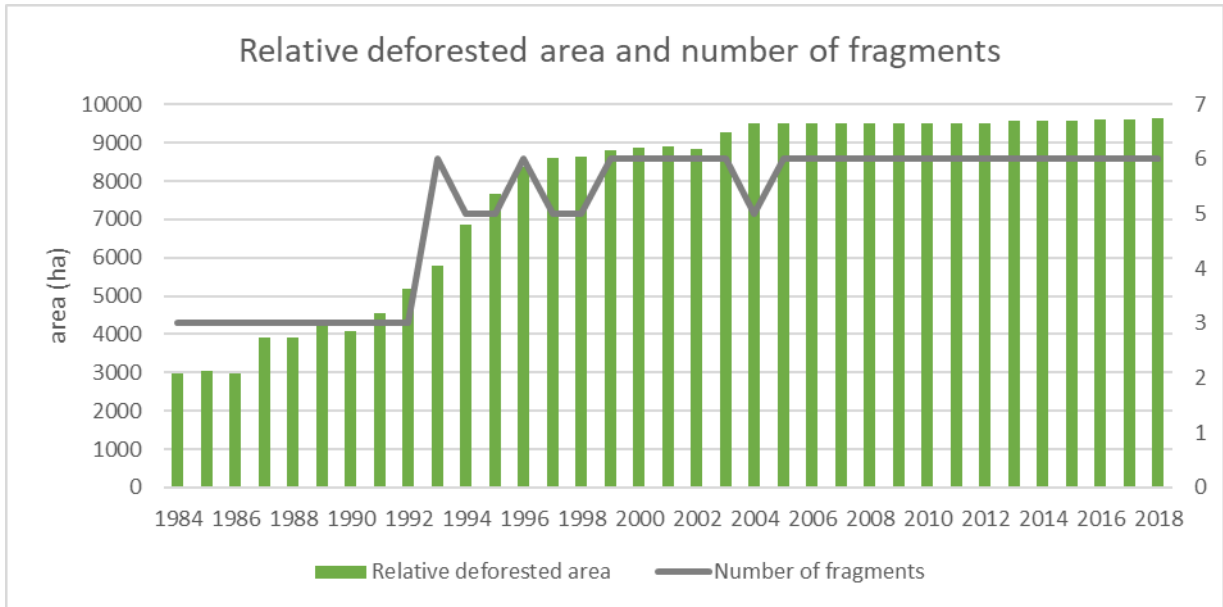
Figure 4.2 Relative area of deforestation (ha) and the number of fragments from 1984 to 2018 in our study area.

4.2.2 Satellite Data

We used 498 images from Landsat 5 Thematic Mapper (TM), 552 images from Landsat 7 Enhanced Thematic Mapper Plus (ETM+) and 104 images of Landsat 8 Operational Land Imager (OLI) from two different Path/Row (227/069 and 227/070) between March 1984 and September 2018. The data was available from U.S. Geological Survey (USGS) EROS Science Processing Architecture (ESPA) ordering system. The images were acquired from TIER 1 collection category, this includes Level-1 Precision, Terrain (L1TP) corrected and radiometrically calibrated data. The Tier 1 is considered the best set of data for time-series analysis (USGS, 2017).

4.2.3 Data Processing

Photosynthetically active (or 'healthy') vegetation has an intense radiation absorption in the red part of the visible light by photosynthetic pigments (chlorophyll), and reflection of near-infrared radiation due to canopy. This feature allows vegetation indices to determine parameters such as vigor, growth stage, photosynthetic activity, percentage of vegetation cover and other biophysical properties of vegetation. The NDVI highlights the differences between the minimum reflection in red, corresponding to the maximum absorption by plant pigments, and the maximum reflection in the near infrared, due to the leaf structure.

$$NDVI = \frac{(NIR - RED)}{(NIR + RED)}$$

NIR - reflection in the near-infrared spectrum

RED - reflection in the red range of the spectrum

NDVI is highly correlated with the greenness of the vegetation, and it is the most index used in research related to the dynamics of vegetation cover. NDVI values range from -1 to 1. Vegetation is associated with positive values. Materials that reflect more intensely in the red portion with respect to near infrared (e.g., clouds, water) show negative NDVI (Rouse, J. W., Jr., 1974). Therefore, in the first step, we extracted the NDVI from each image. The NDVI must be used to estimate the biomass, however it can be considered an approximation to the amount of green biomass and forest productivity. In the long-term, the differences in forest productivity can be seen in differences in the biomass.

We used a tool in the bfastSpatial package in R software (developed by Loïc Dutrieux, Ben DeVries and Jan Verbesselt, 2014, https://github.com/dutri001/bfastSpatial) to create annual mean value composites from May to September (dry season). This period to create the composites was chosen because our study area is in a transition of two Biomes that have, in part, characteristics of a tropical forest. Therefore, this is a region with large cloud cover in the rainy season (from October to April). In addition, in this transitional region there are species from both biomes, where some of these species lose their foliage in the dry season. Therefore, it is important to choose one season (dry or rainy) to create the composites, to avoid misinterpreting the values of NDVI, e.g., the decrease of NDVI could be misinterpreted with the foliage loss. The mean value composites processing was necessary to reduce the seasonal variation in the vegetation. By this approach, we obtained 35 annual composites from 1984 to 2018 (Figure 4.3).
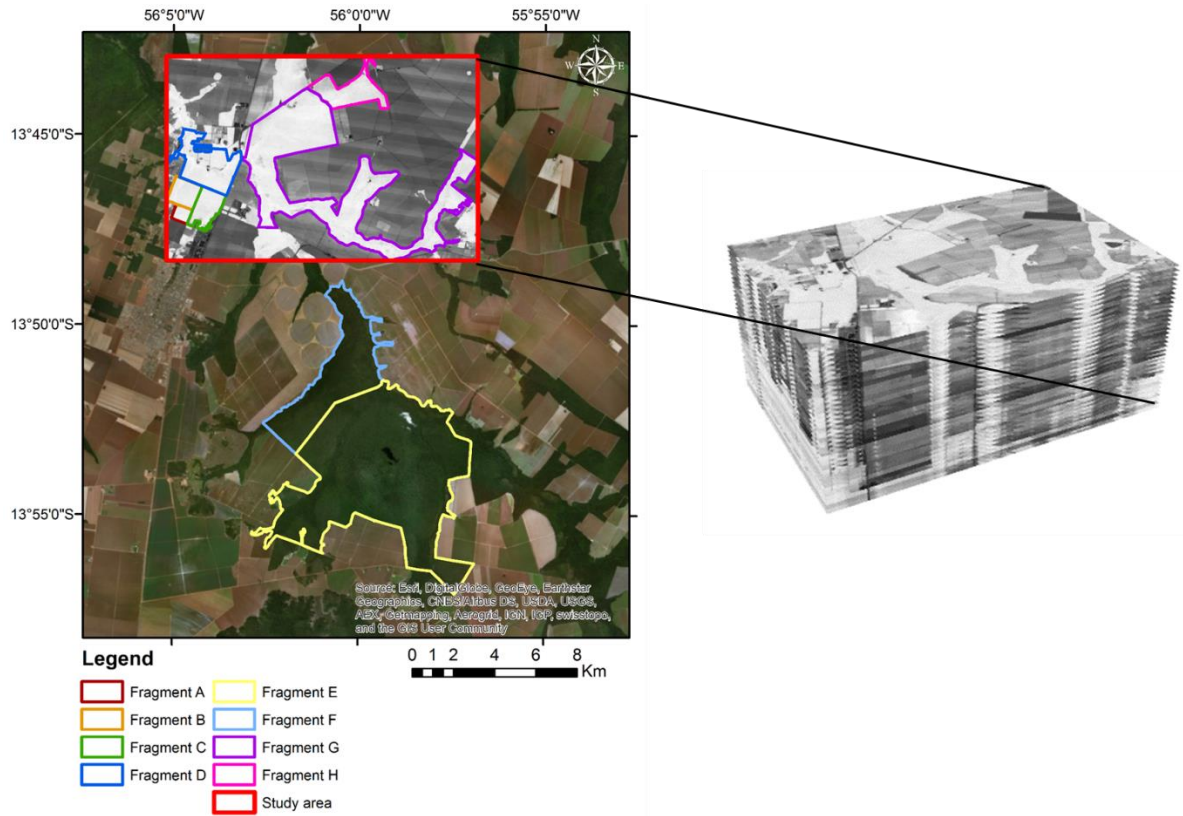
Figure 4.3 NDVI stack of Landsat 5/7/8 images on top of a Google Earth image.

4.2.4   Sampling Design

In order to reach the objective of this study, we created a stratified sampling design to subdivide the strata, such as forest types, rivers, eco-zones, roads, to generate a precise result. The first strata was to extract from the cerradão vegetation type map (Figure 3 A) from Souza Mendes et al. (2019). Additionally, we cut out the cerradão areas that were not within the fragments analyzed in this study (Figure 3 B). For the second strata, we mapped the river basin and created a 100 meters buffer around the rivers of the study region in order to avoid any target that was not forest (Figure 4.3 C). Moreover, we created 80 random points in each of the six fragments, totalling 480 random points (Figure 4.4). Besides, we manually mapped thirty-five forest masks for every year based on the NDVI images, in order to have a mask on the edges on the fragments for each year to see the start of the deforestation process in these areas.
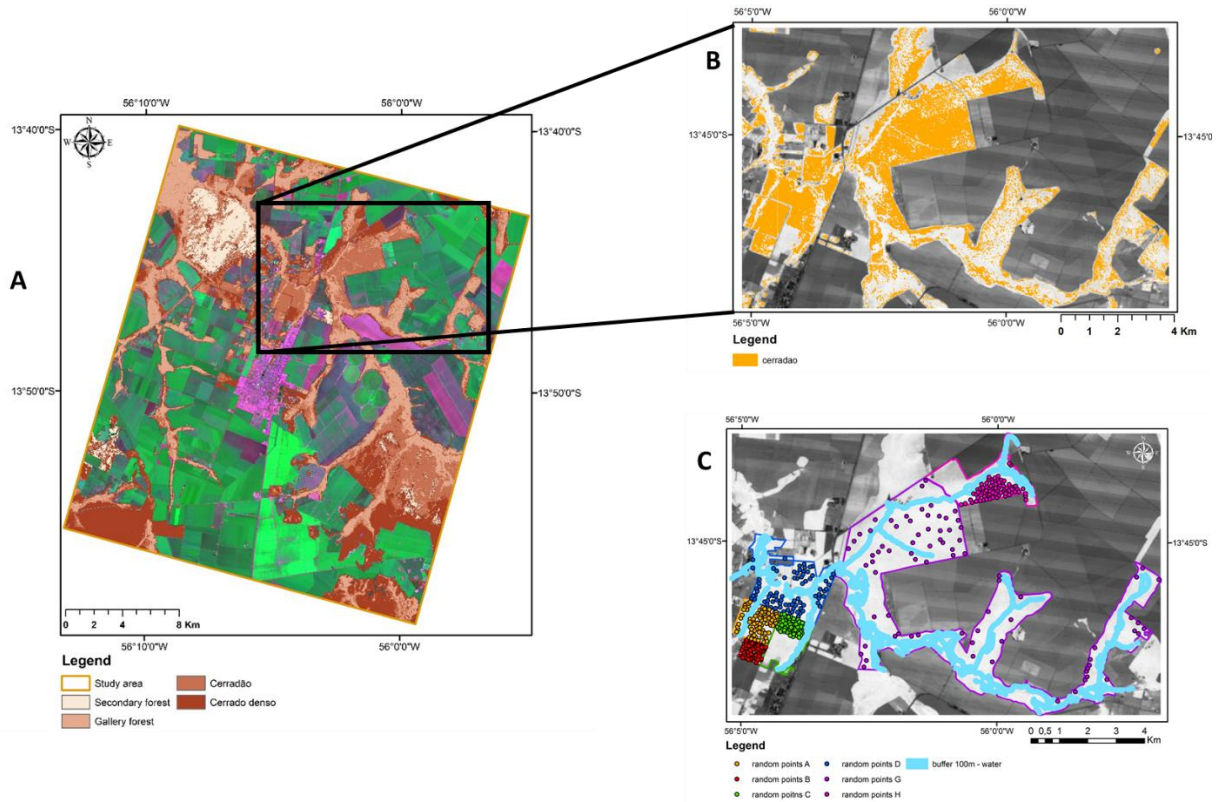
Figure 4.4 Stratified sampling design. Vegetation type map from De Souza Mendes et al. 2019 (A), Cerradão vegetation areas extracted from the A map (first strata) on top of an annual composition from NDVI Landsat 8 in 2017 (B). Buffer of 100 meters from the water (second strata) and 480 random points created in the six fragments on top of an annual composition from NDVI Landsat 8 in 2017 (C).

4.2.5 Data Analysis

To analyze the edge effect, we used the mean values of NDVI (from -1 to 1) and the distance to the nearest edge (meters) from each random point created in the six fragments. Firstly, we used a simple linear regression of the relationship between distance to the nearest edge and NDVI for the thirty-five years, to that we plot the distance to nearest edge in the X-axis and NDVI values in the Y-axis for every year and fragment. Secondly, we calculate a linear regression using the p-value to show how strong and significant theses relations are. Therefore, p-value shows the significance of the correlation between NDVI values and the distance from the edge to the center of the fragment. By these approaches, we created five classes to present the results: '***' represents p-values smaller than 0.00005 with a positive slope; '**' represents p-value between 0.005 and 0.00005 with positive slope; * for p-value smaller than 0.05 and higher 0.005 with positive slope; ns (not significant) for p-value bigger than 0.05; and # for p-value bigger than 0.05 and lower 0.005 with negative slope.

4.3 Results

Table 4.2 shows the linear regression results regarding the relationship between NDVI values and distance to the nearest edge in every fragment and year. In addition, Table 2 indicates the beginning of the deforestation process in each fragment in red color. Across the six fragments, the significance shows a cluster concerning the size of fragments. The biggest fragments (D, G and H) showed a higher significance associated with edge distance compared to the smallest fragments (A, B and C). The fragments G and H were the most significant while in fragment G, twenty-two years out of the thirty-five years recorded the highest significance. In fragment G, twelve years out of the thirty-five years showed the highest significance. Fragment C was the least significance.

Table 4.2 Simple linear regression of the relation between distance to the nearest edge and NDVI values per year for each fragment. The values in red color represent the beginning of deforestation around the fragment.

Year	Fragments					
	A	B	C	D	G	H
1984	***	*	#	***	*	*
1985	**	*	ns	***	***	***
1986	**	*	ns	***	*	***
1987	***	*	#	ns	**	***
1988	ns	*	ns	***	**	***
1989	ns	*	ns	***	**	***
1990	*	***	ns	*	*	*
1991	*	**	ns	*	**	***
1992	*	*	ns	*	*	***
1993	ns	*	ns	**	***	***
1994	#	***	ns	ns	***	***
1995	ns	*	***	***	***	***
1996	#	ns	*	*	*	***
1997	ns	ns	ns	***	**	***
1998	***	ns	ns	**	***	***
1999	*	ns	#	ns	*	***
2000	*	ns	#	*	**	***
2001	**	**	ns	ns	ns	ns
2002	*	***	ns	**	***	***
2003	ns	*	ns	ns	***	*
2004	ns	***	ns	***	***	***
2005	*	ns	*	ns	***	***
2006	***	***	ns	**	ns	**

2007	***	**	*	ns	**	***
2008	*	**	ns	ns	**	*
2009	ns	ns	ns	***	*	***
2010	#	#	ns	***	ns	ns
2011	***	***	ns	ns	***	**
2012	ns	ns	*	ns	*	***
2013	*	ns	ns	**	*	**
2014	*	ns	ns	**	**	ns
2015	ns	ns	***	*	***	**
2016	ns	ns	ns	*	**	*
2017	ns	ns	##	***	***	*
2018	ns	ns	#	ns	ns	***

>0.00005 and positive slope = ***, 0.005 >*>0.00005 and positive slope = **, 0.05>*>0.005 and positive slope = *, >0.05 = ns (not significant), 0.05>*>0.005 and negative slope = #.

Figure 4.5 shows the relation between NDVI and distance to forest border in the fragment G from 1991 to 1994, one year before and two years after the beginning of deforestation. There is a positive relationship between edge distance and NDVI. Two years after the deforestation, i.e. in 1994, Fragment G recorded increases in NDVI values. The largest edge distance before 1992 was around 2,300 m and after the deforestation, this distance decreased to 1,500 m. NDVI in 1993 was lower than in 1992. However, this pattern was also observed with all other fragments (See appendix A, B, C, D, E and F), probably due to the severe drought that occurred in 1992–1993 across the study region (Appendix G).
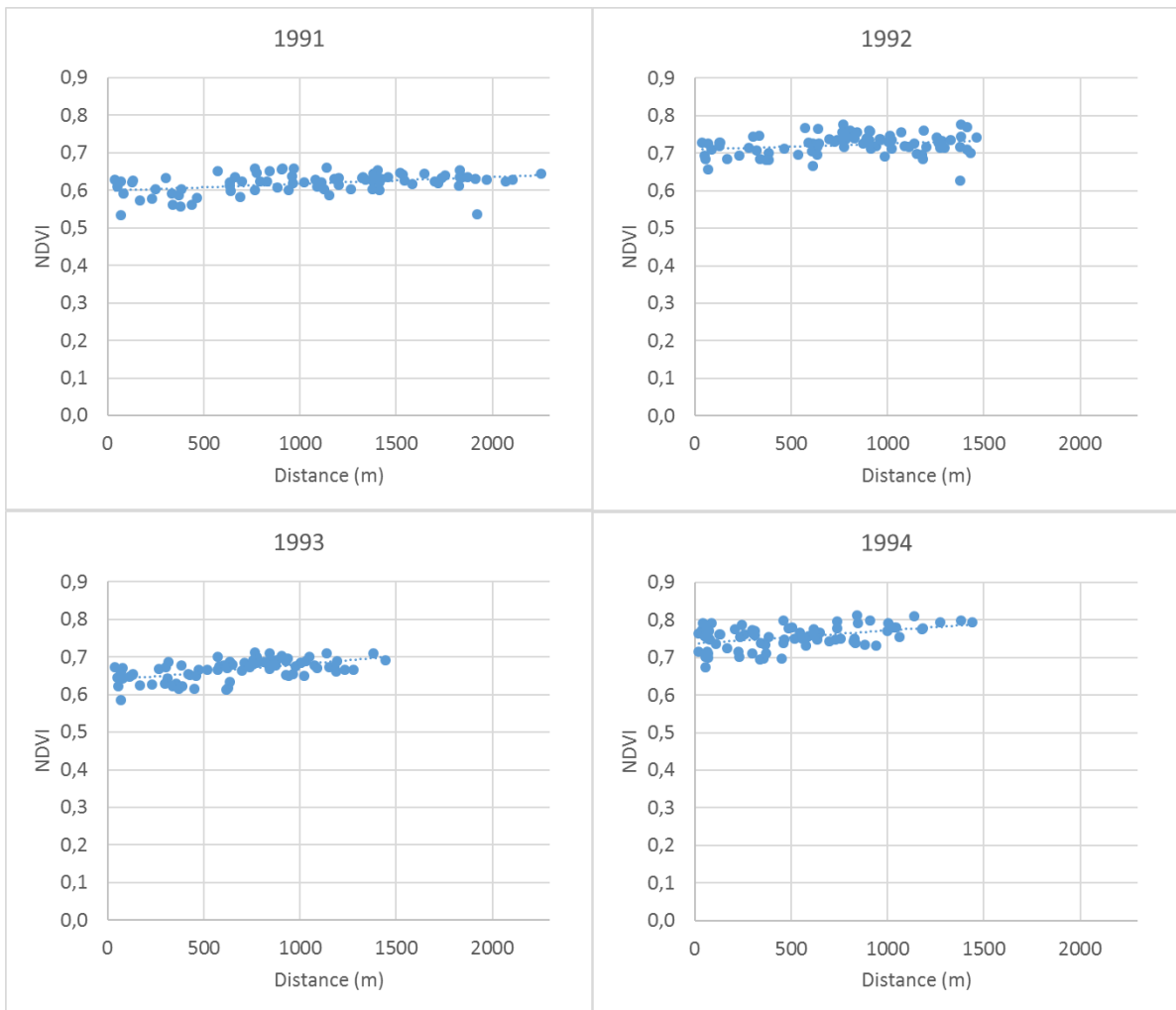
Figure 4.5 Simple linear regression of the relation between edge distance and mean values of NDVI annual compositions, between 1991 and 1994 in the fragment G.

In Fragment H, recorded NDVI in 2002 were higher than the preceding year, i.e. 2003, which showed a positive relationship with edge distance (Figure 4.6). The deforestation process around the area of Fragment H started in 2003. Additionally, there is a decrease in the distance between the point and the nearest edge. Before the deforestation, the maximum distance was 1,000 m and afterwards 600 m. Furthermore, the NDVI values increase two years after the deforestation process started.
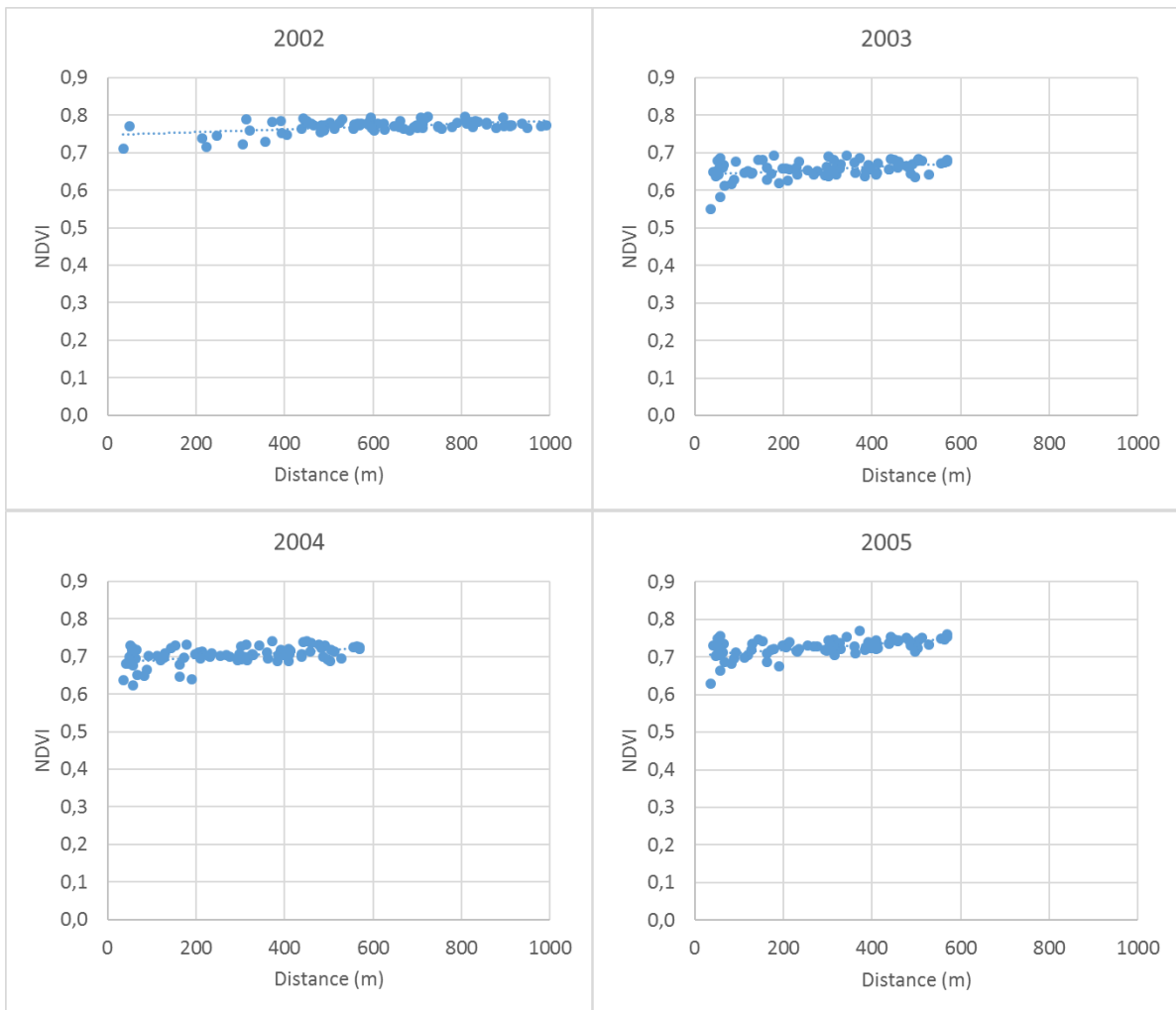
Figure 4.6 Simple linear regression of the relation between edge distance and mean values of NDVI annual compositions, between 2002 and 2005 in the fragment H.

4.4   Discussion

Our findings show a significant and positive relationship between NDVI and edge, thus, the closer a fragment is to the edge, the lower the value of NDVI. Studies related to the edge effect have shown that several environmental variables are changed, such as, humidity is lower at the edge of the fragment, due to the higher radiation at the forest border. Inside the fragment, the humidity is higher because of crone coverage (Matlack, 1993). The increasing tree mortality in the edge is another common edge effect (Laurance et al., 1998b). Biomass and carbon storage can also be affected by the edge effect (Laurance et al., 1997; Brinck et al., 2017). Silva Junior et al. (2020) find a carbon loss associated with edge of 947 Tg C from 2001 to 2015. In this study, which covers the Amazon biome including the AOD, remote sensing was used to first map the forest edges based on the Global Forest Change map and to estimate the carbon loss over the forest edges using LIDAR data. Additionally, Putz et al. (2014) estimated a carbon loss of 599 million tons due to edge effect over ten years in the same

biome. In this study, remote sensing was used to map the fragmentation in the biome using MODIS data. Ordway and Asner (2020) identified a carbon loss around 22% along edges, reductions in canopy height and leaf mass per area in Malaysian Borneo tropical forest using LIDAR. In the same context, Dantas et al. (20116) used Landsat Tree Cover Map to assess the edge effect on the tree cover patterns, which was lower close to the edges.

The largest fragments (D, G, H) showed more positive significance between NDVI and distance to the edge compared to the smallest fragments (A, B, C) (see Table 2). On the other hand, Lagos (2017) showed no difference in the NDVI values regarding the edge effects related to the fragment size in Atlantic Forest biome. In his study, the smallest fragments showed a homogeneous or no edge effect compared to the largest fragments, what are similar trends compared to our results. Our results indicate that edge effects are significant higher in larger fragments than in smaller one. Often fragment studies do not consider this. Additionally, the literature shows that the effects of fragment size on forest species, biomass, carbon storage and species distribution vary greatly in different biomes. Nascimento and Laurance (2006) did not find a significant difference in the density and biomass of primary species in different sizes of fragments (1, 10 and 100 ha) in Amazon biome. Our results show that the largest fragments present more visible edges effects than the smaller fragments. One possible explanation is that these small fragments have higher perturbation, which contributes to a major change in the structure and composition of the vegetation for the whole fragment and resulted in greater homogeneity of NDVI values. The effect of fragment size on vegetation structure and composition in the Cerrado biome has not been widely studied, the few studies in this area were related to the impact on fauna (Rocha et al., 2018). Mendonça et al. (2015) studied the edge effect in cerrado sensu stricto from Sao Paulo. Their results did not show any edge effect in the density, basal area and richness in the arboreal strata. However, small difference in the edge and interior temperature of the fragment was reported, suggesting the same pattern as in the study of Dodonov (2011).

The above studies analyzed the edge effect in a short or medium period. However, the literature shows that the edge effect, depending on the biome, may occur for a short, medium or long period. Our results showed that after one year of deforestation, the NDVI value of all analyzed points decreased slightly and after two to three years, the values increase to the level before. This edge effect differs from studies in tropical rainforests, where fragmentation and edge effect can be observed for several years after deforestation. Laurance et al. (1997) analyzed the edge effect caused by the fragmentation process over 17 years in Amazon biome. The above-ground dry biomass had a sharp decrease within the first 4 years and stabilized thereafter. In contrast, the number of successional trees in the edge increased up to 17 years after the beginning of fragmentation and there was no change in the plots located in the interior of the fragment (Laurance et al., 2006). Additionally, the number of large trees

were less in the years after the fragmentation within 300 m distance to the edge up to 20 years ((Laurance et al., 2000). Our study showed that in the Cerrado biome, edge effect may be short-lived and NDVI re-establish quick after deforestation impact. Nevertheless, we cannot conclude if this vegetation recovery after the deforestation also mean a recovery of ABG and carbon storage in the fragments, because with deforestation trees are mainly cut and reduced. Results from Laurance et al. (1997) seems plausible that AGB and carbon storage decrease more at the edge.

Further studies are needed to analyze the edge effect indicators such as tree density, tree height, DBH and biomass of trees, shrubs and herbaceous layer over a longer time span. One suggestion is the use of time series accompanied by satellite image analysis for NDVI and biomass. However, in essence, it is challenging to find in a highly progressive zone of deforestation (Arc of Deforestation in Brazil) such as areas that are relatively stable over 20 to 30 years.

4.5   Conclusion

In this paper, we evaluated the edge effect with NDVI values in the transitional area between the Cerrado and Amazon biomes. In contrast to other studies with short time periods after deforestation, our research applied an approach to investigate possible edge effects for long time using vegetation index from freely available satellite images (1984-2018). Our findings showed a positive significant change in NDVIs related to the distance from the nearest edge of the larger fragments. For the smaller fragments, most of the years had no or very small significant level between distance and NDVI. In all fragments, there was a quick recover of NDVI after deforestation impact, but this does not mean that AGB or carbon storage re-establishment was proportionate. Furthermore, our results showed that long-term edge effect pattern found in Amazon biome cannot be extrapolated to Cerrado. More detailed studies are therefore needed to understand the long-term dynamics of edge effect in the different biomes. Consequently, evaluate the changes in biomass and carbon for the global important ecotone of Cerrado and Amazonas biome.

Author contributions:

Flávia de Souza Mendes – conceptualization, methodology, validation, formal analysis, investigation, data curation, investigation, writing—original draft preparation, writing—review and editing, visualization, project administration

Kwabena Abrefa Nketia – formal analysis, visualization, review and editing

Niklas Langner – formal analysis, data curation, writing—review and editing

Gerhard Gerold – conceptualization, validation, writing—review and editing, visualization

Veraldo Liesenberg – writing—review and editing, visualization

Stefan Erasmi – conceptualization, methodology, investigation, writing—review and editing, visualization

5.   General Discussion

In order to monitor forest fragmentation and carbon storage in Cerrado biome, we used different approaches, by mapping the different type of vegetation using optical and SAR remote sensing, estimating the biomass and carbon stock from field data collection in the context of edge effect and analyzing the edge effect in long-term by Landsat satellite series.

In the first manuscript, we mapped the forest and non-forest areas and forest type using different combinations of SAR and optical images. First, our results showed the importance of integrating satellite images from different sensors to classify the forest and non-forest area. We compared our data to the data of the forest areas from the Program for the Estimation of Amazon Deforestation (PRODES) project, which is the most important project that has been conducting satellite monitoring of deforestation in the Legal Amazon. It was possible to verify a high underestimation in the forest areas, mainly in the classes gallery forest and Cerrado denso. The PRODES estimated an area of 12,702 ha of forest, and our work estimated an area of 27,326 ha. This difference can be associated to the different spatial resolution used in PRODES (30 meters) and in our study (10 meters). Second, in our results, S2 classifications showed the highest overall accuracy and kappa values. The application of S2 images to map vegetation types in the Cerrado biome is new. In general, Landsat is the most common sensor used to discriminate vegetation types in the Cerrado. Nascimento and Sano (2010) had 85% overall accuracy for mapping vegetation types in this biome. The authors used Landsat 7 ETM+ images to discriminate the Rupestrian Cerrado (Savanna formation) in the Chapada dos Veadeiros National Park in Goias State, which can be difficult due to the spectral confusion with other types of Cerrado vegetation. The optical data are certainly useful to map the vegetation type in Cerrado; however, these images are usually not available during the rainy season and the optical data cannot extract information from the structure of the forest (Asner 2001). Moreover, the availability of images in the rainy season would allow for a higher temporal resolution, which is crucial to better discriminate the vegetation types in the Cerrado biome due its high seasonality. The use of radar images can be a solution to overcome the lack of image availability in the rainy season and the high saturation of optical images in areas of great biomass density. In our radar classification results from the dry and rainy seasons, TanDEM-X (X Band) and ALOS-PALSAR 2 (L Band) dual polarimetric classification from the dry season showed the highest overall accuracy and kappa values. The results of the CI 95% OAA showed the importance of the fusion between optical and radar data to map vegetation type in the Cerrado biome, since the confidence interval with the narrowest range belonged to the classification that used all images from the dry and rainy seasons. The narrower the interval was, the more accurate the classification. The Cerrado vegetation has one of the largest forest diversities, consequently the combination of different sensors (optical and radar) and spatial resolution (low, medium, and high) results in a great improvement in the

accuracy (Saatchi et al. 2010). Of the three classifications that obtained the highest values of accuracy and kappa, two used radar and optical images. This showed the importance of the integration of different sensors in improving the mapping of forest types in Cerrado. A similar result was reported by Sano et al. (2005), who combined optical and radar images to improve the classification of different vegetation types in the Cerrado biome. The study had a high overall classification accuracy, which used both sensors in regions of savanna and grasslands formations. Sano et al. (2005) used data from the dry and rainy seasons and showed the importance of the time series in improving the classification of different types of vegetation. Additionally, Sano et al. (2005) showed better performance of radar data (JERS-1 SAR) compared to optical data (Landsat). In contrast, our results showed that optical data performed better for classification, compared to the radar data. However, Sano et al. (2005) used a higher number of radar images using L Band compared to our study, which increased the efficiency of mapping vegetation, due to the sensitivity to identify the various structures of the forest, consequently better distinguishing the type of forest, as reported by Lucas et al.; Garestier et al.; Santoro et al. (2000; 2009; 2009).

In the second manuscript, we analysed the edge effect on biomass and carbon stock based on field data collected in July and August 2017, we compared our results to other areas in Cerrado biome. In our results, the estimation of AGB for Cerradão was 93.23 Mg ha-1, comparing the results with the reference values of AGB in Cerradão (Table 3), except for the results of Marimon et al. (2014), all Cerradão references values are lower. Marimon et al. (2014) determined a high AGB value of 120.2 Mg ha-1 for a protected Cerradão area, nevertheless the data were collected in the Bacaba Municipal Park (ecological reserve), which probably are more protected than our study area. Additionally, the reference values for the AGB in Cerrado denso were lower than the value of our study, 56.13 Mg ha-1. The reference values of AGB are predominatly not located in AOD, however this region of forest-savanna boundaries is a complex mosaic of dense and open different types of vegetation. Our main hypothesis is that fragmentation leads to a negative edge effect, the closer to the edge, the lower biomass and carbo stock. To test this hypothesis, we use the Kruskal-Wallis test, which showed no significant difference in AGB values in the edge and the center of the fragment for both vegetation types, Cerradão (p= 0.11) and Cerrado denso (p=0.22). The differences between interior and edges were less than those obtained in Amazon forest, e.g. by Laurance et al. (1997), who calculate a loss of 36% of the carbon stock after 10-17 years of fragmentation process in Amazon forest. Since 1970, Cerrado biome lost more than 50% of its vegetation and have highly fragmented landscapes, therefore even interior plots may have been subjected to additive edge effects. Additionally, Stephenson et al. (2014) showed that big tree can stock a large amount of carbon compared to smaller tree and in some of our fragments, the bigger trees were removed by logging. Furthermore, the fieldwork data was

collected in a single dataset from 2017. Laurance et al. (2011) has previously shown the importance to assess the edge effect in the long-term.

In the third manuscript, we monitored edge effects from remote sensing data. Regarding the fragment size, the results show a significant positive relation between NDVI and edge distance in the biggest fragments (D, G and H) compared to the smallest fragments (A, B, C) (Table 1). Om and Khongjee (2010) found a different result. This study showed a positive relation between species richness and fragment size in the subtropical forest of Meghalaya, the smaller the fragment size, the smaller the species richness, because the smallest fragments have a high disturbance which changes the floristic composition, carbon storage (Ma et al. 2017) and species composition (Echeverría et al. 2007). Nevertheless, Lagos (2017) showed no difference in the NDVI values regarding the edge effects related to the fragment size in Atlantic Forest biome, which can be a result of predominant small fragments. Additionally, Nascimento and Laurance (2006) did not find a significant difference in the density and biomass of primary species in different sizes of fragments (1, 10 and 100 ha) in Amazon biome. The literature shows that the effects of fragment size on forest species, biomass, carbon storage and species distribution vary greatly in different biomes. In Amazon and Atlantic biomes, studies related to the edge effect have shown that several variables are changed, such as, humidity (Matlack 1993), plant density (Malcolm 1994), tree mortality (Laurance et al. 1998b), carbon and biomass (Laurance et al. 1997; Brinck et al. 2017). There is no consensus about the edge effect in Cerrado biome. Lima-Ribeiro (2008) analyzed the edge effect on the vegetation structure in Cerradão, Southwest of Goiás State. The results of this study showed a strong positive influence of edge effect on vegetation structure, species distribution and microclimate parameters. Conversely, Dodonov (2011) did not find any edge effect on the tree height and exotic grasses in Cerrado biome in Sao Paulo. Dodonov study showed a small difference in the temperature in the center and border of the fragment; the further from the edge, the lower the temperature. Moreover, Mendonça et al. (2015) studied the edge effect in cerrado sensu stricto from Sao Paulo. The results did not show any edge effect in the density, basal area and richness in the arboreal strata, however, the temperature showed a small difference in the edge and interior of the fragment, presenting the same pattern as the study of Dodonov (2011). Additionally, the subshrub stratum was the only parameter that showed a negative significance edge effect, it increased logarithmically from the edge to the center of the fragment. Likewise, Kulp et al. (2018) showed that the number of shrubs was higher at the edge than at the center of the fragment in Cerradão and Cerrado denso in Nova Mutum, Mato Grosso. Nevertheless, the study showed no significant differences in the AGB and carbon stocks between the edge and the center of the fragment in both vegetation types, Cerradão and Cerrado denso. The results show the need for further and longer-term studies to analyze the edge effect indicators such as tree density, tree height, DBH and biomass of trees, shrubs

and herbaceous layer. One suggestion is the use of time series of in situ data accompanied by satellite image analysis for NDVI and biomass.

6.   Final remarks

In this thesis, we first evaluated the use of optical and radar remote sensing for mapping different types of vegetation in the transitional area between the Cerrado and Amazon biomes. When applying a supervised random forest classification, the highest overall accuracy and kappa coefficient were obtained using only the Sentinel 2A for classification. However, of the three classifications that obtained the highest overall accuracy and kappa values, two used radar and optical images. Bands 5, 11, and 12 of Sentinel 2A, texture images from Sentinel 1A cross-polarization, and coherence of TanDEM-X were the most important images in order to separate each class, as calculated by the random forest variable importance.

Second, we assess the fragmentation and edge effect impact on biomass and carbon stock, the outcomes reveal that fragmentation has no significant impacts on the quantity or the distribution of AGB and aboveground carbon stocks in the study area in Nova Mutum. This is shown by the non-significant differences of the AGB and its carbon stocks between the border of a fragment and its center in both vegetation types as well as by the non-significant differences of the AGB and its carbon stocks between the fragments themselves. Merely by comparing the AGB and its carbon stocks of the Cerradão with the Cerrado denso, the results show significant differences, which are referable to the differences in vegetation physiognomy. Finally, the edge effect on biomass patterns found in the Amazon cannot be compared with those of the Cerrado biome, as it has a long history of human disturbance. Additionally, this analyzes was performed with a single measurement, therefore, to better understand these impacts a long-term analysis is required.

Third, we evaluated the edge effect in long-term based on NDVI values in the transitional area between the Cerrado and Amazon biomes. The method described in this study supported the studies assessing the edge effect on the vegetation. Additionally, our research applied a different approach to investigate possible edge effects using vegetation index from free satellite images. Moreover, our results showed a positive significant change in the NDVI values related to the distance from the nearest edge, the closer to the edge, the lower the NDVI value. Furthermore, our results showed that the long-term edge effect pattern found in Amazon biome cannot be extrapolated to Cerrado due to the NDVI values stabilized two years after deforestation started around the area. More studies need to be done to understand the dynamics of the edge effect in AOD, which directly affect estimations such as biomass and carbon.

Finally, we interpret the results of this thesis as a complex understanding of the possible edge effect due to the fragmentation. In the small scale, using fieldwork data, we could not find any evidence that fragmentation affect the carbon stock, however, we have significant results from remote sensing long-

term data that the NDVI is affected by the edge effect, where the closer to the edge, the smaller the NDVI. The NDVI is a direct approximation of the amount of photosynthesis material and how green the vegetation is. This edge effect identified by the NDVI may be related to tree mortality and the decrease of green biomass and species. Therefore, this may be related to AGB. This research has an important impact to the policies of Carbon Credit in the Cerrado biome. The carbon credit is a tradable certificate that allows the emission of carbon dioxide in exchange for maintaining forest areas and consequently reduce the emission of carbon dioxide and other greenhouse gases. The carbon estimation methodologies in the endangered Amazon/Cerrado ecotone in Brazil are still not accurate since they do not take into account the effects of fragmentation in the carbon stock. To that end, it is recommended to analyze whether the edge effect found in the study area will also be found in other parts of the Cerrado biome. Therefore, monitoring of edge effect using remote sensing data is first recommended as a basis for deciding which areas should in situ data be collected. For a monitoring model of edge effect in the Cerrado, the in-situ data must be correlated with the remote sensing data, which can then be used for better estimation of carbon stocks in different Cerrado vegetation types.

7. References

Abdala, G. C.; Caldas, L. S.; Harisasan, M.; Eiten, G. (1998): Above and belowground organic matter and root:shoot ratio in a cerrado in Central Brazil. In Brazilian Journal of Ecology 2, pp. 11–23.

Acerbi Júnior, Fausto Weimar; Silveira, Eduarda Martiniano de Oliveira; Mello, José Márcio de; Mello, Carlos Rogério de; Scolforo, José Roberto Soares (2015): CHANGE DETECTION IN BRAZILIAN SAVANNAS USING SEMIVARIOGRAMS DERIVED FROM NDVI IMAGES. In Ciênc. agrotec. 39 (2), pp. 103–109. DOI: 10.1590/S1413-70542015000200001.

Achard, Frédéric; Beuchle, René; Mayaux, Philippe; Stibig, Hans-Jürgen; Bodart, Catherine; Brink, Andreas et al. (2014): Determination of tropical deforestation rates and related carbon losses from 1990 to 2010. In Global change biology 20 (8), pp. 2540–2554. DOI: 10.1111/gcb.12605.

Almeida, R. A.; Shimabukuro, Y. E. (2000): Detecting areas disturbed by gold mining activities through JERS-1 SAR images, Roraima State, Brazilian Amazon.

Anupama, K.; Prasad, S.; Reddy, C. S. (2014): Vegetation, land cover and land use changes of the last 200 years in the Eastern Ghats (southern India) inferred from pollen analysis of sediments from a rain-fed tank and remote sensing. In Quat. Int. 325, pp. 93–104. DOI: 10.1016/j.quaint.2014.02.003.

Arantes, A. E.; Ferreira, L. G.; Coe, M. T. (2016): The seasonal carbon and water balances of the Cerrado environment of Brazil: Past, present, and future influences of land cover and land use. In ISPRS Journal of Photogrammetry and Remote Sensing 117, pp. 66–78. DOI: 10.1016/j.isprsjprs.2016.02.008.

Araujo, L. S.; Santos, J. R.; Keil, M.; Lacruz, M.S.P.; Kramer, J.C.M. (Eds.) (2001): Razão entre bandas do SIR-C/X SAR para estimativa de biomassa em áreas de contato floresta e cerrado. X SBSR. Foz do Iguaçu. Foz do Iguaçu, Brazil, April 21-26. Proceedings of X SBSR. Foz do Iguaçu. Foz do Iguaçu, Brazil.

Asner, G. P. (2001): Cloud cover in Landsat observations of the Brazilian Amazon. In Int. J. Remote Sens. 22 (18), pp. 3855–3862. DOI: 10.1080/01431160010006926.

Baker, Timothy R.; Phillips, Oliver L.; Malhi, Yadvinder; Almeida, Samuel; Arroyo, Luzmila; Di Fiore, Anthony et al. (2004): Variation in wood density determines spatial patterns inAmazonian forest biomass. In Glob. Change Biol. 10 (5), pp. 545–562. DOI: 10.1111/j.1365-2486.2004.00751.x.

Balderas Torres, A.; Lovett, J. C. (2013): Using basal area to estimate aboveground carbon stocks in forests: La Primavera Biosphere's Reserve, Mexico. In Philos. Trans. R. Soc. B-Biol. Sci. 86 (2), pp. 267–281. DOI: 10.1093/forestry/cps084.

Bamler, R.; Hartl, P. (1998): Synthetic aperture radar interferometry. In Inverse Problems 14.

References

Baron, Daniel; Erasmi, Stefan (2017): High Resolution Forest Maps from Interferometric TanDEM-X and Multitemporal Sentinel-1 SAR Data. In PFG 85 (6), pp. 389–405. DOI: 10.1007/s41064-017-0040-1.

Barret, B.; Raab, C.; Cawkwell, F.; Grenn, Stuart (2016): Upland vegetation mapping using Random Forests with optical and radar satellite data. In Remote Sensing in Ecology and Conservation.

Basommi, P. L.; Guan, Q. F.; Cheng, D. D. (2015): Exploring Land use and Land cover change in the mining areas of Wa East District, Ghana using Satellite Imagery. In Open Geosci. 7 (1), pp. 618–626. DOI: 10.1515/geo-2015-0058.

Bengtsson, J.; Bullock, J. M.; Egoh, B.; Everson, C.; Everson, T.; O'Connor, T. et al. (2019): Grasslands-more important for ecosystem services than you might think. In Ecosphere 10 (2), e02582. DOI: 10.1002/ecs2.2582.

Benítez-Malvido, J, Lázaro, A, Ferraz, IDK. (2018): Effect of distance to edge and edge interaction on seedling regeneration and biotic damage in tropical rainforest fragments: A long-term experiment. J Ecol.; 106: 2204– 2217. https://doi.org/10.1111/1365-2745.13003.

Beuchle, René; Grecchi, Rosana Cristina; Shimabukuro, Yosio Edemir; Seliger, Roman; Eva, Hugh Douglas; Sano, Edson; Achard, Frédéric (2015): Land cover changes in the Brazilian Cerrado and Caatinga biomes from 1990 to 2010 based on a systematic remote sensing sampling approach. In Applied Geography 58, pp. 116–127. DOI: 10.1016/j.apgeog.2015.01.017.

Bitencourt, Marisa D.; Mesquita, Jr. Humberto N. de; Kuntschik, Gerardo; da Rocha, Humberto R.; Furley, Peter A. (2007): Cerrado vegetation study using optical and radar remote sensing: two Brazilian case studies. In Canadian Journal of Remote Sensing 33 (6), pp. 468–480. DOI: 10.5589/m07-054.

Bourliere, F.; Hadley, M. (1970): The Ecology of Tropical Savannas. In Annu. Rev. Ecol. Syst. 1 (1), pp. 125–152. DOI: 10.1146/annurev.es.01.110170.001013.

Boy, Jens; Strey, Simone; Schönenberg, Regine; Strey, Robert; Weber-Santos, Oscarlina; Nendel, Claas et al. (2018): Seeing the forest not for the carbon: why concentrating on land-use-induced carbon stock changes of soils in Brazil can be climate-unfriendly. In Regional Environmental Change 18 (1), pp. 63–75. DOI: 10.1007/s10113-016-1008-1.

Bradter, Ute; Thom, Tim J.; Altringham, John D.; Kunin, William E.; Benton, Tim G. (2011): Prediction of National Vegetation Classification communities in the British uplands using environmental data at multiple spatial scales, aerial images and the classifier random forest. In J. Appl. Ecol. 48 (4), pp. 1057–1065. DOI: 10.1111/j.1365-2664.2011.02010.x.

Breiman, Leo (2001): Random Forests. In Machine Learning 45 (1), pp. 5–32. DOI: 10.1023/A:1010933404324.

Brinck, Katharina; Fischer, Rico; Groeneveld, Jürgen; Lehmann, Sebastian; Paula, Mateus Dantas de; Pütz, Sandro et al. (2017): High resolution analysis of tropical forest fragmentation and its impact on the global carbon cycle. In ncomms 8, p. 14855. DOI: 10.1038/ncomms14855.

Brown, Sandra (1997): Estimating biomass and biomass change of tropical forests: a primer. Rome: FAO (FAO forestry paper, 134). Available online at http://www.fao.org/docrep/W4095E/W4095E00.htm.

Bustamante, M.; Potter, C.; Corbeels, M.; Scopel, E. (2007): Land Use and Changes in Carbon Budget in the Brazilian Cerrado. In AGUFM 2007, B21B-05.

Carvalho, L.; Rahman, M.; Hay, G.; Yackel, J. (Eds.) (2010): Optical and SAR imagery for mapping vegetation gradientsin Brazilian savannas: Synergy between pixel-based andobject-based approaches. International Conference of Geographic Object-Based Image. Ghent.

Casenave, Javier Lopez de; Pelotto, Juan Pablo; Protomastro, Jorge (1995): Edge-interior differences in vegetation structure and composition in a Chaco semi-arid forest, Argentina. In Forest Ecology and Management 72 (1), pp. 61–69. DOI: 10.1016/0378-1127(94)03444-2.

Castro, A.A.J.F. (1994): Comparação florística de espécies do cerrado. In Silvicultura 15, pp. 16–18.

Castro, E. A. (1995): Biomass, nutrient pools and response to fire in the Brazilian Cerrado. MSc. Oregon State University, Oregon.

Castro, Elmar Andrade de.; Kauffmann, J. Boone (1998): Ecosystem structure in the Brazilian Cerrado: a vegetation gradient of aboveground biomass, root mass and consumption by fire. In J. Trop. Ecol. 14 (3), pp. 263–283. DOI: 10.1017/S0266467498000212.

Chabi, Adéyèmi; Lautenbach, Sven; Orekan, Vincent Oladokoun Agnila; Kyei-Baffour, Nicholas (2016): Allometric models and aboveground biomass stocks of a West African Sudan Savannah watershed in Benin. In Carbon Balance Manage 11 (1), pp. 1–18. DOI: 10.1186/s13021-016-0058-5.

Chaplin-Kramer, Rebecca; Ramler, Ivan; Sharp, Richard; Haddad, Nick M.; Gerber, James S.; West, Paul C. et al. (2015): Degradation in carbon stocks near tropical forest edges. In Nature communications 6, p. 10158. DOI: 10.1038/ncomms10158.

Chave, J.; Andalo, C.; Brown, S.; Cairns, M. A.; Chambers, J. Q.; Eamus, D. et al. (2005): Tree allometry and improved estimation of carbon stocks and balance in tropical forests. In Oecologia 145 (1), pp. 87–99. DOI: 10.1007/s00442-005-0100-x.

Chave, Jerome; Condit, Richard; Aguilar, Salomon; Hernandez, Andres; Lao, Suzanne; Perez, Rolando (2004): Error propagation and scaling for tropical forest biomass estimates. In Philos. Trans. R. Soc. B-Biol. Sci. 359 (1443), pp. 409–420.

References

Chave, Jérôme; Réjou-Méchain, Maxime; Búrquez, Alberto; Chidumayo, Emmanuel; Colgan, Matthew S.; Delitti, Welington B. C. et al. (2014): Improved allometric models to estimate the aboveground biomass of tropical trees. In Global change biology 20 (10), pp. 3177–3190. DOI: 10.1111/gcb.12629.

Climate data and Openstreemap org (2012): Klima & Wetter in Nova Mutum. Available online at https://de.climate-data.org/location/43166/, checked on 01-26-2018.

Cloude, S. R.; Pottier, E. (1996): A review of target decomposition theorems in radar polarimetry. In IEEE Trans. Geosci. Remote Sensing 34 (2), pp. 498–518. DOI: 10.1109/36.485127.

Cole, Monica M. (1963): Vegetation and Geomorphology in Northern Rhodesia: An Aspect of the Distribution of the Savanna of Central Africa. In The Geographical Journal 129 (3), p. 290. DOI: 10.2307/1794828.

Collinson, A. S. (1988): Introduction to World Vegetation. Dordrecht: Springer Netherlands. Available online at https://ebookcentral.proquest.com/lib/gbv/detail.action?docID=3568460.

Colwell, R. N. (1984): From photographic interpretation to Remote Sensing. In Photogrammetric Engineering and Remote Sensing 50(9):1305.

Congalton, Russell G. (1991): A review of assessing the accuracy of classifications of remotely sensed data. In Remote Sensing of Environment 37 (1), pp. 35–46. DOI: 10.1016/0034-4257(91)90048-B.

Coutinho, L. M. (2007): O bioma cerrado. In A. L. Klein (Ed.): Eugen Warming e o cerrado brasileiro: um século depois. São Paulo: Imprensa Oficial do Estado, p. 77-91.

Cremon, Édipo; Fátima Rossetti, Dilce de; Zani, Hiran (2014): Classification of Vegetation over a Residual Megafan Landform in the Amazonian Lowland Based on Optical and SAR Imagery. In Remote Sensing 6 (11), pp. 10931–10946. DOI: 10.3390/rs61110931.

Cunha, Hélida Ferreira (2007): COMPOSIÇÃO E FRAGMENTAÇÃO DO CERRADO EM GOIÁS USANDO SISTEMA DE INFORMAÇÃO GEOGRÁFICA (SIG). In BGG 27 (2). DOI: 10.5216/bgg.v27i2.2661.

d'Albertas, Francisco; Costa, Karine; Romitelli, Isabella; Barbosa, Jomar Magalhães; Vieira, Simone Aparecida; Metzger, Jean Paul (2018): Lack of evidence of edge age and additive edge effects on carbon stocks in a tropical forest. In Forest Ecology and Management 407, pp. 57–65. DOI: 10.1016/j.foreco.2017.09.042.

Dantas de Paula, Mateus; Groeneveld, Jürgen; Huth, Andreas (2016): The extent of edge effects in fragmented landscapes: Insights from satellite measurements of tree cover. In Ecological Indicators 69, pp. 196–204. DOI: 10.1016/j.ecolind.2016.04.018.

de Souza Mendes, F. de (2016): The potential of SENTINEL-1/-2 for mapping the forest edge and fragmentation in the Cerrado Biome of Mato Grosso, Brazil. LSP-ESA 2016. ESA. Prague, 2016.

DeFries, Ruth; Herold, Martin; Verchot, Louis; Macedo, Marcia N.; Shimabukuro, Yosio (2013): Export-oriented deforestation in Mato Grosso: harbinger or exception for other tropical forests? In Philosophical transactions of the Royal Society of London. Series B, Biological sciences 368 (1619), p. 20120173. DOI: 10.1098/rstb.2012.0173.

Delitti, Welington Braz Carvalho; Meguro, Marico; Pausas, Juli Garcia (2006): Biomass and mineralmass estimates in a "cerrado" ecosystem. In Rev. bras. Bot. 29 (4), pp. 531–540. DOI: 10.1590/S0100-84042006000400003.

Di Gregorio, Antonio (2005): Land cover classification system : classification concepts and user manual : LCCS. Rev. Rome: Food and Agriculture Organization of the United Nations. Available online at http://worldcatlibraries.org/wcpa/oclc/807041447.

Dodonov, Pavel (2011): Influência de borda sobre vegetação e microclima no cerrado paulista. Universidade Federal de São Carlos, São Carlos. Available online at https://repositorio.ufscar.br/bitstream/ufscar/2009/1/3492.pdf.

Dodonov, Pavel; HARPER, KAREN A.; Silva-Matos, Dalva M. (2013): The role of edge contrast and forest structure in edge influence: vegetation and microclimate at edges in the Brazilian cerrado. In Plant Ecol. 214 (11), pp. 1345–1359. DOI: 10.1007/s11258-013-0256-0.

Echeverría, Cristian; Newton, Adrian C.; Lara, Antonio; Benayas, José María Rey; Coomes, David A. (2007): Impacts of forest fragmentation on species composition and forest structure in the temperate landscape of southern Chile. In Global Ecol Biogeography 16 (4), pp. 426–439. DOI: 10.1111/j.1466-8238.2007.00311.x.

Eiten, George (1973): The cerrado vegetation of Brazil. In Bot. Rev 39 (1), p. 70. DOI: 10.1007/BF02860070.

EMBRAPA (1999): Sistema brasileiro de classificação de solos. Embrapa Solos. Rio de Janeiro.

Evans, T. L.; Costa, M. (2013): Landcover classification of the Lower Nhecolandia subregion of the Brazilian Pantanal Wetlands using ALOS/PALSAR, RADARSAT-2 and ENVISAT/ASAR imagery. In Remote Sens. Environ. 128, pp. 118–137. DOI: 10.1016/j.rse.2012.09.022.

F. G. Assis, Luiz Fernando; Ferreira, Karine Reis; Vinhas, Lubia; Maurano, Luis; Almeida, Claudio; Carvalho, Andre et al. (2019a): TerraBrasilis: A Spatial Data Analytics Infrastructure for Large-Scale Thematic Mapping. In ISPRS International Journal of Geo-Information 8 (11), p. 513. DOI: 10.3390/ijgi8110513.

F. G. Assis, Luiz Fernando; Ferreira, Karine Reis; Vinhas, Lubia; Maurano, Luis; Almeida, Claudio; Carvalho, Andre et al. (2019b): TerraBrasilis: A Spatial Data Analytics Infrastructure for Large-Scale Thematic Mapping. In IJGI 8 (11), p. 513. DOI: 10.3390/ijgi8110513.

Fearnside, P.M (2005): Deforestation in Brazilian Amazonia. History, Rates, and Consequences. In Conservation Biology 19 (3), pp. 680–688. DOI: 10.1111/j.1523-1739.2005.00697.x.

Fearnside, Philip M. (2018): Brazil's Amazonian forest carbon: the key to Southern Amazonia's significance for global climate. In Reg. Envir. Chang. 18 (1), pp. 47–61. DOI: 10.1007/s10113-016-1007-2.

Fearnside, Philip Martin; Righi, Ciro Abbud; Graça, Paulo Maurício Lima de Alencastro; Keizer, Edwin W.H.; Cerri, Carlos Clemente; Nogueira, Euler Melo; Barbosa, Reinaldo Imbrozio (2009): Biomass and greenhouse-gas emissions from land-use change in Brazil's Amazonian "arc of deforestation". The states of Mato Grosso and Rondônia. In Forest Ecology and Management 258 (9), pp. 1968–1978. DOI: 10.1016/j.foreco.2009.07.042.

Fehrmann, Lutz (2007): Alternative Methoden zur Biomasseschätzung auf Einzelbaumebene unter spezieller Berücksichtigung der k-Nearest Neighbour (k-NN) Methode. PhD. Georg-August-Universität Göttingen, Göttingen. Available online at https://ediss.uni-goettingen.de/bitstream/11858/00-1735-0000-0006-B0F5-F/1/fehrmann.pdf.

Felfili, J. (2005): Manual para o monitoramento de parcelas permanentes nos biomas Cerrado e Pantanal. Brasìlia DF: Universidade de Brasìlia Departamento de Engenharia Florestal. Available online at http://worldcatlibraries.org/wcpa/oclc/709525470.

Felfili, M. (2008): Proposição de critérios florísticos, estruturais e de produção para o manejo do cerrado sensu stricto do Brasil Central. Doutorado. Universidade de Brasília, Brasília.

Fensham, R. J.; Powell, O.; Horne, J. (2011): Rail survey plans to remote sensing. vegetation change in the Mulga Lands of eastern Australia and its implications for land use. In Rangeland J. 33 (3), pp. 229–238. DOI: 10.1071/rj11007.

Ferreira, L. G.; Huete, A. R. (2004): Assessing the seasonal dynamics of the Brazilian Cerrado vegetation through the use of spectral vegetation indices. In International Journal of Remote Sensing 25 (10), pp. 1837–1860. DOI: 10.1080/0143116031000101530.

Ferreira, Leandro V.; Laurance, William F. (1997): Effects of Forest Fragmentation on Mortality and Damage of Selected Trees in Central Amazonia. In Conserv. Biol. 11 (3), pp. 797–801. DOI: 10.1046/j.1523-1739.1997.96167.x.

Ferreira, M. E.; Ferreira, L. G.; Sano, E. E.; Shimabukuro, Y. E. (2007): Spectral linear mixture modelling approaches for land cover mapping of tropical savanna areas in Brazil. In International Journal of Remote Sensing 28 (2), pp. 413–429. DOI: 10.1080/01431160500181507.

Ferreira, N. C.; Ferreira.; L. G., Ferreira, M. E.; Bustamante, M and Ometto, J (2011): Assessing deforestation related carbon emission in the Brazilian Savanna based on moderate resolution imagery. In 2011 IEEE International Geoscience and Remote Sensing Symposium, pp. 748-751. DOI: 10.1109/IGARSS.2011.6049238.

Ferreira, R.L.C (1997): Estrutura e dinâmica de uma floresta secundária de transição, Rio Vermelho e Serra Azul de Minas, MG. Tese de doutorado. Universidade Federal de Viçosa, Viçosa.

Furtado, Luiz Felipe de Almeida; Silva, Thiago Sanna Freire; Novo, Evlyn Márcia Leão de Moraes (2016): Dual-season and full-polarimetric C band SAR assessment for vegetation mapping in the Amazon várzea wetlands. In Remote Sensing of Environment 174, pp. 212–222. DOI: 10.1016/j.rse.2015.12.013.

Ganem, Sena. S. (2008): Ocupação humana e impactos no bioma Cerrado: dos bandeirantes. Brasília, DF.

Garestier, F.; Dubois-Fernandez, P. C.; Guyon, D.; Le Toan, T. (2009): Forest Biophysical Parameter Estimation Using L- and P-Band Polarimetric SAR Data. In IEEE Trans. Geosci. Remote Sensing 47 (10), pp. 3379–3388. DOI: 10.1109/TGRS.2009.2022947.

Giambelluca, Thomas W.; Scholz, Fabian G.; Bucci, Sandra J.; Meinzer, Frederick C.; Goldstein, Guillermo; Hoffmann, William A. et al. (2009): Evapotranspiration and energy balance of Brazilian savannas with contrasting tree density. In Agricultural and Forest Meteorology 149 (8), pp. 1365–1376. DOI: 10.1016/j.agrformet.2009.03.006.

Girolamo Neto, C.Di.; Fonseca, Leila Maria Garcia; Körting, Thales Sehn (2017): ASSESSMENT OF TEXTURE FEATURES FOR BRAZILIAN SAVANNA CLASSIFICATION: A CASE STUDY IN BRASÍLIA NATIONAL PARK. In Brazilian Journal of Cartography 69/5, pp. 891–901.

Gizachew, Belachew; Solberg, Svein; Næsset, Erik; Gobakken, Terje; Bollandsås, Ole Martin; Breidenbach, Johannes et al. (2016): Mapping and estimating the total living biomass and carbon in low-biomass woodlands using Landsat 8 CDR data. In Carbon balance and management 11 (1), p. 13. DOI: 10.1186/s13021-016-0055-8.

Goedert, Wenceslau J. (1986): Solos dos Cerrados. Tecnologias e estratégias de manejo. Brasília, D.F.: EMBRAPA, Centro de Pesquisa Agropecuária dos Cerrados; Nobel.

Goodland, Roberto (1971): A Physiognomic Analysis of the `Cerrado' Vegetation of Central Brasil. In Journal of Ecology 59 (2), p. 411. DOI: 10.2307/2258321.

References

Göpel, Jan; Schüngel, Jan; Schaldach, Rüdiger; Meurer, Katharina H. E.; Jungkunst, Hermann F.; Franko, Uwe et al. (2018): Future land use and land cover in Southern Amazonia and resulting greenhouse gas emissions from agricultural soils. In Reg. Envir. Chang. 18 (1), pp. 129–142. DOI: 10.1007/s10113-017-1235-0.

Goudie, Andrew; Cuff, David J. (Eds.) (2002): Encyclopedia of global change. Environmental change and human society. Oxford: Oxford Univ. Press.

Grecchi, R. C.; Gwyn, Q. H. J.; Benie, G. B.; Formaggio, A. R.; Fahl, F. C. (2014): Land use and land cover changes in the Brazilian Cerrado. A multidisciplinary approach to assess the impacts of agricultural expansion. In Appl. Geogr. 55, pp. 300–312. DOI: 10.1016/j.apgeog.2014.09.014.

Gross, Michael (2017): Brazil's fragmented forests. In Current Biology 27 (14), R681-R684. DOI: 10.1016/j.cub.2017.07.001.

Haack, Barry; Bechdol, Matthew (2000): Integrating multisensor data and RADAR texture measures for land cover mapping. In Computers & Geosciences 26 (4), pp. 411–421. DOI: 10.1016/S0098-3004(99)00121-1.

Haralick, Robert M.; Shanmugam, K.; Dinstein, Its'Hak (1973): Textural Features for Image Classification. In IEEE Trans. Syst., Man, Cybern. SMC-3 (6), pp. 610–621. DOI: 10.1109/TSMC.1973.4309314.

Harper, Karenn A.; MACDONALD, S. ELLEN; BURTON, PHILIP J.; CHEN, JIQUAN; Brosofske, Kimberley, D.; SAUNDERS, SARI C. et al. (2005): Edge Influence on Forest Structure and Composition in Fragmented Landscapes. In Conservation Biology 19 (3), pp. 768–782. DOI: 10.1111/j.1523-1739.2005.00045.x.

He, Kate S.; Zhang, Jianting; Zhang, Qiaofeng (2009): Linking variability in species composition and MODIS NDVI based on beta diversity measurements. In Acta Oecologica 35 (1), pp. 14–21. DOI: 10.1016/j.actao.2008.07.006.

Henderson, Floyd M.; Lewis, Anthony J.; Ryerson, Robert A. (Eds.) (1998): Principles and applications of imaging radar. American Society for Photogrammetry and Remote Sensing. 3. ed. New York: Wiley (Manual of remote sensing, / ed. by Robert A. Ryerson. Publ. in cooperation with the American Society for Photogrammetry and Remote Sensing ; Vol. 2).

Henry, M.; Bombelli, A.; Trotta, C.; Alessandrini, A.; Birigazzi, L.; Sola, G. et al. (2013): GlobAllomeTree: international platform for tree allometric equations to support volume, biomass and carbon assessment. In iForest 6 (6), pp. 326–330. DOI: 10.3832/ifor0901-006.

References

Hermuche, P. M.; Sano, E. E. (2011): Identificação da floresta estacional decidual no Vão do Paraná, estado de Goiás, a partir da analise da reflectância acumulada de imagens do sensor ETM+/Landsat-7. In Revista Brasileira de Cartografia 63 (3), pp. 415–425.

Hernandez, P.; Ponzoni, F. J.; Pereira, M. N. (1998): Phytophysiognomic and land use mapping of partial Alto Taquari Basin using TM/Landsat and HRV/SPOT images. In Pesqui. Agropecu. Bras. 33, pp. 1755–1762.

Hirota, Marina; Nobre, Carlos; Oyama, Marcos Daisuke; Bustamante, Mercedes M. C. (2010): The climatic sensitivity of the forest, savanna and forest-savanna transition in tropical South America. In The New phytologist 187 (3), pp. 707–719. DOI: 10.1111/j.1469-8137.2010.03352.x.

Hoffmann, William A.; Adasme, Ryan; HARIDASAN, M.; Carvalho, Marina T. de; Geiger, Erika L.; Pereira, Mireia A. B. et al. (2009): Tree topkill, not mortality, governs the dynamics of savanna-forest boundaries under frequent fire in central Brazil. In Ecology 90 (5), pp. 1326–1337. DOI: 10.1890/08-0741.1.

Holzner, S. (2013): Estimation of Aboveground Biomass in Brazilian Gallery Forests. MSc. Georg-August-University Göttingen, Göttingen.

IBGE (2001): Mapa de Solos do Brasil. IBGE; EMBRAPA. Rio de Janeiro. Available online at http://ftp//geoftp.ibge.gov.br/informacoes_ambientais/pedologia/mapas/brasil/solos.pdf, checked on 10/24/2019.

IBGE (2004): Mapa de Biomas do Brasil, primeira aproximação. Rio de Janeiro.

IBGE (2015): Indicadores de desenvolvimento sustentável: Brasil 2015 10.

Inglada, Jordi; Vincent, Arthur; Arias, Marcela; Marais-Sicre, Claire (2016): Improved Early Crop Type Identification By Joint Use of High Temporal Resolution SAR And Optical Image Time Series. In Remote Sensing 8 (5), p. 362. DOI: 10.3390/rs8050362.

INPE (2011): Program for the Estimation of Amazon Deforestation (PRODES). INPE. São José dos Campos.

Jandl, Robert; Lindner, Marcus; Vesterdal, Lars; Bauwens, Bram; Baritz, Rainer; Hagedorn, Frank et al. (2007): How strongly can forest management influence soil carbon sequestration? In Geoderma 137 (3), pp. 253–268. DOI: 10.1016/j.geoderma.2006.09.003.

Janssen, Thomas A.J.; Ametsitsi, George K.D.; Collins, Murray; Adu-Bredu, Stephen; Oliveras, Imma; Mitchard, Edward T.A.; Veenendaal, Elmar M. (2018): Extending the baseline of tropical dry forest loss in Ghana (1984–2015) reveals drivers of major deforestation inside a protected area. In Biological Conservation 218, pp. 163–172. DOI: 10.1016/j.biocon.2017.12.004.

References

Jensen, John R. (2014a): Remote sensing of the environment. An earth resource perspective. Segunda edición, Indian Subcontinental edition. India: Dorling Kindersley; Pearson (Always Learning).

Jensen, John R. (2014b): Remote sensing of the environment. An earth resource perspective / John R. Jensen. 2nd ed., Pearson new international ed. Harlow, Essex: Pearson.

Jorge, Luiz Alberto Blanco; Garcia, Gilberto José (1997): A study of habitat fragmentation in Southeastern Brazil using remote sensing and geographic information systems (GIS). In Forest Ecology and Management 98 (1), pp. 35–47. DOI: 10.1016/S0378-1127(97)00072-8.

Kauffman, J. Booone; Hughes, R. Flint; Heider, Chris (2009): Carbon pool and biomass dynamics associated with deforestation, land use, and agricultural abandonment in the neotropics. In Ecol. Appl. 19 (5), pp. 1211–1222. DOI: 10.1890/08-1696.1.

Kauffman, J. Boone; Cummings, D. L.; Ward, D. E. (1994): Relationships of Fire, Biomass and Nutrient Dynamics along a Vegetation Gradient in the Brazilian Cerrado. In Journal of Ecology 82 (3), p. 519. DOI: 10.2307/2261261.

Kershaw, J. A.; Ducey, M. J.; Beers, T. W.; Husch, B. (2016): Forest Mensuration: Wiley. Available online at https://books.google.de/books?id=ymhxDQAAQBAJ.

Klink, C. A.; Machado, R. B. (2005): A conservação do cerrado brasileiro. In Megadiversidade 1, pp. 147–155.

Krieger, Gerhard; Moreira, Alberto; Fiedler, Hauke; Hajnsek, Irena; Werner, Marian; Younis, Marwan; Zink, Manfred (2007): TanDEM-X: A Satellite Formation for High-Resolution SAR Interferometry. In IEEE Trans. Geosci. Remote Sensing 45 (11), pp. 3317–3341. DOI: 10.1109/TGRS.2007.900693.

Kulp, L. (2018): Estimation of aboveground biomass and carbon stocks in the Cerrado forests, Mato Grosso, Brazil. MSc. Georg-August-Universität Göttingen, Göttingen.

Kulp, L.; de Souza Mendes, F. de; Gerold, G. (2018): Aboveground biomass and carbon stocks in the Cerrado forests, Mato Grosso, Brazil. In GEO-ÖKO 39 (16161 – 0983), pp. 5–47.

Lagos, M. do C. C. (2017): Efeito de borda em fragmentos do bioma Cerrado e Mata Atlântica. Available online at http://repositorio.bc.ufg.br/tede/bitstream/tede/7610/5/Tese%20-%20Maria%20do%20Carmo%20Correa%20Lagos%20-%202017.pdf.

Lapola, David M.; Martinelli, Luiz A.; Peres, Carlos A.; Ometto, Jean P. H. B.; Ferreira, Manuel E.; Nobre, Carlos A. et al. (2014): Pervasive transition of the Brazilian land-use system. In Nature Clim Change 4 (1), pp. 27–35. DOI: 10.1038/nclimate2056.

Laurance, W. F.; Ferreira L.V.; Rankin De Merona J.M.; Laurance S.G.; Hutchings R.W.; Lovejoy T.E (1997): Biomass Collapse in Amazonian Forest Fragments. In Science 278 (5340), pp. 1117–1118. DOI: 10.1126/science.278.5340.1117.

Laurance, William F.; Camargo, José L.C.; Luizão, Regina C.C.; Laurance, Susan G.; Pimm, Stuart L.; Bruna, Emilio M. et al. (2011): The fate of Amazonian forest fragments: A 32-year investigation. In Biological Conservation 144 (1), pp. 56–67. DOI: 10.1016/j.biocon.2010.09.021.

Laurance, William F.; Delamônica, Patricia; Laurance, Susan G.; Vasconcelos, Heraldo L.; Lovejoy, Thomas E. (2000): Rainforest fragmentation kills big trees. In Nature 404 (6780), p. 836. DOI: 10.1038/35009032.

Laurance, William F.; Ferreira, Leandro V.; Merona, Judy M. Rankin-De; Laurance, Susan G.; Hutchings, Roger W.; Lovejoy, Thomas E. (1998a): Effects of Forest Fragmentation on Recruitment Patterns in Amazonian Tree Communities. In Conservation Biology 12 (2), pp. 460–464. DOI: 10.1111/j.1523-1739.1998.97175.x.

Laurance, William F.; Ferreira, Leandro V.; Rankin-de Merona, Judy M.; Laurance, Susan G. (1998b): RAIN FOREST FRAGMENTATION AND THE DYNAMICS OF AMAZONIAN TREE COMMUNITIES. In Ecology 79 (6), pp. 2032–2040. DOI: 10.1890/0012-9658(1998)079[2032:RFFATD]2.0.CO;2.

Laurance, William F.; Laurance, Susan G.; Delamonica, Patricia (1998c): Tropical forest fragmentation and greenhouse gas emissions. In Forest Ecology and Management 110 (1), pp. 173–180. DOI: 10.1016/S0378-1127(98)00291-6.

Laurance, William F.; Nascimento, Henrique E. M.; Laurance, Susan G.; Andrade, Ana C.; Fearnside, Philip M.; Ribeiro, José E. L.; Capretz, Robson L. (2006): Rain forest fragmentation and the proliferation of successional trees. In Ecology 87 (2), pp. 469–482. DOI: 10.1890/05-0064.

Le Toan, T.; Kong, Jin Au (1992): Microwave interaction and analysis of polarimetric data. Retrieval of forest biomass, executive summary. Toulouse: ESA.

Lee, Jong-Sen; Pottier, Eric (2009): Polarimetric radar imaging. From basics to applications / Jong-Sen Lee, Eric Pottier. Boca Raton, Fla.: CRC; London : Taylor & Francis [distributor] (Optical science and engineering, 143).

Liesenberg, Veraldo; Galvão, Lênio Soares; Ponzoni, Flávio Jorge (2007): Variations in reflectance with seasonality and viewing geometry. Implications for classification of Brazilian savanna physiognomies with MISR/Terra data. In Remote Sensing of Environment 107 (1-2), pp. 276–286. DOI: 10.1016/j.rse.2006.03.018.

Lilienfein, Juliane; Wilcke, Wolfgang; Vilela, Lourival; Ayarza, Miguel Angelo; Lima, Samuel do Carmo; Zech, Wolfgang (2003): Soil Fertility under Native Cerrado and Pasture in the Brazilian Savanna. In Soil Science Society of America Journal 67 (4), p. 1195. DOI: 10.2136/sssaj2003.1195.

Lima-Ribeiro, Matheus de Souza (2008): Efeitos de borda sobre a vegetação e estruturação populacional em fragmentos de Cerradão no Sudoeste Goiano, Brasil. In Acta Bot. Bras. 22 (2), pp. 535–545. DOI: 10.1590/S0102-33062008000200020.

Liu, Y. Y.; van Dijk, Aijm; de Jeu, R. A. M.; Canadell, J. G.; McCabe, M. F.; Evans, J. P.; Wang, G. J. (2015): Recent reversal in loss of global terrestrial biomass. In Nat. Clim. Chang. 5 (5), pp. 470–474. DOI: 10.1038/nclimate2581.

Lötsch, Fritz; Zöhrer, F.; Haller, Karl Eberhard; Brünig, E. F. (1973): Statistics of forest inventory and information from aerial photographs. 2. ed. München: BLV Verl. Ges (Forest inventory, / F. Lötsch; F. Zöhrer; K. E. Haller ; Vol. 1).

Louis, J.; Debaecker, V.; Pflug, B.; Main-Knorn, M.; Bieniarz, J.; Mueller-Wilm, U. et al. (Eds.) (2016): Sentinel-2 Sen2Cor: L2A Processor for Users. ESA Living Planet Symposium 2016. Living Planet Symposium 2016.

Lucas, R. M.; Milne, A. K.; Cronin, N.; Witte, C.; Denham, R. (2000): The potential of synthetic aperture radar (SAR) for quantifying the biomass of Australia's woodlands. In Rangeland J. 22 (1), p. 124. DOI: 10.1071/RJ0000124.

Ma, Lei; Shen, Chunyu; Lou, Duo; Fu, Shenglei; Guan, Dongsheng (2017): Ecosystem carbon storage in forest fragments of differing patch size. In Sci Rep 7 (1), pp. 1–8. DOI: 10.1038/s41598-017-13598-4.

Macedo, Marcia N.; DeFries, Ruth S.; Morton, Douglas C.; Stickler, Claudia M.; Galford, Gillian L.; Shimabukuro, Yosio E. (2012): Decoupling of deforestation and soy production in the southern Amazon during the late 2000s. In Proc. Natl. Acad. Sci. U. S. A. 109 (4), pp. 1341–1346. DOI: 10.1073/pnas.1111374109.

Machado, R. B.; Ramos Neto, M. B.; Pereira, P.G.P.; Caldas, E. F.; Gonçalves, D. A.; Santos, N. S. et al. (2004): Estimativas de perda da área do Cerrado brasileiro. Conservação Internacional. Brasília.

Malcolm, Jay R. (1994): Edge Effects in Central Amazonian Forest Fragments. In Ecology 75 (8), p. 2438. DOI: 10.2307/1940897.

Malhado, Ana Cláudia Mendes; Pires, Gabrielle Ferreira; Costa, Marcos Heil (2010): Cerrado conservation is essential to protect the Amazon rainforest. In AMBIO: A Journal of the Human Environment 39 (8), pp. 580–584. DOI: 10.1007/s13280-010-0084-6.

Malhi, Yadvinder; WOOD, DANIEL; Baker, Timothy R.; WRIGHT, JAMES; Phillips, Oliver L.; COCHRANE, THOMAS et al. (2006): The regional variation of aboveground live biomass in old-growth Amazonian forests. In Glob. Change Biol. 12 (7), pp. 1107–1138. DOI: 10.1111/j.1365-2486.2006.01120.x.

Maracahipes Santos, Leonardo; Lenza, Eddie; dos Santos, Josias Oliveira; Marimon, Beatriz Schwantes; Eisenlohr, Pedro V.; Marimon Junior, Ben Hur; Feldpausch, Ted R. (2015): Diversity, floristic composition, and structure of the woody vegetation of the Cerrado in the Cerrado–Amazon transition zone in Mato Grosso, Brazil. In Brazilian Journal of Botany 38 (4), pp. 877–887. DOI: 10.1007/s40415-015-0186-2.

Marimon, Beatriz S.; Marimon-Junior, Ben Hur; Feldpausch, Ted R.; Oliveira-Santos, Claudinei; Mews, Henrique A.; Lopez-Gonzalez, Gabriela et al. (2014): Disequilibrium and hyperdynamic tree turnover at the forest–cerrado transition zone in southern Amazonia. In Plant Ecol. Divers. 7 (1-2), pp. 281–292. DOI: 10.1080/17550874.2013.818072.

Marques, Eduardo Q.; Marimon-Junior, Ben Hur; Marimon, Beatriz S.; Matricardi, Eraldo A. T.; Mews, Henrique A.; Colli, Guarino R. (2019): Redefining the Cerrado–Amazonia transition: implications for conservation. In Biodivers Conserv 01 (4), p. 24. DOI: 10.1007/s10531-019-01720-z.

Matlack, Glenn R. (1993): Microenvironment variation within and among forest edge sites in the eastern United States. In Biological Conservation 66 (3), pp. 185–194. DOI: 10.1016/0006-3207(93)90004-K.

Mayaux, Philippe; Grandi, Gianfranco de; Malingreau, Jean-Paul (2000): Central African Forest Cover Revisited. In Remote Sensing of Environment 71 (2), pp. 183–196. DOI: 10.1016/S0034-4257(99)00073-5.

McGarigal, K., Cushman, S.A., Neel, M.C. & Ene, E. (2002) FRAGSTATS: Spatial Pattern Analysis Program for Categorical Maps. Computer software program produced by the authors at the University of Massachusetts, Amherst. Available at the following web site: www.umass.edu/landeco/research/fragstats/fr

Menaut, J. C. (1983): The Vegetation of African Savannas. In: Bourlière F (ed) Tropical savannas. 13 volumes. Amsterdam: Elsevier.

Mendonça, A. H. (2010): Avaliação do efeito de borda sobre a vegetação do cerrado sensu stricto inserido em matriz de pastagem. Master Thesis, Escola de Engenharia de São Carlos, Universidade de São Paulo, São Carlos. doi:10.11606/D.18.2010.tde-12082010-141506.

Mendonça, Augusto H.; Russo, Cibele; Melo, Antônio C.G.; Durigan, Giselda (2015): Edge effects in savanna fragments: a case study in the cerrado. In Plant Ecology & Diversity 8 (4), pp. 493–503. DOI: 10.1080/17550874.2015.1014068.

Mermoz, Stéphane; Le Toan, Thuy; Villard, Ludovic; Réjou-Méchain, Maxime; Seifert-Granzin, Joerg (2014): Biomass assessment in the Cameroon savanna using ALOS PALSAR data. In Remote Sensing of Environment 155, pp. 109–119. DOI: 10.1016/j.rse.2014.01.029.

Mermoz, Stéphane; Réjou-Méchain, Maxime; Villard, Ludovic; Le Toan, Thuy; Rossi, Vivien; Gourlet-Fleury, Sylvie (2015): Decrease of L-band SAR backscatter with biomass of dense forests. In Remote Sensing of Environment 159, pp. 307–317. DOI: 10.1016/j.rse.2014.12.019.

Mesquita JR, H. N.; Bittencourt, M. D.; Kuntschik, G. (Eds.) (2001): Gradient analysis of cerrado vegetation physiognomies by SAR image processing (JERS-1). X Simpósio Brasileiro de Sensoriamento Remoto,. Foz do Iguacú.

Michelakis, Dimitrios; Stuart, Neil; Brolly, Matthew; Woodhouse, Iain H.; Lopez, German; Linares, Vinicio (2015): Estimation of Woody Biomass of Pine Savanna Woodlands From ALOS PALSAR Imagery. In IEEE J. Sel. Top. Appl. Earth Observations Remote Sensing 8 (1), pp. 244–254. DOI: 10.1109/JSTARS.2014.2365253.

Miguel, Eder Pereira; Rezende, Alba Valéria; Leal, Fabrício Assis; Matricardi, Eraldo Aparecido Trondoli; Encinas, José Marcelo Imana; Miranda, João Felipe Nunes (2017a): Floristic, structural, and allometric equations to estimate arboreal volume and biomass in a cerradão site. In SCA 38 (4), p. 1691. DOI: 10.5433/1679-0359.2017v38n4p1691.

Miguel, Eder Pereira; Rezende, Alba Valéria; Pereira, Reginaldo Sergio; Azevedo, Gileno Brito de; Mota, Fabrícia Conceição Menez; Souza, Álvaro Nogueira de; Joaquim, Maísa Santos (2017b): Modeling and prediction of volume and aereal biomass of the tree vegetation in a Cerradão area of Central Brazil. In Interciencia: Revista de ciencia y tecnología de América 42 (1), pp. 21–27.

Minami, Patricia; Ribeiro, Edilene Silva; Martins, Verônica Gratão; Moreira, Elton Lopes (2017): FLORISTICA E FITOSSOCIOLOGIA EM MATA DE GALERIA E CERRADÃO NO MUNICÍPIO DE NOVA MUTUM – MT, BRASIL. In Biodiversidade 16 (1). Available online at http://periodicoscientificos.ufmt.br/ojs/index.php/biodiversidade/article/download/4973/3351.

Miranda, Sabrina do Couto de; Bustamante, Mercedes; Palace, Michael; Hagen, Stephen; Keller, Michael; Ferreira, Laerte Guimarães (2014): Regional Variations in Biomass Distribution in Brazilian Savanna Woodland. In Biotropica 46 (2), pp. 125–138. DOI: 10.1111/btp.12095.

References

Mitchard, E. T. A.; Saatchi, S. S.; White, L. J. T.; Abernethy, K. A.; Jeffery, K. J.; Lewis, S. L. et al. (2012): Mapping tropical forest biomass with radar and spaceborne LiDAR in Lopé National Park, Gabon. Overcoming problems of high biomass and persistent cloud. In Biogeosciences 9 (1), pp. 179–191. DOI: 10.5194/bg-9-179-2012.

Mitchard, E.T.A.; Saatchi, S. S.; Lewis, S. L.; Feldpausch, T. R.; Woodhouse, I. H.; Sonké, B. et al. (2011): Measuring biomass changes due to woody encroachment and deforestation/degradation in a forest–savanna boundary region of central Africa using multi-temporal L-band radar backscatter. In Remote Sensing of Environment 115 (11), pp. 2861–2873. DOI: 10.1016/j.rse.2010.02.022.

MMA (2002): Mapa interativo. Vegetation coverage in the Cerrado. LAPIG. Available online at http://maps.lapig.iesa.ufg.br/lapig.html, checked on 01-25-2018.

MMA (2006): Cobertura vegetal dos biomas brasileiros. São Luiz: Folha SA-23-Z-A. EMBRAPA CERRADOS: MMA. Available online at http://mapas.mma.gov.br/geodados/brasil/vegetacao/vegetacao2002/, checked on 03-20-2018.

MMA (2014): PPCerrado. Plano de Ação para prevenção e controle do desmatamento e das quimadas no Cerrado : 2a fase (2014-2015). Brasília, DF: Ministério do Meio Ambiente, Secretaria Executiva, Departamento de Políticas para o Combate ao Desmatamento.

MMA (2015): Mapeamento do Uso e Cobertura da Terra do Cerrado. Projeto TerraClass Cerrado 2013. Brasília.

Morais, Vinícius Augusto; Scolforo, José Roberto Soares; Silva, Carlos Alberto; Mello, José Marcio de; Gomide, Lucas Rezende; Oliveira, Antônio Donizette de (2013): Carbon and biomass stocks in a fragment of cerradão in Minas Gerais state, Brazil. In CERNE 19 (2), pp. 237–245. DOI: 10.1590/S0104-77602013000200007.

Müller, Hannes; Rufin, Philippe; Griffiths, Patrick; Barros Siqueira, Auberto José; Hostert, Patrick (2015): Mining dense Landsat time series for separating cropland and pasture in a heterogeneous Brazilian savanna landscape. In Remote Sensing of Environment 156, pp. 490–499. DOI: 10.1016/j.rse.2014.10.014.

Munyati, C.; Economon, E. B.; Malahlela, O. E. (2013): Effect of canopy cover and canopy background variables on spectral profiles of savanna rangeland bush encroachment species based on selected Acacia species (mellifera, tortilis, karroo) and Dichrostachys cinerea at Mokopane, South Africa. In J. Arid. Environ. 94, pp. 121–126. DOI: 10.1016/j.jaridenv.2013.02.010.

Murcia, Carolina (1995): Edge effects in fragmented forests: implications for conservation. In Trends in Ecology & Evolution 10 (2), pp. 58–62. DOI: 10.1016/S0169-5347(00)88977-6.

Myers, N.; Mittermeier, R. A.; Mittermeier, C. G. (2000): Biodiversity hotspots for conservation priorities. [S.l.] (Nature, vol. 403, 24 february 2000).

Nascimento, Erika Regina Prado; Sano, Edson Eyji (2010): Identificação de Cerrado Rupestre por meio de imagens multitemporais do Landsat: proposta metodológica. In Soc. nat. 22 (1), pp. 93–106. DOI: 10.1590/S1982-45132010000100007.

Nascimento, Henrique E. M.; Laurance, William F. (2004): Biomass dynamics in Amazonian forest fragments. In Ecological Applications 14 (sp4), pp. 127–138. DOI: 10.1890/01-6003.

Nascimento, Henrique E. M.; Laurance, William F. (2006): Efeitos de área e de borda sobre a estrutura florestal em fragmentos de floresta de terra-firme após 13-17 anos de isolamento. In Acta Bot. Bras. 36 (2), pp. 183–192. DOI: 10.1590/S0044-59672006000200008.

Nepstad, Daniel; McGrath, David; Stickler, Claudia; Alencar, Ane; Azevedo, Andrea; Swette, Briana et al. (2014): Slowing Amazon deforestation through public policy and interventions in beef and soy supply chains. In Science (New York, N.Y.) 344 (6188), pp. 1118–1123. DOI: 10.1126/science.1248525.

Nogueira, Euler Melo; Fearnside, Philip Martin; Nelson, Bruce Walker; Barbosa, Reinaldo Imbrozio; Keizer, Edwin Willem Hermanus (2008): Estimates of forest biomass in the Brazilian Amazon: New allometric equations and adjustments to biomass from wood-volume inventories. In Forest Ecology and Management 256 (11), pp. 1853–1867. DOI: 10.1016/j.foreco.2008.07.022.

Nogueira, Euler Melo; Fearnside, Philip Martin; Nelson, Bruce Walker; França, Mabiane Batista (2007): Wood density in forests of Brazil's 'arc of deforestation': Implications for biomass and flux of carbon from land-use change in Amazonia. In Forest Ecology and Management 248 (3), pp. 119–135. DOI: 10.1016/j.foreco.2007.04.047.

Nogueira, Euler Melo; Yanai, Aurora M.; Fonseca, Frederico O. R.; Fearnside, Philip Martin (2015): Carbon stock loss from deforestation through 2013 in Brazilian Amazonia. In Global change biology 21 (3), pp. 1271–1292. DOI: 10.1111/gcb.12798.

Nogueira, Euler Melo; Yanai, Aurora Miho; Vasconcelos, Sumaia Saldanha de; Alencastro Graça, Paulo Maurício Lima de; Fearnside, Philip Martin (2018): Carbon stocks and losses to deforestation in protected areas in Brazilian Amazonia. In Reg. Envir. Chang. 18 (1), pp. 261–270. DOI: 10.1007/s10113-017-1198-1.

Oliveira, Paulo Tarso S.; Nearing, Mark A.; Moran, M. Susan; Goodrich, David C.; Wendland, Edson; Gupta, Hoshin V. (2014): Trends in water balance components across the Brazilian Cerrado. In Water Resour. Res. 50 (9), pp. 7100–7114. DOI: 10.1002/2013WR015202.

Oliveira Filho, A. T.; Ratter, J. A. (2013): Vegetation Physiognomies and Woody Flora of the Cerrado Biome. In P. S, R. J (Eds.): The Cerrados of Brazil: Ecology and Natural History of a Neotropical Savanna. With assistance of Oliveira Filho, A.T. & RATTER, J.A.: Columbia University Press, pp. 91–120.

Olofsson, Pontus; Foody, Giles M.; Herold, Martin; Stehman, Stephen V.; Woodcock, Curtis E.; Wulder, Michael A. (2014): Good practices for estimating area and assessing accuracy of land change. In Remote Sensing of Environment 148, pp. 42–57. DOI: 10.1016/j.rse.2014.02.015.

Olson, David M.; Dinerstein, Eric; Wikramanayake, Eric D.; Burgess, Neil D.; Powell, George V. N.; Underwood, Emma C. et al. (2001): Terrestrial Ecoregions of the World. A New Map of Life on Earth. In BioScience 51 (11), p. 933. DOI: 10.1641/0006-3568(2001)051[0933:TEOTWA]2.0.CO;2.

Om, Prakash Tripathi; Khongjee, Rangdajied Reynald (2010): Effect of forest fragment size on tree diversity and population structure of humid subtropical forest of Meghalaya, India. In Biodiversity Science 18 (2), p. 222. DOI: 10.3724/SP.J.1003.2010.222.

Ottmar, R. D.; Vihnanek, R. E.; Miranda, H. S.; Sato, M. N.; Andrade, S. M. A. (2001): Séries de estereo-fotografias para quantificar a biomassa da vegetac¸a~o do Cerrado do Brasil Central. Available online at http://redd.mma.gov.br/images/apresentacoes/gttredd_reuniao6_heloisamiranda_estereofotografias.pdf, checked on 04-25-2018.

Paneque-Galvez, J.; Mas, J. F.; More, G.; Cristobal, J.; Orta-Martinez, M.; Luz, A. C. et al. (2013): Enhanced land use/cover classification of heterogeneous tropical landscapes using support vector machines and textural homogeneity. In Int. J. Appl. Earth Obs. Geoinf. 23, pp. 372–383. DOI: 10.1016/j.jag.2012.10.007.

Paula, Mateus Dantas de; Costa, Cecília Patrícia Alves; Tabarelli, Marcelo (2011): Carbon Storage in a Fragmented Landscape of Atlantic Forest: The Role Played by Edge-Affected Habitats and Emergent Trees. In Tropical Conservation Science 4 (3), pp. 349–358. DOI: 10.1177/194008291100400310.

Peixoto, K. S.; Marimon-Junior, B. H.; Marimon, B. S.; Elias, F.; Farias, J.; Freitag, R. et al. (2017): Unravelling ecosystem functions at the Amazonia-Cerrado transition: II. Carbon stocks and CO2 soil efflux in cerradão forest undergoing ecological succession. In Acta Oecologica 82, pp. 23–31. DOI: 10.1016/j.actao.2017.05.005.

Penariol, L. V., & Madi-Ravazzi, L. (2013): Edge-interior differences in the species richness and abundance of drosophilids in a semideciduous forest fragment. SpringerPlus, 2(1), 114. https://doi.org/10.1186/2193-1801-2-114.

Pereira, Luciana; Furtado, Luiz; Novo, Evlyn; Sant'Anna, Sidnei; Liesenberg, Veraldo; Silva, Thiago (2018): Multifrequency and Full-Polarimetric SAR Assessment for Estimating Above Ground Biomass and Leaf Area Index in the Amazon Várzea Wetlands. In Remote Sensing 10 (9), p. 1355. DOI: 10.3390/rs10091355.

Pfadenhauer, Jörg; Klötzli, Frank (2014): Vegetation der Erde. Grundlagen, Ökologie, Verbreitung. Berlin: Springer Spektrum. Available online at http://ebooks.ciando.com/book/index.cfm/bok_id/1869205.

Pottier, E.; Lee, J.; Ferro-Famil, L. (2007): PolSARPro_v4.2.0-Tutorial-Part1 Radar Polarimetry-4 Polarimetric decompositions.

Prabhakara, Kusuma; Hively, W. Dean; McCarty, Gregory W. (2015): Evaluating the relationship between biomass, percent groundcover and remote sensing indices across six winter cover crop fields in Maryland, United States. In International Journal of Applied Earth Observation and Geoinformation 39, pp. 88–102. DOI: 10.1016/j.jag.2015.03.002.

Pütz, Sandro; Groeneveld, Jürgen; Henle, Klaus; Knogge, Christoph; Martensen, Alexandre Camargo; Metz, Markus et al. (2014): Long-term carbon loss in fragmented Neotropical forests. In Nature communications 5, p. 5037. DOI: 10.1038/ncomms6037.

Queiroga, J. L. (2001a): Estudos de bordas de fragmentos de cerrado em areas de agricultura do Maranhao. Universidade Estadual de Londrina, Londrina. Laboratório de Ecologia da Paisagem.

Queiroga, J. L. (2001b): Estudos de bordas de fragmentos de cerrado em areas de agricultura do Maranhao. Universidade Estadual de Londrina, Londrina. Laboratório de Ecologia da Paisagem.

Ramankutty, Navin; Foley, Jonathan A.; Olejniczak, Nicholas J. (2002): People on the Land. Changes in Global Population and Croplands during the 20 th Century. In AMBIO: A Journal of the Human Environment 31 (3), pp. 251–257. DOI: 10.1579/0044-7447-31.3.251.

Ratana, Piyachat; Huete, Alfredo R.; Ferreira, Laerte (2005): Analysis of Cerrado Physiognomies and Conversion in the MODIS Seasonal–Temporal Domain. In Earth Interact. 9 (3), pp. 1–22. DOI: 10.1175/1087-3562(2005)009<0001:AOCPAC>2.0.CO;2.

Ratter, J. A.; Richards, P. W.; Argent, G.; Gifford, D. R. (1973): Observations on the Vegetation of Northeastern Mato Grosso: I. The Woody Vegetation Types of the Xavantina-Cachimbo Expedition Area. In Philos. Trans. R. Soc. B-Biol. Sci. 266 (880), pp. 449–492. DOI: 10.1098/rstb.1973.0053.

Rezende, A. V.; Vale, A. T. D.; Sanquetta, C. R.; Figueiredo Filho, A.; Felfili, J. M. (2006): Comparação de modelos matemáticos para estimativa do Comparação de modelos matemáticos para estimativa do

volume, biomassa e estoque de carbono da vegetação lenhosa de um cerrado sensu stricto em Brasília, DF. In Scientia Forestalis 71, pp. 65–76.

Ribeiro, J. F.; WALTER, B. M. T. (1998): Fitofisionomias do bioma cerrado.

Ribeiro, Natasha S.; Saatchi, Sassan S.; Shugart, Herman H.; Washington-Allen, Robert A. (2008): Aboveground biomass and leaf area index (LAI) mapping for Niassa Reserve, northern Mozambique. In J. Geophys. Res. 113 (G3), p. 1331. DOI: 10.1029/2007JG000550.

Ribeiro, Sabina Cerruto; Fehrmann, Lutz; Soares, Carlos Pedro Boechat; Jacovine, Laércio Antônio Gonçalves; Kleinn, Christoph; Oliveira Gaspar, Ricardo de (2011): Above- and belowground biomass in a Brazilian Cerrado. In Forest Ecology and Management 262 (3), pp. 491–499. DOI: 10.1016/j.foreco.2011.04.017.

Rocha, Ednaldo Cândido; Brito, Daniel; Silva, Paulo Machado e.; Silva, Jhefferson; Bernardo, Paulo Vitor dos Santos; Juen, Leandro (2018): Effects of habitat fragmentation on the persistence of medium and large mammal species in the Brazilian Savanna of Goiás State. In Biota Neotrop. 18 (3), p. 2703. DOI: 10.1590/1676-0611-bn-2017-0483.

Rosich, B.; Meadows, P. (2004): Absolute calibration of ASAR Level 1 products generated with PF-ASAR. 1st ed.

Rouse, J. W., Jr. (1974): Monitoring the vernal advancement and retrogradation (green wave effect) of natural vegetation. Priority no. http://hdl.handle.net/2060/19740022555.

Rudorff, Bernardo F. T.; Adami, Marcos; Risso, Joel; Aguiar, Daniel Alves de; Pires, Bernardo; Amaral, Daniel et al. (2012): Remote Sensing Images to Detect Soy Plantations in the Amazon Biome—The Soy Moratorium Initiative. In Sustainability 4 (5), pp. 1074–1088. DOI: 10.3390/su4051074.

Saatchi, S. S.; Nelson, B.; Podest, E.; Holt, J. (2010): Mapping land cover types in the Amazon Basin using 1 km JERS-1 mosaic. In International Journal of Remote Sensing 21 (6-7), pp. 1201–1234. DOI: 10.1080/014311600210146.

Saatchi, Sassan; Marlier, Miriam; Chazdon, Robin L.; Clark, David B.; Russell, Ann E. (2011): Impact of spatial variability of tropical forest structure on radar estimation of aboveground biomass. In Remote Sensing of Environment 115 (11), pp. 2836–2849. DOI: 10.1016/j.rse.2010.07.015.

Sabattini, J. A. (2015): Land cover and land use changes of native forests categories. the case of the Atencio District, Argentina, in the period from 1984 to 2013. In For. Syst. 24 (2), p. 11. DOI: 10.5424/fs/2015242-06680.

Sabins, Floyd F. (1999): Remote sensing for mineral exploration. In Ore Geology Reviews 14 (3-4), pp. 157–183. DOI: 10.1016/S0169-1368(99)00007-4.

Sampaio, Alexandre Bonesso, & Scariot, Aldicir. (2011): Edge effect on tree diversity, composition and structure in a deciduous dry forest in Central Brazil. Revista Árvore, 35(5), 1121-1134. https://doi.org/10.1590/S0100-67622011000600018.

Sankaran, Mahesh; Hanan, Niall P.; Scholes, Robert J.; Ratnam, Jayashree; Augustine, David J.; Cade, Brian S. et al. (2005): Determinants of woody cover in African savannas. In Nature 438 (7069), pp. 846–849. DOI: 10.1038/nature04070.

Sano, E. E.; Ferreira, L. G.; Asner, G. P.; Steinke, E. T. (2007a): Spatial and temporal probabilities of obtaining cloud-free Landsat images over the Brazilian tropical savanna. In International Journal of Remote Sensing 28 (12), pp. 2739–2752. DOI: 10.1080/01431160600981517.

Sano, E. E.; Pinheiro, G.C.C; Meneses, P. R. (2001): Assessing JERS-1 synthetic aperture radar data for vegetation mapping in the Brazilian savanna. In Journal of the Remote Sensing society in Japan 21 (2), pp. 158–167.

Sano, E. E.; Rosa, R.; Brito, J. L. S.; Ferreira, L. G. (2007b): Mapeamento de Cobertura Vegetal do Bioma Cerrado: estratégias e resultados, pp. 1–33.

Sano, E. E.; Rosa, R.; Brito, J. L. S.; Ferreira, L. G. (2008): Semidetailed land use mapping in the Cerrado. In Pesqui. Agropecu. Bras. 43 (1), pp. 153–156.

Sano, Edson E.; Ferreira, Laerte G.; Huete, Alfredo R. (2005): Synthetic Aperture Radar (L band) and Optical Vegetation Indices for Discriminating the Brazilian Savanna Physiognomies. A Comparative Analysis. In Earth Interact. 9 (15), pp. 1–15. DOI: 10.1175/EI117.1.

Sano, Edson E.; Rosa, Roberto; Brito, Jorge L. S.; Ferreira, Laerte G. (2010): Land cover mapping of the tropical savanna region in Brazil. In Environmental Monitoring and Assessment 166 (1-4), pp. 113–124. DOI: 10.1007/s10661-009-0988-4.

Santoro, M.; Fransson, J.E.S.; Eriksson, L.E.B.; Magnusson, M.; Ulander, L.M.H.; Olsson, H. (2009): Signatures of ALOS PALSAR L-Band Backscatter in Swedish Forest. In IEEE Trans. Geosci. Remote Sensing 47 (12), pp. 4001–4019. DOI: 10.1109/TGRS.2009.2023906.

Santos, J. R.; Lacruz, M. S. Pardi; Araujo, L. S.; Keil, M. (2010): Savanna and tropical rainforest biomass estimation and spatialization using JERS-1 data. In International Journal of Remote Sensing 23 (7), pp. 1217–1229. DOI: 10.1080/01431160110092867.

Santos, J. R.; Xaud, M. R.; Pardi Lacruz, M. S. (Eds.) (1998): Analysis of the backscattering signals of JERS-1 image from savanna and tropical rainforest biomass in Brazilian Amazonia. International Symposium on Resource and Environmental Monitoring. Budapest, 1-4 September. Budapest.

Sarmiento, G. (1983): The savannas of Tropical America. Ecosystems of the world 13: tropical savannas. Amsterdan, Oxford, New York: Elsevier Scientific Publishing Company.

Sawyer, D. R. (2016): Ecosystem Profile: Cerrado Biodiversity Hotspot.

Scariot, A. (2005): Cerrado. Ecologia, biodiversidade e conservação. Brasília, DF: Ministério do Meio Ambiente.

Schlund, Michael; Poncet, Felicitas von; Hoekman, Dirk H.; Kuntz, Steffen; Schmullius, Christiane (2014): Importance of bistatic SAR features from TanDEM-X for forest mapping and monitoring. In Remote Sensing of Environment 151, pp. 16–26. DOI: 10.1016/j.rse.2013.08.024.

Scholes, R. J.; Archer, S. R. (1997): TREE-GRASS INTERACTIONS IN SAVANNAS. In Annu. Rev. Ecol. Syst. 28 (1), pp. 517–544. DOI: 10.1146/annurev.ecolsys.28.1.517.

Schreier, Günter (1993): SAR geocoding. Data and systems. Karlsruhe: Wichmann.

Schwieder, Marcel; Leitão, Pedro J.; da Cunha Bustamante, Mercedes Maria; Ferreira, Laerte Guimarães; Rabe, Andreas; Hostert, Patrick (2016): Mapping Brazilian savanna vegetation gradients with Landsat time series. In International Journal of Applied Earth Observation and Geoinformation 52, pp. 361–370. DOI: 10.1016/j.jag.2016.06.019.

Schumacher, F. X. (1933): Logarithmic expression of timber-tree volume. In J Agric Res 47, pp. 719–734.

Scolforo, J. R.; Mello, J. M.; Oliveira, A. D. (2008): Inventário florestal de Minas Gerais. Cerrado: florística, estrutura, diversidade, similaridade, distribuição diamética e de altura, volumetria, tendências de crescimento e áreas aptas para manejo florestal. Lavras: UFLA.

Silva Junior, Celso; Aragão, Luiz; Fonseca, Marisa; Almeida, Catherine; Vedovato, Laura; Anderson, Liana (2018): Deforestation-Induced Fragmentation Increases Forest Fire Occurrence in Central Brazilian Amazonia. In Forests 9 (6), p. 305. DOI: 10.3390/f9060305.

Silveira, S. (2015): Biomas brasileiros. In: SANDERLEI SILVEIRA. Available online at http://sanderlei.com.br/PT/Ensino-Fundamental/Santa-Catarina-Historia-Geografia-31, checked on 12/12/2017.

Small, David (2011): Flattening Gamma. Radiometric Terrain Correction for SAR Imagery. In IEEE Trans. Geosci. Remote Sensing 49 (8), pp. 3081–3093. DOI: 10.1109/TGRS.2011.2120616.

Soares-Filho, Britaldo; Rajão, Raoni; Macedo, Marcia; Carneiro, Arnaldo; Costa, William; Coe, Michael et al. (2014): Land use. Cracking Brazil's Forest Code. In Science (New York, N.Y.) 344 (6182), pp. 363–364. DOI: 10.1126/science.1246663.

References

Soterroni, Aline C.; Ramos, Fernando M.; Mosnier, Aline; Fargione, Joseph; Andrade, Pedro R.; Baumgarten, Leandro et al. (2019): Expanding the Soy Moratorium to Brazil's Cerrado. In Science advances 5 (7), eaav7336. DOI: 10.1126/sciadv.aav7336.

Souza, Priscila Bezerra de; Saporetti Junior, Amilcar Walter; Soares, Michellia Pereira; Viana, Rodney Haulien Oliveira; Camargos, Virgínia Londe de; Meira Neto, João Augusto Alves (2010): Florística de uma área de cerradão na floresta nacional de Paraopeba - Minas Gerais. In CERNE 16 (1), pp. 86–93. DOI: 10.1590/S0104-77602010000100010.

Souza Mendes, Flávia de; Baron, Daniel; Gerold, Gerhard; Liesenberg, Veraldo; Erasmi, Stefan (2019): Optical and SAR Remote Sensing Synergism for Mapping Vegetation Types in the Endangered Cerrado/Amazon Ecotone of Nova Mutum—Mato Grosso. In Remote Sensing 11 (10), p. 1161. DOI: 10.3390/rs11101161.

Steffen, Will; Rockström, Johan; Richardson, Katherine; Lenton, Timothy M.; Folke, Carl; Liverman, Diana et al. (2018): Trajectories of the Earth System in the Anthropocene. In Proc. Natl. Acad. Sci. U. S. A. 115 (33), pp. 8252–8259. DOI: 10.1073/pnas.1810141115.

Stephenson, N. L.; Das, A. J.; Condit, R.; Russo, S. E.; Baker, P. J.; Beckman, N. G. et al. (2014): Rate of tree carbon accumulation increases continuously with tree size. In Nature 507 (7490), pp. 90–93. DOI: 10.1038/nature12914.

Steubing, L.; Fangmeier, A. (1992): Pflanzenökologisches Praktikum. Gelände- und Laborpraktikum der terrestrischen Pflanzenökologie UTB für Wissenschaft Große Reihe, 8062. Stuttgart.

Sun, G.; Ranson, K.J; Kharuk, V.I (2002): Radiometric slope correction for forest biomass estimation from SAR data in the Western Sayani Mountains, Siberia. In Remote Sensing of Environment 79 (2), pp. 279–287. DOI: 10.1016/S0034-4257(01)00279-6.

Torello-Raventos, Mireia; Feldpausch, Ted R.; Veenendaal, Elmar; Schrodt, Franziska; Saiz, Gustavo; Domingues, Tomas F. et al. (2013): On the delineation of tropical vegetation types with an emphasis on forest/savanna transitions. In Plant Ecol. Divers. 6 (1), pp. 101–137. DOI: 10.1080/17550874.2012.762812.

Trancoso, Ralph; Sano, Edson E.; Meneses, Paulo R. (2014): The spectral changes of deforestation in the Brazilian tropical savanna. In Environmental Monitoring and Assessment 187 (1), p. 4145. DOI: 10.1007/s10661-014-4145-3.

Vale, Ailton Teixeira do; Fiedler, Nilton César; Silva, Gilson Fernandes da (2010): Avaliação energética da biomassa do cerrado em função do diâmetro das árvores. In Ciênc. Florest. 12 (2), p. 115. DOI: 10.5902/198050981686

van Breugel, Michiel; Ransijn, Johannes; Craven, Dylan; Bongers, Frans; Hall, Jefferson S. (2011): Estimating carbon stock in secondary forests: Decisions and uncertainties associated with allometric biomass models. In Forest Ecology and Management 262 (8), pp. 1648–1657. DOI: 10.1016/j.foreco.2011.07.018.

Walker, B. H. (1987): Determinants of Tropical Savannas. Oxford, UK: IRL Press Ltd.

Walter, B.H (2006): Fitofisionomias do bioma Cerrado: síntese terminológica e relações florísticas. These de doutorado em Ecologia. Universidade de Brasília, Brasília.

Yague-Martinez, N.; Zan, F. de; Prats-Iraola, P. (2017): Coregistration of Interferometric Stacks of Sentinel-1 TOPS Data. In IEEE Geosci. Remote Sensing Lett. 14 (7), pp. 1002–1006. DOI: 10.1109/LGRS.2017.2691398.

Yu, Yifan; Saatchi, Sassan (2016): Sensitivity of L-Band SAR Backscatter to Aboveground Biomass of Global Forests. In Remote Sensing 8 (6), p. 522. DOI: 10.3390/rs8060522.

USGS EROS. Landsat Collection 1 Level 1 Product Definition; USGS: Sioux Falls, SD, USA, 2017.

Zaiatz, Ana Paula Soares Rodrigues; Zolinn, Cornélio Alberto; VENDRUSCULO, Laurimar Goncalves; LOPES, Tarcio Rocha; PAULINO, Janaina (2018): Agricultural land use and cover change in the Cerrado/Amazon ecotone: A case study of the upper Teles Pires River basin. In Acta Amazonica 48 (2), pp. 168–177. DOI: 10.1590/1809-4392201701930.

Zanne, Amy E.; Lopez-Gonzalez, G.; Coomes, David A.; Ilic, Jugo; Jansen, Steven; Lewis, Simon L. et al. (2009): Data from: Towards a worldwide wood economics spectrum.

Zimmermann, Julia; Higgins, Steven I.; Grimm, Volker; Hoffmann, John; Münkemüller, Tamara; Linstädter, Anja (2008): Recruitment filters in a perennial grassland: the interactive roles of fire, competitors, moisture and seed availability. In Journal of Ecology 96 (5), pp. 1033–1044. DOI: 10.1111/j.1365-2745.2008.01409.x.
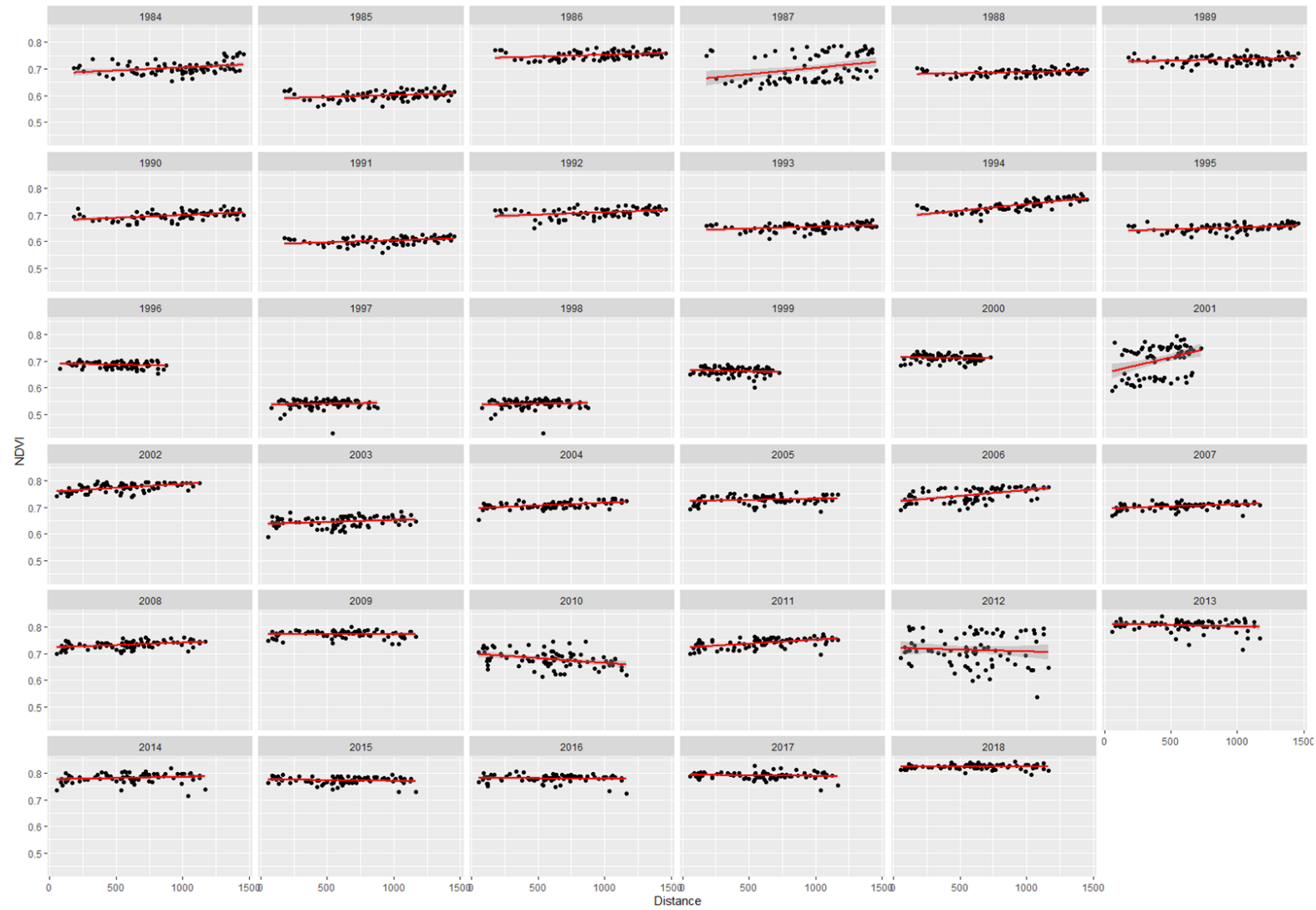
Appendix A

Figure A. Simple linear regression of the relation between edge distance and mean values of NDVI annual compositions of the fragment A.
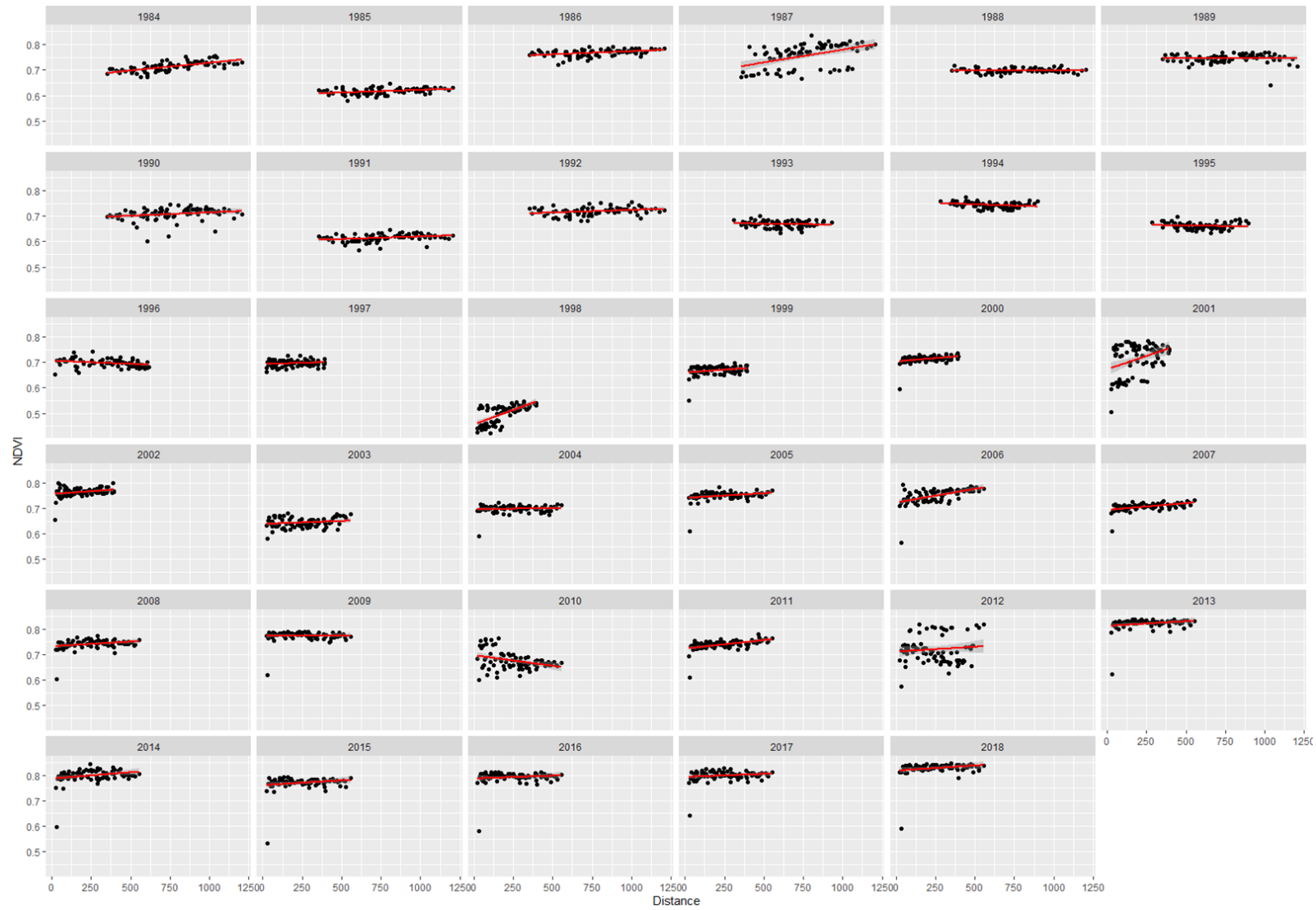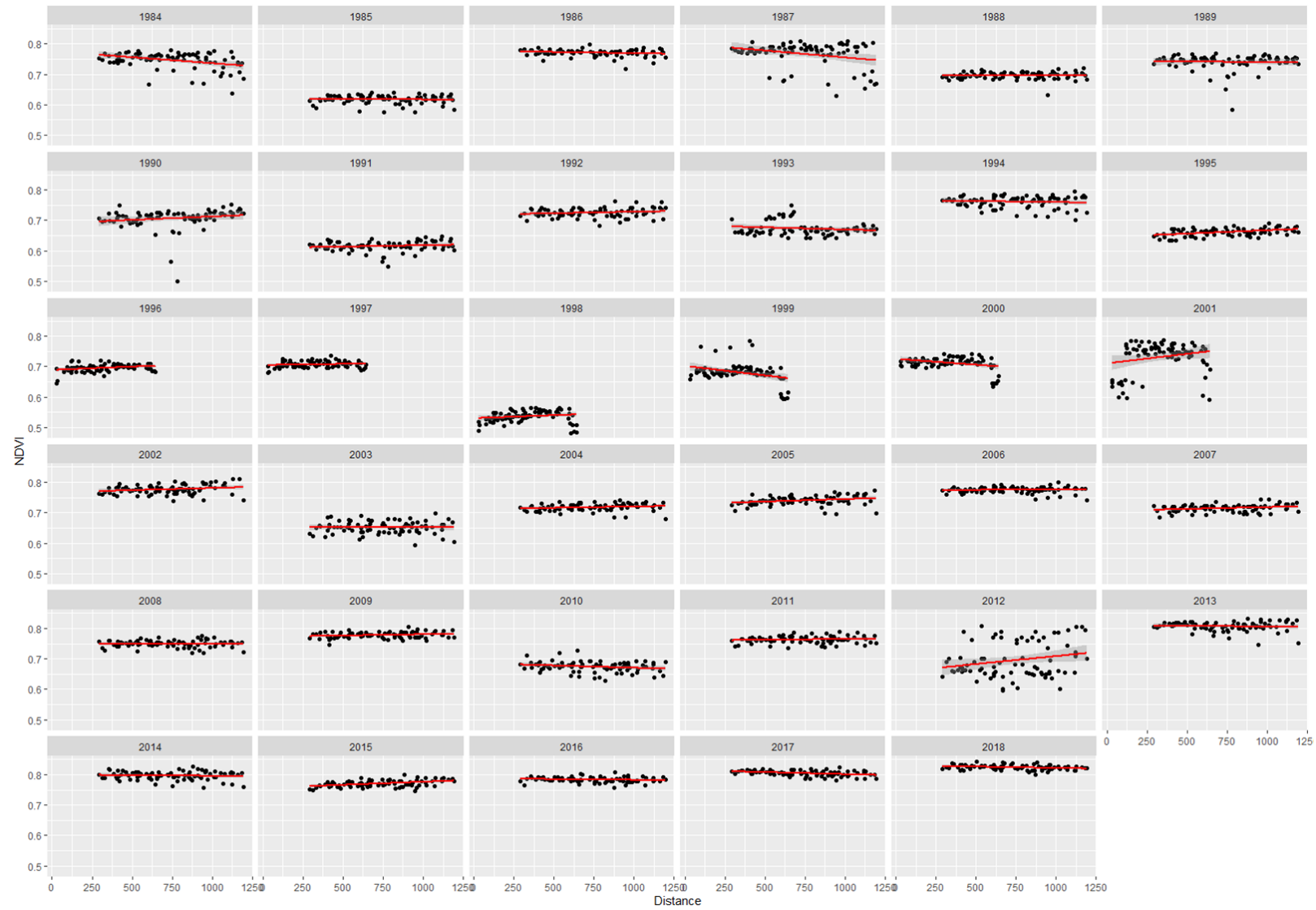
Appendix B

Figure B. Simple linear regression of the relation between edge distance and mean values of NDVI annual compositions of the fragment B.
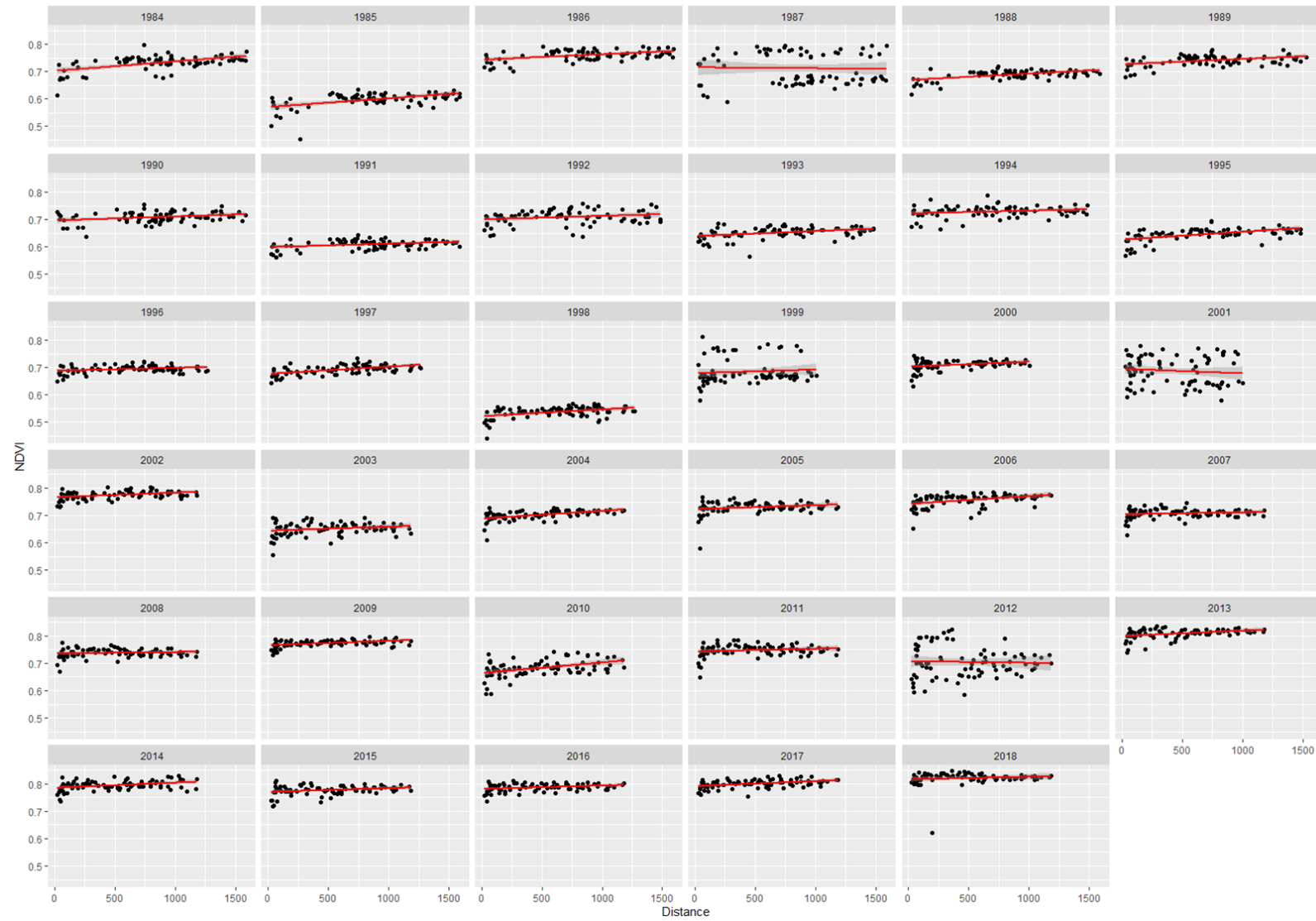
Appendix C

Figure C. Simple linear regression of the relation between edge distance and mean values of NDVI annual compositions of the fragment C.
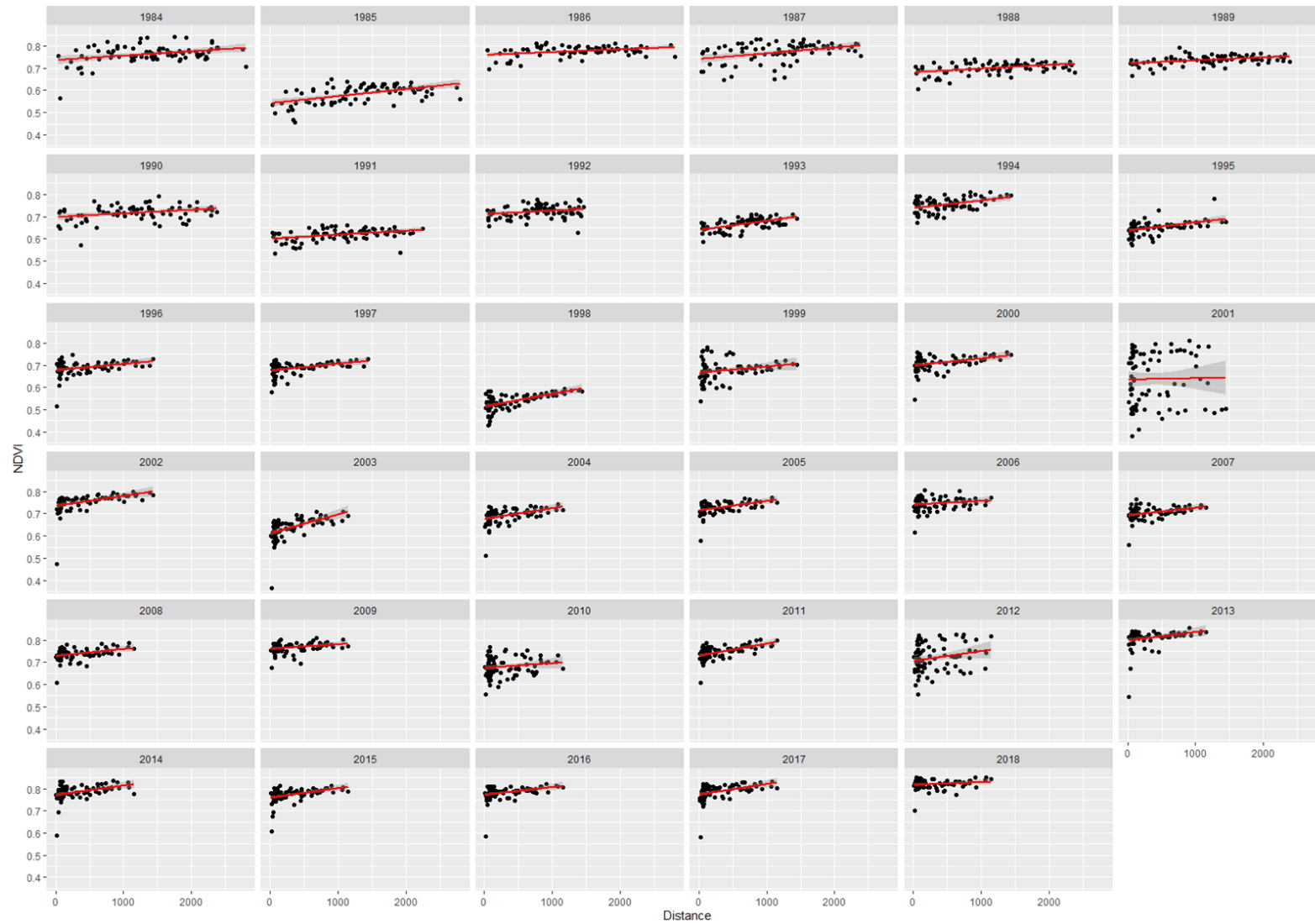
Appendix D
Figure D. Simple linear regression of the relation between edge distance and mean values of NDVI annual compositions of the fragment D.
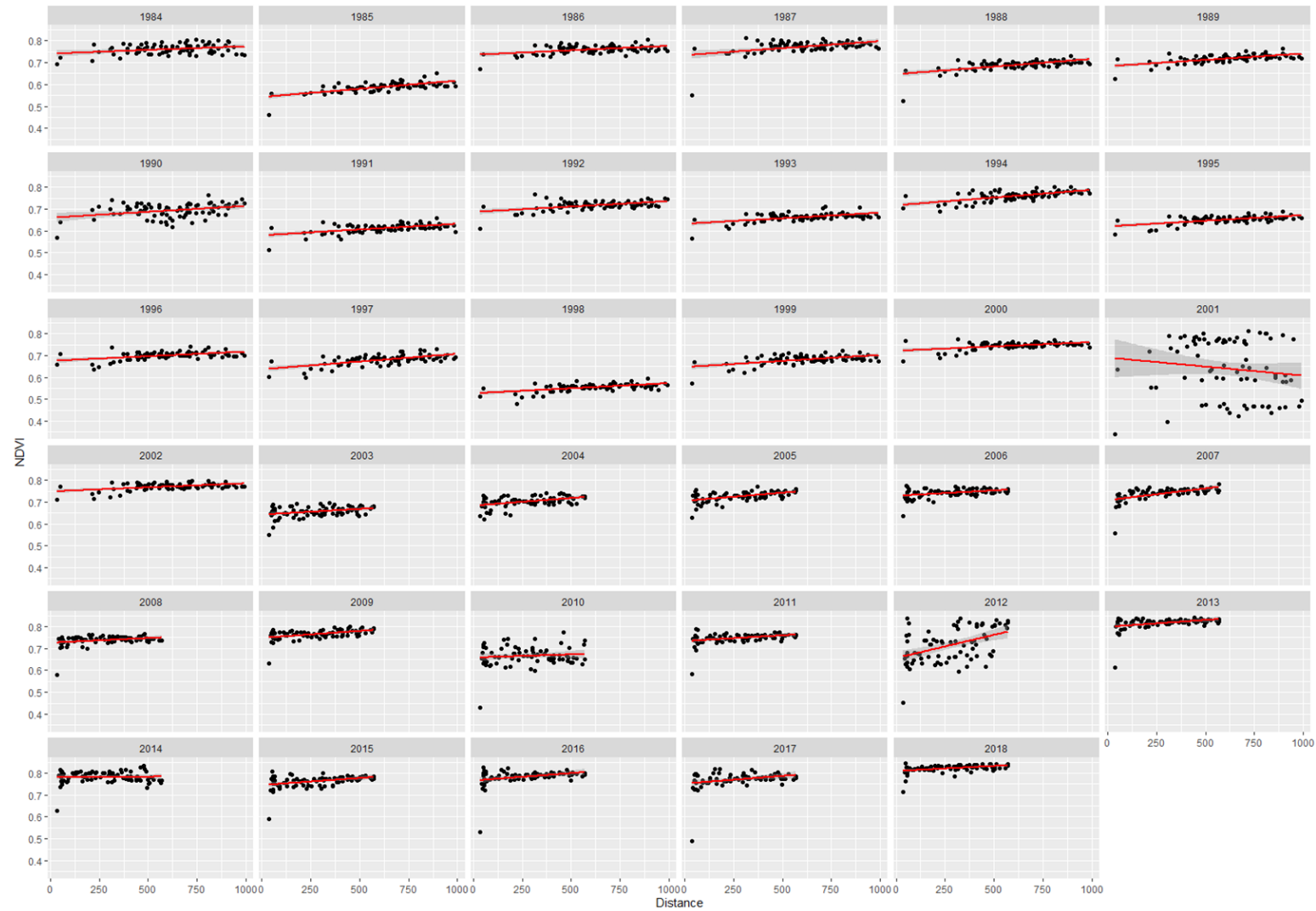
Appendix E

Figure E. Simple linear regression of the relation between edge distance and mean values of NDVI annual compositions of the fragment G.

Appendix F

Figure F. Simple linear regression of the relation between edge distance and mean values of NDVI annual compositions of the fragment H.

Figure G. Historical (1984–2017) precipitation data collected from the Diamatino fluviometric station located near to the study area.